Interpretation of sponge fossil faunas:
A neontological approach to a paleontological problem

by

Pablo Aragonés Suarez

A thesis submitted in partial fulfillment of the requirements for the degree of

Master of Science

Department of Biological Sciences
University of Alberta

Abstract

The tempo and mode of early animal evolution remains one of the biggest conundrums in biology. Stratigraphy shows that there is a gap, not attributable to poor preservation, of at least ~100 Myr between the oldest animal fossils and the divergence times implied by molecular phylogenies. Sponges, due to their position in the metazoan tree, are a good candidate for the earliest fossil evidence for the diversification of animals. Nevertheless, the search for the earliest animals represents a major challenge due to the lack of criteria by which to recognize such organisms in the fossil record. Here I describe a way to quantify the sponge filtration or 'sponge pump character' by analyzing the ratio between the two major components of the aquiferous system: external surface area–SA and osculum cross-sectional area–OSA, which allows comparison between extant sponges and many fossil forms. Second, I addressed the question of whether sponges make use of induced flow, an often-made assumption when interpreting fossils as sponges.

The analysis includes the three major classes of Porifera: Demospongiae, Hexactinellida and Calcarea, both are represented by extant and fossil taxa from two extremes of the Phanerozoic, the Cambrian and Eocene. The data show that this ratio is narrow, 0.01 – 0.001 in modern sponges, and the slope of the ratio can be used to distinguish classes of sponges. I then examined the ratio of OSA/SA for the putative Ediacaran sponge *Thectardis avalonensis*, and found it to be similar to some Cambrian sponge genera. Moreover, the slope of the ratio across different sizes of *T. avalonensis* is similar to that of demosponges. However, the original argument for the Poriferan affinity of *T. avalonensis* was based on the idea that the main mechanisms that sponges use to filter water is through current induced flow, meaning that shape

alone drives the flow in and out of a sponge at no extra metabolic cost. I tested this hypothesis in the second chapter of this thesis by analyzing data from tank experiments in the demosponge *Geodia barretti.* The analysis of the filtration to respiration ratio showed increased filtration at ambient currents below 10 cm s^{-1} but a reduction at higher ambient current speeds, which contrast the traditional view of shape induced flow. Instead, these results support the evidence that sponges have a high degree of control over their filtration, with the consequence that induce flow should not be taken as a criterion for ascribing to the sponges any structure based on this assumption.

Overall, my work shows that a more solid understanding of the biology of modern sponges provides a wealth of information with which to examine the Precambrian record of sponges in particular, and the greater picture of early animal evolution in general. This is because having a correct interpretation of the fossil record is essential to properly calibrating molecular phylogenies.

Preface

A version of Chapter 2 has been submitted for publication to Paleobiology as Aragonés, P. and Leys, S.P. Extant sponge morphology provide insights into the fossil record. SPL was the supervisory author and helped in designing the experimental questions and hypotheses. I was in charge of data collection, analysis and writing.

Chapter 3 is planned for publication as Aragonés, P., Kahn, A.S., Matveev E., Bannister R., and Leys, S.P. Evidence of sense-induced flow in the deep-sea demosponge *Geodia barretti.* SPL designed the experiment and collected the raw data and I did data analysis and wrote the chapter.

Dedication

Esta tesis está dedicada a la memoria de mi abuelito Enrique Moisés Suarez Méndez† quien me enseñó a mantener la vista siempre fija en mis objetivos.

Quiero agradecer a mi familia. Mi mamá, Lilia América Suarez Fajardo; mi papá, Pablo Elías Aragonés Coello; mi hermano Josenrique y mi perra Chichi†. Quiero hacer una mención especial a las personas que por motivos relacionados o no a la pandemia causada por el virus SARS-COV-2, han fallecido en el transcurso de este año. Sobre todo, al Inge Papirrín† de Ciudad Guzmán, Jalisco, cuna de grandes artistas.

Quisiera también agradecer con todo mi corazón a tanta gente que me acompañó en el camino, que no cabrían todos aquí. Así que solo me limitaré a enlistar a los más inmediatos y de influencia directa en el desarrollo de este trabajo y de mi bienestar emocional en estos últimos dos años. A mi hermano Josenrique, que me apoyó en mis proyectos más locos. Gracias a él, tengo mi sitio web, y mi podcast La Biozona. Nada sería posible sin ti, ñaño. A todo el equipo de colaboradores, y oyentes, de La Biozona por creer en mí. A los conductores de En Caso De Que El Mundo Se Desintegre, el Pirata y el Señor Lagartija, que siempre han estado ahí. Y a los desintegrados todos. Por supuesto, el resto de la lista no está en orden de importancia sino más bien, es el orden en el que estas personas llegaron a mi vida. Conservo muchos amigos en México, pero en particular Lupita Briones, Dámaris Morón y Thelma Arenas me han apoyado mucho durante el transcurso de esta tesis. Gracias a mi amiga Hailleen Varela que, desde Brasil me apoyó en los momentos más difíciles y me despejaba la mente con sus pláticas sobre astrofísica y Relatividad General. A mis amigos de Edmonton, 'AREPAS'. Najmeh, José Leonardo, Gustavo, Ana, Lucía, Laura, Enrique y Carlo. Y a todo el equipo de EHBA, dónde me distraía dando clases de español.

Acknowledgments

This thesis was only possible thanks to many people. First and foremost, I planned, conducted and wrote about this research under the careful guidance and insight of my supervisor Dr. Sally Leys, who always helped me to get the best out of my abilities. I learned a lot under her tutelage and for that, I'm much obliged. I thank my committee members, Dr. Lindsey Leighton and Dr. John Paul Zonneveld for their suggestions and support, as well my external examiner Dr. Richard Palmer. Thank you to my fellow lab mate and excellent diver Nikita Sergeenko, for his help in specimen collection in Bamfield, BC, as well as the diving crew in Bamfield Marine Science Centre. Thanks also to: a) Nelson Lauzon who helped me build and set up the flow flume in Bamfield and Dr. Amanda Khan who performed the flow experiments with *Geodia barretti* in Norway, b) the personnel of the Royal Tyrell Museum for their help in photographing specimens, c) Jean Bernard Caron and the Royal Ontario Museum for providing pictures of Burgess Shale sponges, some of which were included in my analysis, d) Dr. Michelle Kelly for her kindness providing excellent pictures of lithistids and e) Dr. Andrzej Pisera for sharing his insight of the sponge fossil record. I'm very grateful to all of the members of the Leys Lab for their invaluable feedback. Special thanks to Evgeni Matveev who introduced me to the fascinating world of R coding and Christianne Nylund from whom I learned a lot about pedagogy and helped me succeed in my teaching. Finally, thanks to Dr. Christina Barron-Ortiz and all of the members of the Royal Alberta Museum department of Quaternary Paleontology, and to the members of the Astronomy and Paleontology clubs, to Dr. Sharon Morsink and everyone at the Observatory of the University of Alberta.

This work was funded by the University of Alberta Department of Biological Sciences, Mitacs Graduate Fellowship, and an NSERC Discovery Grant to Dr. Sally Leys.

Table of Contents

List of Tables

List of Figures

List of Symbols

OSA: Osculum cross-sectional area, or osculum area, in cm^2

SA: Surface area, the external surface (estimated entire area of exopinacoderm) of a sponge, in cm^2

U_o: Excurrent jet speed at the osculum, cm s^{-1}

Q: Volumetric flow rate, usually expressed in ml hr^{-1}

FR: The ratio of volumetric flow rate to oxygen removed per unit time

CC: The estimated number of choanocyte chambers

H: Head loss, or the system pressure loss due to friction, in μm H_20

Pp: The pumping power in μW

η: The metabolic cost of pumping, expressed as a percentage (%)

Glossary of Terms

Gross morphology: the external appearance of the sponge, the size and shape and anatomical elements such as the external surface and osculum.

Aquiferous system: the internal branching canal system through which the sponge gets its food and oxygen. It is composed of ostia, subdermal space, incurrent canals, the choanocyte chambers, excurrent canals, atrium and osculum.

Ostium: Pl. Ostia. The first incoming aperture to the aquiferous system of a sponge. Usually in the size range of 10 to 20 μm.

Atrium: Internal cavity of the sponge, and last element of the aquiferous system before the osculum.

Osculum: Pl. Oscula. The final element of the aquiferous system, the opening through which the water leaves the sponge. It is usually circular to ovoid, but there are a range of geometries. Beside shape, it is the most prominent easy-to-distinguish feature of a sponge.

Choanocytes: A beating flagellated collar-cell type that lines the interior of the choanocyte chambers. Described by some as the iconic cell type of sponges.

Choanocyte chambers: Internal spheroid structures of varied sizes and number of choanocytes depending on the species. Sits roughly mid-way in the aquiferous system of the sponges, and its function is to trap food particles and generate internal flow.

Ambient current speed: the speed of the water current around the sponge, also termed ambient flow.

Excurrent speed: the speed of the water jet exiting the osculum of the sponge.

Oxygen removed: A proxy for respiration and hence metabolic expenditure of the sponge. This metric is obtained by subtracting the oxygen concentration in the water expelled by the sponge from the ambient-water oxygen concentration. Also termed oxygen removal or oxygen consumption.

Putative sponge fossil: A fossil with controversial affinity. In this case said to be a sponge by the authors who first described it, but which has not reached consensual status in the research community.

Chapter 1. Interpretation of sponge fossils in the context of early animal evolution

1.1. Early animal evolution

Animal evolution corresponds only to the last fraction (roughly 540 million years) of the history of life on Earth (roughly 3.5 billion years). Nevertheless, we do consider the emergence of animals as a major transition in evolution (Maynard Smith and Szathmary 1995). Yet, details of the timing of this event are not fully resolved to everyone's satisfaction. Geologists have traditionally divided Earth's history at the point of the first appearance of fossilized animals in the rock record, and the Precambrian-Phanerozoic distinction is still widely used among paleontologists as this point (Peng et al. 2012). The apparently sudden emergence of multicellular animals at the base of the Cambrian greatly puzzled Darwin (1859) who argued that eventual fossil discoveries would solve this conundrum. We now know that phylum-level lineages were long established by the early Cambrian, c.a. 541 Ma (Butterfield 2007, Peterson et al. 2005) and there is evidence for earlier animal fossils that push back the origin of animals at least to the late Neoproterozoic, e.g., the vendobionts of Ediacara and fossil embryos of Doushantou (635–542 Ma) (Jensen et al. 1998, Yin et al. 2007). Although some of these have disputed affinities, we do find bilaterian-like ichnofossils at ~555 Ma (Evans et al. 2020). There is still a rather large gap compared to molecular clock estimates, which suggest that the divergence of major animal clades occurred at 800 Ma or earlier (Peterson et al. 2008). The lack of consensus is exacerbated by, or maybe due to, the fact that we do not have criteria with which to recognize early animals definitively in the fossil record (Antcliffe et al. 2014).

Understanding the relationship of the non-bilaterian taxa to the Bilateria (i.e., the rest of Metazoa) is key to the understanding of the evolution of metazoan traits and to knowing what to look for in the rock record. Molecular sequence analysis of such deep branching is obscured by saturation and long-branch attraction resulting in an as yet incomplete knowledge of the higher-level relationships among Metazoa (Edgecombe et al. 2011, Philippe et al. 2011). Nevertheless, molecular systematics has greatly advanced our understanding of the relationship within Metazoan lineages. Trees combining both molecular and morphological characters support the monophyly of the major Metazoan groups, Deuterostomia (Ambulacraria + Chordata) and Protostomia (Spiralia + Ecdysozoa) and support the group Bilateria + Cnidaria as a clade

(Edgecombe et al. 2011, Eernisse and Peterson 2004, Gröger and Schmid 2001, Peterson et al. 2008). Yet, the relationships of Porifera, Ctenophora, and Placozoa are not well-resolved. And although the debate is ongoing, a compelling body of evidence places sponges as the sister group of the rest of Metazoa (Feuda et al. 2017, Whelan et al. 2017). This is relevant, because sponges have a highly specialized morphology that has not changed since they first appeared in the fossil record and provides us with some features that we can potentially observe in early sponge candidates. Some of the phylogenetic studies also claim paraphyly of Porifera, with the clades Silicia (Demospongiae + Hexactinellida), Homoscleromorpha and Calcarea. In those studies, Calcarea is identified as the sister group of the rest of Metazoa. This implies that the common ancestor of metazoans had a water canal system (Eernisse and Peterson 2004, Peterson and Butterfield 2005).

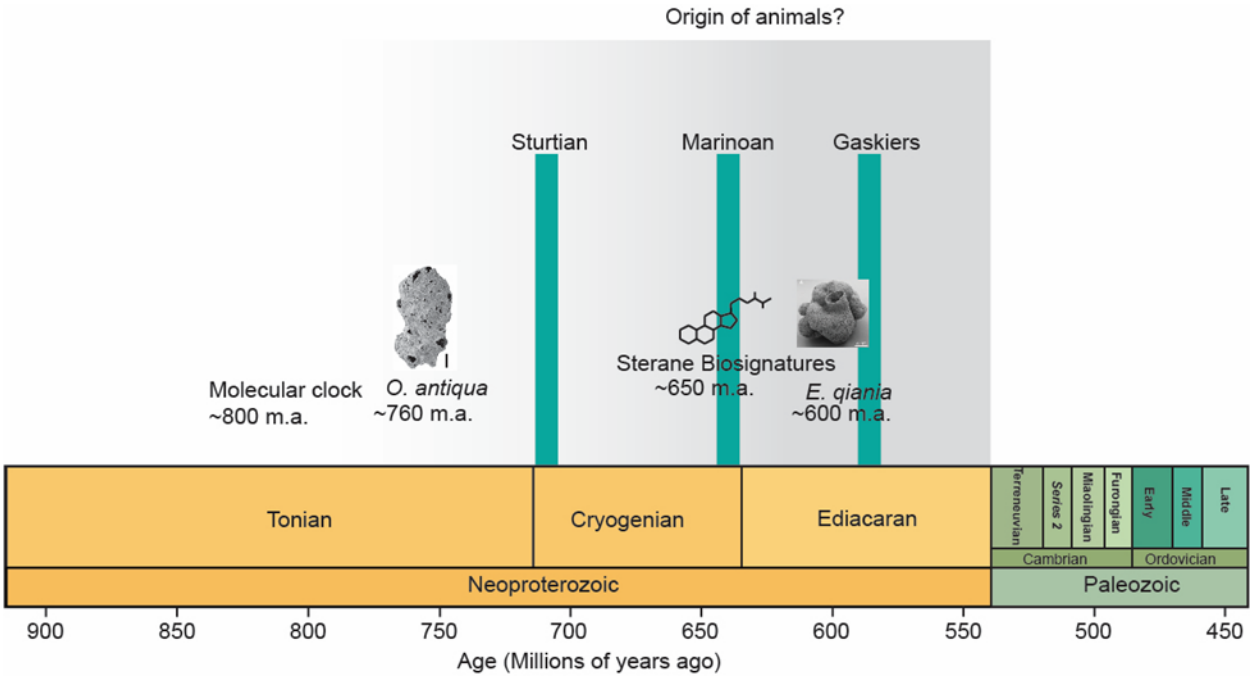

Figure 1.1. Graphic timeline of the evolution of metazoan showing position of fossils, *Otavia antiqua* (Brain et al. 2012) at 750 ma, proposed as either a testate amoeba or sponge, and *Eocyathispongia qiania* at 650 ma, proposed as a sponge (Yin et al. 2015). The appearance of sterane molecules considered to reflect the presence of sponge biomolecules is also shown at 700 ma (Zumberge et al. 2018). Molecular clocks suggest animals evolved at 800 ma or earlier, but the oldest Metazoan ichnofossils lie at ~555 ma.

1.2. Sponge phylogeny

More than 800 described species of sponges are currently divided into four extant classes: Calcarea, Homoscleromorpha, Hexactinellida, and Demospongiae (the most diverse group, with up to 85% of species) (Hooper and Van Soest 2002, Van Soest et al. 2012) and the still contentious extinct group Archaeocyatha. The Calcarea are characterized by the production of extracellular calcite spicules, the Hexactinellida by triaxonic siliceous spicules and tissue arranged in syncytia. Homoscleromorpha, a former subclass within Demospongiae with tetraxonic siliceous spicules, has been recognized as a distinct class based on molecular data and the lack of cell types such as collencytes, spongocytes and lophocytes (Ereskovsky et al. 2014). Finally, the Demospongiae are characterized by monaxonic, tetraxonic or polyaxonic siliceous spicules and spongin filaments (Hooper and Van Soest 2002). However, a mix of calcarean and demosponge characters occurs in early sponges (Nadhira et al. 2019). So the last common ancestor of Porifera could have been a thin-walled sponge with bimineral (calcite and silica) hexactine spicules (Nadhira et al. 2019), although relationships are not fully resolved, and it could as well have lacked spicules or any kind of mineralization altogether. Also, it is important to note that the sponge fossil record is dominated by lithistid sponges (a polyphyletic demosponge group) (Botting et al. 2017) due to the nature of their skeleton, and so sponges with loose skeletons and/or living in high energy environments are likely underrepresented in the record.

1.3. Sponge biology and morphology

Sponge is the vernacular name for all the members the phylum Porifera. This group of animals composes a large portion of, and sometimes dominates, tropical reef fauna in terms of biomass. Significantly, sponges conspicuously inhabit both marine and freshwater habitats in a large range of depths and latitudes. Sponges display many colors (e.g., yellow, purple, black, green…) and a huge range of sizes (from a few millimeters up to a few meters in diameter). They also display a myriad of growth forms, being tubular, spherical, conical, and encrusting sheets (Brusca and Brusca 2003). Porifera are non-bilateral invertebrates lacking a distinctive body symmetry, and this complicates their description and identification at the species level in the field (Bell 2008).

The main taxonomic features are spicules made of calcium carbonate, silicon or protein (spongin, a derivative form of collagen) arranged in a mesh-like skeleton, although some members of the phylum that possess a massive skeleton do not exhibit this trait e.g., *Vaceletia,* and stromatoporoids (Stearn 1983).

Sponge bodies are organized around an aquiferous system, in which the hierarchical branching system of canals follows this structure: Water enters through the ostia (10 – 20 µm diameter apertures that cover portions of the surface of the body) to a subdermal space. Then water enters the incurrent canals which lead towards the choanocyte chambers, which are the units that power the pump via the continuous beating of the flagella of many choanocyte cells. There are tens of these cells in each chamber, depending on the species. Importantly the chambers are arranged in parallel, which means water only passes through one, and only one, choanocyte chamber through its whole journey. The entrance of the choanocyte chambers is the prosopyle, and the exit is the apopyle. Inside, the water flows through the collar of the choanocyte, and the particles are trapped on mucus. A gasket or secondary reticulum effectively divides the incurrent and excurrent flow, giving rise to a unidirectional stream of water, so that in natural conditions the water flows from the ostia to the osculum and never in reverse (Bidder 1923).

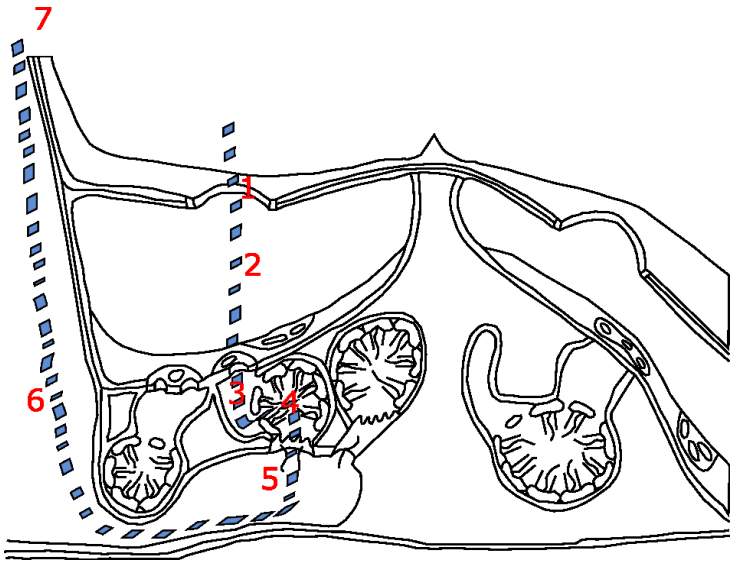

Figure 1.2. Diagram showing the water path (blue dashed line) through the aquiferous system of a sponge. (1) Ostia (2) Subdermal space (3) Incurrent canals, (4) Choanocyte chambers, (5) Excurrent canals, (6) Atrium, and (7) Osculum. Modified from Elliott and Leys (2007).

Sponges are a crucial element for the nutrient cycling of the ecosystems in which they thrive. Moreover, they can also be seen as ecosystems of their own, as we now recognize the concept of the sponge holobiont. The sponge holobiont involves the sponge host, the microbiota and the interactions between them. This is a very important distinction, as different sponge taxa will host a particular microbiota, and their immune system can distinguish between foreign and symbiotic microbes (Pita et al. 2018). The sponge microbiota is both specific and exceptionally diverse, displaying more than 30 bacterial phyla, the candidate bacterial phylum Poribacteria, and at least two archaeal lineages (Schmitt et al. 2012, Simister et al. 2012, Webster et al. 2010). Even more striking is the clear – and long recognized – distinction in microbial abundances within their tissues, as either high or low with no intermediaries (Poppell et al. 2014). Low Microbial Abundance (LMA) sponges have a microbial density similar to that of sea water (10^5-10^6 cells cm^{-3} of sponge tissue). In contrast, bacteriosponges (sensu Reiswig 1981) or High Microbial Abundance sponges (HMA, sensu Hentschel et al. 2003) harbour in their mesohyl up to 5 orders of magnitude more microbial cells per volume of tissue (10^8-10^{10} cells cm^{-3} of sponge tissue) (Hentschel et al. 2006, Vacelet and Donadey 1977).

1.4. Induced flow

In terms of structure and function, a sponge is a highly specialized and efficient biological pump. As sedentary animals, and with the notable exception of the carnivorous sponge family Cladorhizidae, almost all members of the phylum Porifera get their nutrients and oxygen through water filtration. The volumetric excurrent flow rate of sponges can be quite high, up to 900 their body volume per hour, and with 99% efficiency when removing bacteria (Reiswig 1974). All this water is moved through the canals via the internal flow generated by the choanocyte chambers (Bidder 1923, Bowerbank 1864, Grant 1825). However, in several publications, Vogel suggested both theoretically, and with *in-situ* and tank experiments, that the sponge pump seems to be enhanced by ambient currents (Vogel 1974, 1977, 1978, Vogel and Bretz 1972). He termed this phenomenon current-induced flow, stating that sponges, as current aligned hollow tubes, could filter more water simply by letting water run through them at no extra metabolic cost from choanocyte beating.

Over the years it has become widely accepted that sponges use this passive mechanism to filter water and oxygenate their tissues (e.g., Kumala et al. 2017, McMurray et al. 2014, Savarese 1995, Schlappy et al. 2010). Most importantly, for the purpose of this thesis, the hypothesized ability of sponges to make use of induced flow has been used indiscriminately to elucidate the affinities of a wide range of *incertae sedis* fossils (e.g., Sperling et al. 2007). Because affinities of early fossil assemblages can have a significant impact in our understanding of the history of animal life it is important that our assumptions are based on our better understanding of extant sponge physiology (Botting and Nettersheim 2018).

Substantial data suggest that the thin-walled glass sponge *Aphrocallistes vastus* does not act as a passive conduit, but rather exhibits complex behavioral responses to currents (Mavteev et al., in prep). In Chapter 3 of this thesis I tested whether the globular sponge *Geodia barretti*, for which there is a full dataset including flow and morphometrics, uses 'current-induced flow' by measuring oxygen removal (respiration) and excurrent flow (filtration) during different ambient current speeds in a large tank experiment.

1.5. Sponge taphonomy

Another important element for the correct interpretation of the fossil record is the understanding of how fossils are formed in the first place. As a prerequisite for fossilization, decaying tissues need to be preserved long enough for the mineralization to occur, and so the likelihood of entering the rock record ultimately depends on the very nature of the tissues themselves: e.g., rapidly decaying soft tissue vs hard and mineralized skeletal elements. Therefore, it is often said, and for good reasons, that the fossil record is incomplete and biased; but it is also true that experimentation can help us investigate in which ways it is biased.

Taphonomy is the paleontological discipline that deals with the question of how we get from a living organism to a fossil. Experimental taphonomy can be informative about how likely it is for a particular group of organisms to be preserved in the fossil record and also in what type of rocks they are more likely to occur. For instance, Precambrian fossils with exceptional preservation are often found in silicified rocks (Barghoorn and Tyler 1965, Xiao et al. 2005, Zhang et al. 1998). Phosphate minerals are also found in the matrix of exceptionally preserved fossils in those and other faunas (Allison and Briggs 1993). Many sponges occur in these types

of rocks, although we find them as flattish compressions with not much internal detail. To answer the question as to how likely it is to find fine details of tissues and cell types in fossils, I performed a short taphonomic experiment focused only on testing the decaying time for sponge tissue, and explored whether this time can be lengthened by reducing conditions and high concentrations of minerals in the surrounding water. My main findings were that sponge soft tissue decays quickly, within 15 days, even in strongly reducing conditions, but that the articulation of the skeleton (which often relies on collagen in the form of spongin) can be retained for at least 4 weeks, allowing for incipient mineral crystals to attach to the spicules (see Appendix 1 for details).

1.6. Morphometrics

The analysis of form is a central problem in biology, because all biologists must deal with shape and size in some way. The analysis of form must also consider adaptation – the fitness of a structure to perform a function beneficial to an organism – for structures do not evolve in a vacuum but in relation to other biological variates and physical variables (Gould 1971). To this end, the field of morphometrics was, and continues to be, greatly advanced in this century (Goloboff and Catalano 2011, Richtsmeier et al. 2002, Rohlf 2015, Rohlf and Corti 2000, Warton et al. 2006). The new methods of Geometric Morphometrics conceive shape in a Riemann manifold space and have vastly replaced the traditional Euclidean space approach of conventional Morphometrics (Kendall 1989, Mitteroecker and Huttegger 2009). This replacement allows for a more detailed study of complex shapes, like those of vertebrate skeletons (Thomas and Reif 1993) but also invertebrates, e.g., bryozoans (Carter et al. 2010) and brachiopods (Tyler and Leighton 2011).

The morphometric revolution did not neglect sponges. Notably, D'Arcy Thompson made a first attempt to describe the relationships between the shape of a sponge and its function in 'On Growth and Form', where he ascribes spicule geometry to be a reflection of surface tension acting upon an aggregate of cells (Thompson 1917, reprinted as Thompson 1992). Sponges are non-bilaterally symmetrical animals with huge morphological plasticity (Bell and Collins 2008, Kaandorp and Leiva 2004). Therefore, sponges do not possess a regular shape, or homologous points, that we can use to study their form in a geometric-morphometric context. Consequently,

morphometric studies of sponges have largely been based on their spicules (e.g., Bavestrello et al. 2008), with a few exceptions (e.g., Kaandorp et al. 2008). But because a) form can be decomposed and described as simply as a ratio of magnitudes that can be plotted against a degree of freedom (usually mass, or length) and b) scaling – the change in the ratios with respect to mass or size – is necessarily paired with profound changes of physical phenomena acting upon shapes at different scales (Thompson 1917, as reprinted in Thompson 1992), it follows that even sponges should respond to the allometric power law equation ($Y=kX^b$) and their shape can be studied in terms of interspecies or intraspecies change in slope (Gould 1966). Because these mathematical relations are symmetrical, we should be able to infer the attributes of the sponge pumping rate, even in fossils, from their form. Spicules can be analyzed using Geometric Morphometrics, but we need a sort of general morphometric character to compare extant taxa with those in deep branches of the tree (and in groups with no spicules, no cellular detail nor internal structure like the water vascular system).

1.7. Thesis objectives

This thesis tests the ability to describe a sponge's function from its form. The ultimate aim is to apply that approach to the fossil record to ask whether a fossil could have been a sponge if no spicules are present. The main objectives that I address in this thesis are: A) to describe the relation of gross morphology, the pump, and the pump units; B) to describe the pump character of extant sponges using the gross morphology of extant sponges, and compare this character with the fossil counterparts; and C) to test the induced flow hypothesis in a deep-sea demosponge. In Chapter 2 I discuss the ratio of the osculum to surface area as the sponge pump character using collected data (new measurements and unpublished imagery), and from the literature, and assess whether this 'character' can be applied to known sponge fossils. I then ask: does the putative sponge fossil, *Thectardis avalonensis* exhibit this distinctive sponge character? If modern and known fossil sponges all share a morphometric scaling character that is indicative of a pump, then putative fossils either a) are not related to sponges, or b) if they were sponges, the filtration requirements must have been different from what Phanerozoic sponges experience. In addition, a better understanding of the sponge pump and its scaling with gross morphology can help us estimate the pumping rate of ancient sponge reefs, such as those that existed in the Tethys Sea.

Chapter 3 deals with the idea of induced flow as a mechanism that reduces the cost of pumping in sponges. I test whether there is evidence for passive flow in the demosponge *Geodia barretti*, a deep-sea demosponge from Norway that is a good candidate to show evidence of passive flow due to the apical position of the osculum and its occurrence in a resource-poor habitat.

Chapter 2. Extant sponge morphology and insights into the fossil record

2.1. Introduction

The tempo and mode of early animal evolution remains one of the biggest conundrums in biology. It is now known that phylum-level lineages were long established by the early Cambrian, c.a. 541 Ma (Butterfield 2007, Peterson and Butterfield 2005) and there is evidence for earlier animal fossils that push back the origin of animals at least to the late Neoproterozoic, e.g., the vendobionts of Ediacara and fossil embryos of Doushantuo (635–542 Ma) (Jensen et al. 1998, Yin et al. 2007), but most of these have disputed affinities, including the bilaterian-like ichnofossils at ~555 Ma (Evans et al. 2020). The apparent sudden emergence of multicellular animals at the base of the Cambrian greatly puzzled Darwin (1859) who argued that eventually fossil discoveries would solve this conundrum. However, except for *Namacalathus* from the Ediacaran, which was recently described as a putative lophotrochozoan (Shore et al. 2021), there are still no body fossils widely accepted to be metazoans. This leaves a large gap in time between fossils and the molecular clock estimates that place the divergence of major animal clades at 800 Ma or earlier (Peterson and Butterfield 2005). The lack of consensus on timing of appearance of the first multicellular animals is exacerbated by, or maybe due to, the fact that we lack criteria by which to recognize early animals definitively in the fossil record (Antcliffe et al. 2014).

Our current understanding of the phylogenetic relationships of early branching taxa is key to interpreting the evolution of metazoan traits and knowing what to look for in the rock record. Molecular sequence analysis of such deep branching is obscured by saturation and long-branch attraction resulting in a yet incomplete knowledge of the higher-level relationships among Metazoa (Edgecombe et al. 2011, Philippe et al. 2011, Philippe et al. 2009). Nevertheless, molecular systematics have greatly advanced our understanding of the relationships within Metazoan lineages. Trees combining both molecular and morphological characters support the monophyly of the major Metazoan groups, Deuterostomia (Ambulacraria + Chordata) and Protostomia (Spiralia + Ecdysozoa) and support the group Bilateria + Cnidaria (Edgecombe et al. 2011, Eernisse and Peterson 2004, Gröger and Schmid 2001, Peterson et al. 2005). Yet, the

relationships of Porifera, Ctenophora, and Placozoa are not well-resolved. Although the debate is ongoing, a compelling body of evidence places sponges as the sister group of the rest of Metazoa (Feuda et al. 2017, Whelan et al. 2015, Whelan et al. 2017, Wörheide et al. 2012). This is relevant because sponges have a highly specialized morphology that has not changed since they first appeared in the fossil record. Stasis in their general shape is likely because the sponge body plan is highly specialized for filtration (Manuel et al. 2003), and so a sponge, or a sponge-type animal, should be a good candidate when looking for fossil evidence of early diversification of animals. It is not known, however, when the sponge 'filtering' body plan arose (Cunningham et al. 2017, Dohrmann and Wörheide 2017, Erpenbeck and Wörheide 2007).

Molecular clock data suggest that Porifera diverged from the metazoan lineage as early as 800 Ma to 650 Ma – the Tonian to Cryogenian interval (Cunningham et al. 2017, Peterson and Butterfield 2005)– and the earliest irrefutable sponge fossils are c.a. 535 Ma (Antcliffe et al. 2014). There is a gap of at least ~100 Myr and up to 300 Myr between the oldest sponge fossil recognized as such, and the oldest signal from the biochemical record of sponge-derived steranes, which agree with the molecular clocks estimates (Botting and Nettersheim 2018, Zumberge et al. 2018).

Some candidate fossils have been proposed which might fill in this gap, but their affinities to sponges are contentious (Antcliffe 2013, Brain et al. 2012, Love et al. 2009, Schuster et al. 2018). Most of these fossils are represented only by scarce spicule-like elements that can also be explained by abiogenesis (Antcliffe et al. 2014). Sponge tissues (or other organic materials) are highly unlikely to be preserved unless in anoxic and reducing conditions for sufficient time to allow replacement of tissue by minerals (Supplementary Fig. 1); thus, it is very unlikely that choanocyte chambers or pinacocytes would be found in the fossil record as proposed by Yin (2015). However, despite the fact that sponge tissues do not preserve well, the organization retained by the spicules can still preserve a general body outline (Supplementary Fig. 2). Putative metazoan body-fossil candidates of unknown affinity include *Otavia antiqua* (Brain et al. 2012), a 0.3 to 5 mm organism from the Otavi and Nama Group in the Okavuvu Formation in Namibia dated at 760 Ma; *Eocyathispongia qiania* (Yin et al. 2015), from the Doushantou Formation in central Guizhou, China dated at 600 Ma; and *Thectardis avalonensis* (Clapham et al. 2004), from the Mistaken Point and Drook formations dated at 575 Ma. All of these have a proposed poriferan affinity, or alternatively are considered possible amoebae

(*Otavia*), or are thought to represent a state (stage) of other known vendobionts (*Thectardis*) (Antcliffe et al. 2014, Porter and Knoll 2000, Sperling et al. 2011).

A reassessment of fossils is therefore needed to close the sponge fossil gap or recognize its true existence. Fossils necessarily lag behind the actual date of origin of a clade, because the likelihood of finding a fossil depends on the abundance and biomass of the organisms that preceded them. As we lack other ways to time-calibrate molecular clocks, it has become obvious that establishing hard-point benchmarks is important. These benchmarks can be direct fossil evidence or molecular footprints, but both are still subject to interpretation; e.g., the sterane biomarkers used to claim the presence of crown group demosponges at 715 Ma (Zumberge et al. 2018) are also found in pelagophyte algae (Nettersheim et al. 2019). Some putative body fossils do not show spicules, and although that does not negate a sponge affinity, how can we recognize a sponge without spicules in the fossil record? As morphology is often our main, if not the only, source of paleontological data, it becomes valuable to explore the relation between form and function in modern groups (e.g., Gould 1976) and to determine if it is possible to extrapolate it to the past.

A body of literature suggests a mathematical relationship exists between the form of a sponge and its excurrent flow (or feeding) (Bidder 1923, Morganti et al. 2019, Reiswig 1971a). Sponge bodies are organized around a branching aquiferous system (Bergquist 1978, Leys and Hill 2012). Water enters canals through ostia, ~20 μm diameter holes on the surface of the body, through incurrent canals to the choanocyte chambers whose beating flagella generate the suction to drive the water flow. Chambers are arranged in parallel, and a gasket of cells or mucus around the collars effectively divides the incurrent and excurrent flow, giving rise to a unidirectional stream of water, from ostium to excurrent vent, the osculum (Asadzadeh et al. 2020, Leys et al. 2011). The pressure drop across the sponge body relies on the continuity of flow and consequently there is a predictable relationship between the area of the incurrent and excurrent openings (Reiswig 1975a, Vogel 1977). Recently it has been found that the pumping power of a sponge (as determined by its excurrent flow) is proportional to the size of a sponge (Morganti et al. 2019, Strehlow et al. 2017). Moreover, the area of the osculum alone can be used to predict the excurrent flow (Morganti et al. 2021b). It has been found that depth-induced morphological changes do not affect the performance of the sponge pump (Gökalp et al. 2020), and overall, the size-corrected total osculum area to surface area ratio is constant regardless of different habitats

(depths) in which the sponge lives. These studies strongly suggest that there might be a fixed relationship between the cross-sectional area of the incurrent and excurrent openings that is optimal for the energy budget of the sponge.

Here we examine a range of morphological characters which contribute directly to the sponge 'pump' and then test which metric best characterizes this physiological quality in extant sponges. We then apply that metric to a range of test data representing fossils from known sponge fauna from the Phanerozoic era, the Cambrian and Eocene, and finally we test whether this metric can be used to infer whether to the Precambrian fossil *Thectardis avalonensis* has the characteristics of a sponge pump.

2.2. Materials and Methods

Morphometric data

The taxonomic span of the whole dataset covers three major classes of Porifera, Demospongiae, Calcarea and Hexactinellida. Morphometric data were gathered from modern and fossil sponge genera from a range of sources (Table 1, Fig. 2). Individuals of *Haliclona* cf. *permollis* (N=17) were measured from images taken using a GoPro6 camera and a plastic ruler as a scale, in tide pools near the Bamfield Marine Science Centre, Bamfield, British Columbia, Canada. *H.* cf. *permollis* is encrusting and has multiple oscula per patch and so patches with multiple oscula were considered as individuals. Images of *Geodia barretti* (N=4) and *Sycon coactum* (N=4) came from unpublished data previously gathered by one of us (SPL). Data for *Aphrocallistes vastus* (N=10) came from Leys et al. (2011). Data for *Haliclona mollis* (N=10), *Neopetrosia problematica* (N=5), *Tethya californiana* (N=5), *Cliona delitrix* (N=9), *Callyspongia vaginalis* (N=12) came from unpublished data associated with Ludeman et al., (2017). Data for fossil sponges covers the two extremes of the Phanerozoic, the Cambrian (N=42 specimens from 12 species), images from the ROM virtual fossil gallery (Royal Ontario Museum, 2011) and Paleogene periods (N=37 specimens from 16 species, images from Frisone et al. (2016)), and the Ediacaran putative sponge *Thectardis avalonensis* (N=125, data from Clapham et al. (2004)).

Linear measurements of sponge body size or gross morphology (length, width, osculum diameter), were made using ImageJ (FIJI, v. 1.43r; National Institutes of Health, Bethesda, MD,

USA). Shape was estimated as the closest surface (*i.e.*, sphere, cylinder, cone, frustum or ellipsoid) to calculate the sponge surface area, *SA* and volume, *V* (Table 2.1). To calculate the area of the osculum, (*OSA,* following conventional terminology), oscula were either approximated using the formula for the area of a circle or ellipsoid or directly measured using the area tool of ImageJ; the difference between these two procedures was less than 5% in a sample of 20 measurements (Appendix 1, Supplementary Table). The measurements used were chosen to be comparable between both modern and fossil sponges.

Quantification of the sponge pump

To correlate the morphological metrics with filtration capacity in modern sponges, the pump, the density of choanocyte chambers (*cc*) was counted from scanning electron micrographs (SEM) available for *G. barretti, Cal. vaginalis, Cli. delitrix, T. californiana, N. problematica, H. mollis* (unpublished data). Tissue preparation for SEM was reported in Ludeman et al. (2017).

Oscular flow rates came from a range of sources. Excurrent flow rates were measured for *T. californiana* and *N. problematica* that were collected by SCUBA divers near the Bamfield Marine Science Centre. Five individuals of each were transferred quickly to a tank with flow-through seawater from 30 m depth and left undisturbed with the exception of a daily flush by pipette to remove excess surface sediment that comes from the seawater system. Excurrent speed from the osculum was measured using a custom-made thermistor flow meter (LaBarbera and Vogel 1976) calibrated with a Vectrino II Acoustic Doppler Velocimeter (Nortek, Norway). Data were recorded every second and binned in 10-second medians to calculate an average of 10 minutes. Images of each osculum were captured using a GoPro6 camera. Excurrent flow rates for *Cal. vaginalis*, *Cli. delitrix* and *H. mollis* were obtained from supplementary data in Ludeman et al. (2017) and for *Aphrocallistes vastus*, from supplementary data in Leys et al. (2011).

The volumetric (oscular) flow rate (Q; l s^{-1}) was estimated using the formula $Q = OSA \cdot U_o$, where *OSA* is the osculum area (cm^2) and U_o is the excurrent speed (cm s^{-1}).

Data analysis & statistics

To assess the extent of allometry the data were log transformed prior to analysis. Because the data were not normally distributed (Shapiro-Wilk test, $W=0.54$, $P<0.05$), a non-parametric Kruskal-Wallis test was used to compare the osculum area to surface area ratio between species,

and a Dunn post hoc test with Bonferroni corrected p-values was used to evaluate significance. The Reduced Major Axis slope of the OSA/SA ratio was considered the sponge pump 'character' and compared between modern and fossil sponge groups using an analysis of covariance (ANCOVA). Correlation and regression analyses were used to understand the contribution of each morphological variable to the pumping rate of the modern species. Data were manipulated in MS Excel, statistical analyses were performed in Sigma Plot v14 (Systat), and PAST (Hammer et al. 2001). Graphs were plotted in MS Excel, PAST (v4.03), and Sigma Plot v14 (Systat) and figures were assembled in Adobe Illustrator (CS 5) or Inkscape v1.0.2.

Table 2.1. Extant and fossil species used and methods of estimating shapes and sources of data. Origin of data: (1) images collected and measured; (2) images from source cited, measurements this work; (3) images and measurement from source cited. Sources: II Ludeman et al. 2017; III Leys et al. 2011; IV Frisone et al. 2016; V ROM virtual Gallery URL https://burgess-shale.rom.on.ca.

Species	Class/Age	Idealized Shape	n	Origin of data	Source
Tethya californiana	D/H	sphere	5	1	I
Neopetrosia problematica	D/H	crustose	5	1	I
Geodia barretti	D/H	sphere	4	1	I
Haliclona permollis	D/H	crustose	17	1	I
Callyspongia vaginalis	D/H	cylinder	12	3	II
Cliona delitrix	D/H	boring	9	3	II
Haliclona mollis	D/H	crustose	10	3	II
Aphrocallistes vastus	H/H	cylinder	10	3	III
Laocoetis emiliana	H/E	cylinder	9	2	IV
Laocoetis patula	H/E	cone	2	2	IV
Stauractinella eocenica	H/E	sphere	3	2	IV
Anomochone sp.	H/E	cylinder	2	2	IV
Hexactinella clampensis	H/E	cone	2	2	IV
Ventriculites sp.	H/E	cylinder	1	2	IV
Camerospongia visentinae	H/E	cone	2	2	IV
Camerospongia tuberculata	H/E	cylinder	2	2	IV
Coronispongia confossa	H/E	cone	3	2	IV
Cavispongia scarpai	H/E	cone	2	2	IV
Siphonia sp	H/E	sphere	2	2	IV
Rhoptrum sp	D/E	cylinder	2	2	IV
Ozotrachelus conicus	D/E	cylinder	2	2	IV
Vaceletia progenitor	D/E	cylinder	1	2	IV
Jereopsis clavaeformis	D/E	sphere	1	2	IV
Verruculina ambigua	D/E	cone	1	2	IV
Eiffelia globosa	C/C	sphere	2	2	V
Capsospongia undulata	D/C	cone	3	2	V
Crumillospongia biporosa	D/C	sphere	3	2	V
Diagoniella hindei	H/C	cone	8	2	V
Eiffelospongia hirsuta	C/C	sphere	2	2	V
Fieldospongia billilineata	D/C	cone	2	2	V
Hazelia spp.	D/C	cone	10	2	V
Wapkia elongata	D/C	cylinder	2	2	V

Takakkawia lineata	D/C	cylinder	3	2	V
Vauxia spp.	D/C	cone	1	2	V
Hamptoniella foliata	D/C	cone	2	2	V
Pirania muricata	D/C	cylinder	4	2	V

Figure 2.1. **Method of surface area calculation of extant and fossil sponge.** A) extant species *Haliclona* cf. *permollis* in situ at Bamfield, B) the mid-Cambrian *Vauxia gracilenta* from the Burgess Shale held in the Royal Tyrrell Museum and C) *Tethya californiana* D) *Neopetrosia problematica* E) *Sycon coactum* (A', B', C', D', E) schematic representation of how the surface area and the osculum area (white in A' cyan in B', C', D' and E') were obtained. This gives a measure of the osculum to surface area OSA/SA ratio, as an approximation of the proportion of the incurrent to excurrent areas.

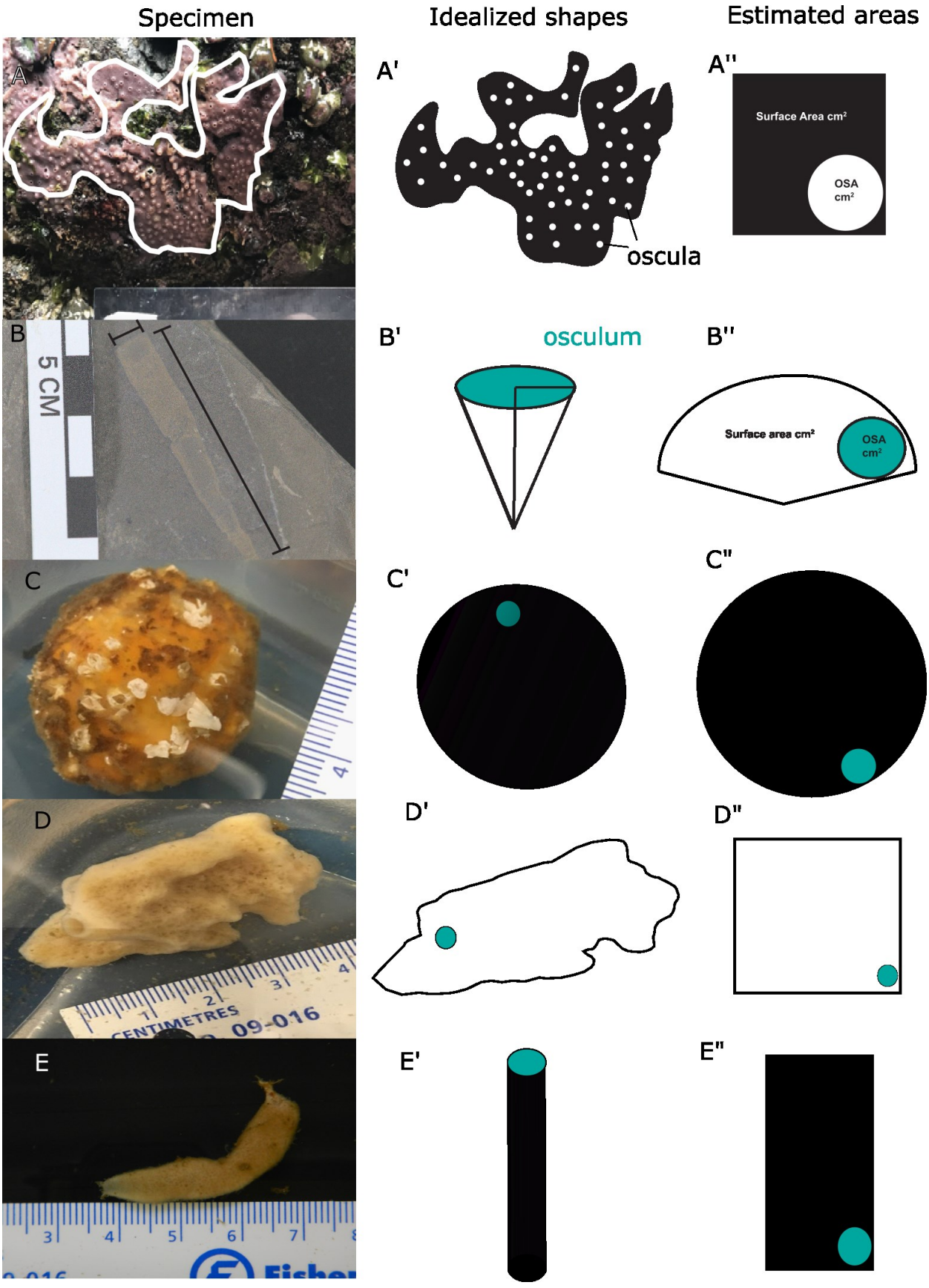
Specimen
Idealized shapes
Estimated areas
A
A'
A''
Surface Area cm²
OSA cm²
oscula
B
5 CM
B'
osculum
B''
Surface area cm²
OSA cm²
C
C'
C''
D
D'
D''
CENTIMETRES
09-016
E
E'
E''

2.3. Results

Sponge morphology and the sponge pump character

The relationship between the morphology of each sponge and the properties of the sponge pump, hereafter called the 'sponge pump character' was examined by comparing morphometrics for *a)* gross morphology (osculum area and surface area of the whole sponge), *b)* the pump unit (estimated density of choanocyte chambers) and *c)* the excurrent speed (Uo) and oscular (volumetric) flow rate (Q) (Fig. 3).

The cross-sectional area of the osculum (OSA) was proportional to the surface area (SA) of the sponge (r_s= 0.89, p<0.001) (Fig. 3A) (Table 2). The surface area of the sponge was directly proportional to the total number of choanocyte chambers in the sponge (r_s= 0.68, p= 0.09) (Fig. 3B) and the number of choanocyte chambers was directly proportional to the oscula (volume) flow rate (r_s= 0.86, p= 0.01) (Fig. 3C). Therefore, the volume pumped (oscula flow rate, Q) was also positively correlated with surface area of the whole sponge (r_s= 0.88, p< 0.001) (Fig. 3D), and with the volume of the sponge (r_s= 0.68, p<0.001) (Fig. S3). The excurrent speed was well correlated with the osculum area for demosponges only (r_s=0.87 p<0.001) (Fig. 3E) but was less well correlated with area of the osculum when both demosponges and hexactinellids were included (r_s= 0.2, p=0.07) (Fig 3E inset). It is noteworthy that the density of choanocyte chambers was not correlated with the oscula flow rate (Fig. S4), but instead was constant across all flow rates. The ratio of the osculum area to the surface area OSA/SA therefore represents a proportion that reflects the excurrent flow rate of the whole sponge. Indeed, the osculum to surface area ratio was negatively correlated with the excurrent speed (r_s=0.84, p<0.001) (Fig. 3F). The osculum to surface area OSA/SA ratio is therefore a morphological character that correlates well with the sponge pump as measured by its excurrent flow.

Testing the OSA/SA as a metric for the sponge pump for modern and fossil sponges

First, we examined variability of the OSA/SA among individuals of a species. Variability of the OSA/SA ratio for individuals of *Haliclona* cf. *permollis* was minimal (R^2=0.91 p<0.001) (Supplementary Tables 2, 3; Supplementary Figs. 5, 6). We then compared the OSA/SA ratio across species and found that the average OSA/SA for any species was not informative about the sponge pump character by itself (Fig. 4A, B). The OSA/SA ratio for modern sponges was

consistently lower than for fossil species (Fig. 4A). Furthermore, if all modern and fossil species were grouped together by class, the OSA/SA could also not distinguish sponges by class (Fig. 4B). For example, a Dunn post hoc test with Bonferroni corrected p-values showed that the OSA/SA ratio was not different between Demospongiae and Hexactinellida ($p=0.23$), but it was different between demosponges and *Thectardis* ($p<0.05$). However, the difference between Hexactinellida and *Thectardis* was not significant ($p>0.05$) indicating this value alone (OSA/SA) was not a useful metric for the sponge pump across sponges, whether modern or fossil.

However, when we compared plots of OSA/SA for each species, we found that the slopes of OSA/SA for fossil and modern sponges of the same class were not significantly different, but the slopes of the OSA/SA were different for different classes of sponges (Fig. 5). The slopes of OSA/SA ratio for all individuals in modern and fossil Demospongiae were not different (Fig. 5A), and the slopes of the OSA/SA ratio of modern and fossil Hexactinellida also did not differ (Fig. 5B) (Table 3). However, the slopes of the OSA/SA ratio from all demosponges differed from that of all hexactinellids (Fig. 5C).

Finally, we compared the slope of the OSA/SA for the putative sponge *Thectardis avalonensis* (Clapham et al. 2004) to hexactinellids and demosponges, and found it to be different from Hexactinellida, but not different from that of Demospongiae (Fig. 5D).

Table 2. Slopes of the correlation on log scale of pumping rate to size and shape of extant sponges. Osculum Area (OSA), sponge Surface Area (SA), Volumetric (oscula) flow rate (Q), Excurrent speed (Uo), Number of choanocyte chambers (CC).

X Y pair	equation	R^2	r_s	p	slope	intercept	Slope 95% bootstrapped CI N=1999	Intercept 95% bootstrapped CI N=1999
OSA SA	$Y=-3.26X^{1.63}$	0.8	0.89	8.95E-13	1.63	-3.26	1.38, 1.87	-3.77, -2.78
SA Q	$Y=-3.01X^{1.76}$	0.8	0.88	2.37E-10	1.78	-3.01	1.46, 2.026	-3.65, -2.44
OSA Uo	$Y=0.64X^{0.58}$	0.8	0.87	4.12E-10	0.58	0.6	0.47, 0.65	0.58, 0.71
OSASA Uo	$Y=-1.4X^{-0.97}$	0.2	-0.85	1.00E-02	-0.97	-1.4	-1.17, -0.71	-1.65, -1.01
SA No. CC	$Y=2.35X^{1.9}$	0.5	0.68	9.06E-02	1.9	2.35	-0.87, 3.27	0.17, 4.3
Q No. CC	$Y=5.4X^{1.23}$	0.7	0.86	1.42E-02	1.23	5.4	0.54, 1.82	5.11, 6.46

Figure 2.2. Correlation of pumping rate to size ratio of extant sponges plotted on a log scale. A) Osculum area (cm^2) to surface area (cm^2). B) Estimated number of choanocyte chambers to surface area (cm^2). C) Estimated number of choanocyte chambers, to volumetric flow (Q, ml s^{-1}). D) Volumetric flow rate (Q, ml s^{-1}) to surface area (cm^2). E) Excurrent speed (U_o, cm s^{-1}) to osculum area (cm^2). F) Excurrent speed (U_o) to ratio of osculum area/surface area (OSA/SA). Species are *Tethya californiana* (open diamond), *Neopetrosia problematica* (black diamond), *Haliclona mollis* (black square), *Geodia barretti* (white circle), *Cliona delitrix* (inverted white triangle), *Callyspongia vaginalis* (black triangle), *Aphrocallistes vastus* (black circle).

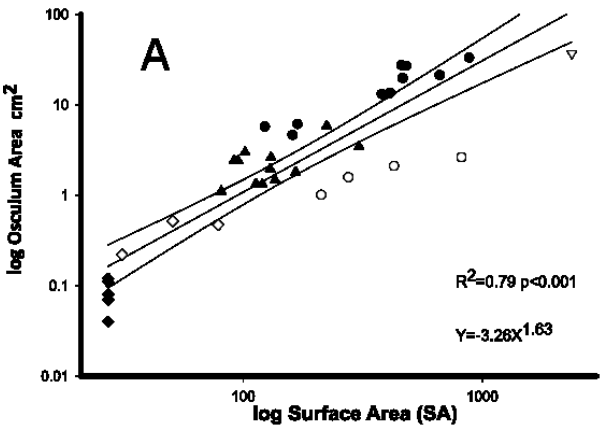
A
log Osculum Area cm2
log Surface Area (SA)
R2=0.79 p<0.001
Y=-3.26X1.63

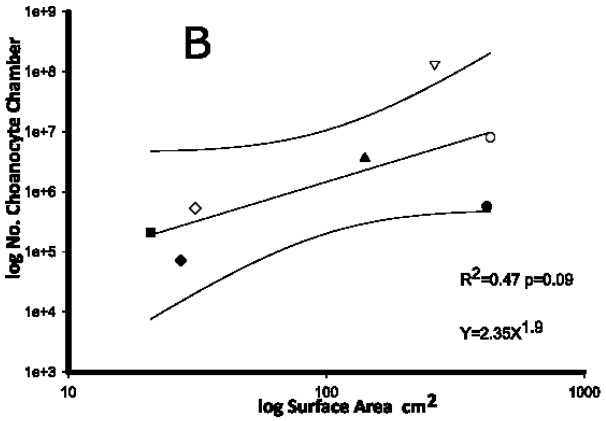
B
log No. Choanocyte Chamber
log Surface Area cm2
R2=0.47 p=0.09
Y=2.35X1.9

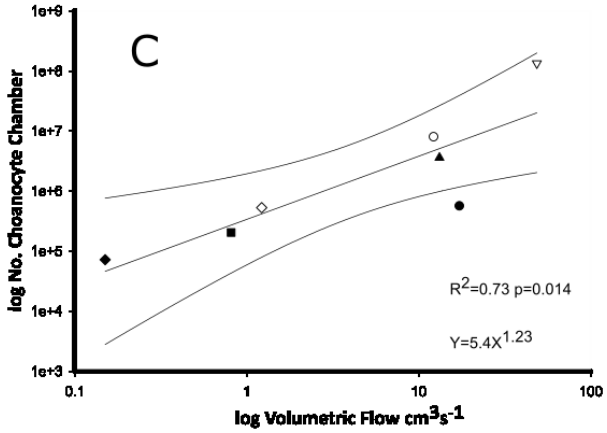
C
log No. Choanocyte Chamber
log Volumetric Flow cm3s-1
R2=0.73 p=0.014
Y=5.4X1.23

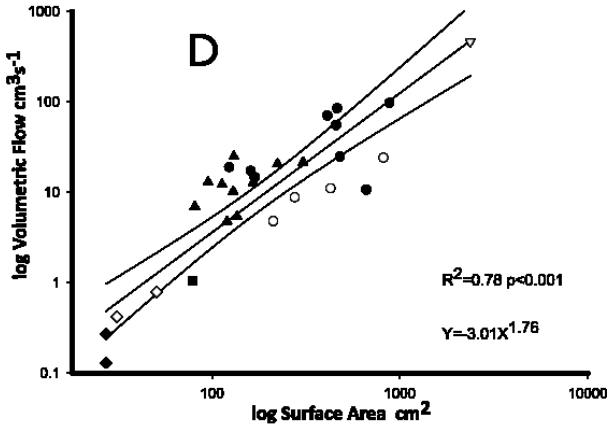
D
log Volumetric Flow cm3s-1
log Surface Area cm2
R2=0.78 p<0.001
Y=-3.01X1.76

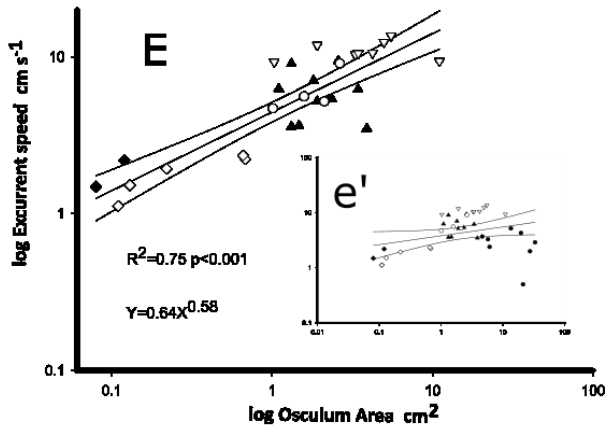
E
e'
log Excurrent speed cm s-1
log Osculum Area cm2
R2=0.75 p<0.001
Y=0.64X0.58

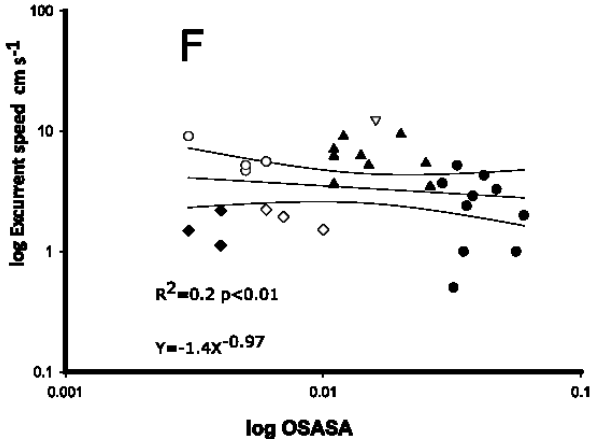
F
log Excurrent speed cm s-1
log OSASA
R2=0.2 p<0.01
Y=-1.4X-0.97

Figure 2.3. Ratio of the osculum area to surface area (OSA/SA) of fossil (*Diagoniella, Eiffelospongia, Hazelia, Vauxia, Pirania, Laocoetis, Stauractinella, Camerospongia, Thectardis*) and modern (*Haliclona*, *Neopetrosia*, *Callyspongia*, *Cliona*, *Tethya, Aphrocallistes*) genera. (A) Individual species/genera. (B) Genera grouped into higher taxa for modern and fossil genera. Modern sponges have a ratio of 0.01-0.02. Sources: Clapham et al., 2014; Ludeman et al., 2017; Frisone et al., 2016; Leys et al., 2011; ROM virtual Gallery URL https://burgess-shale.rom.on.ca and unpublished data.

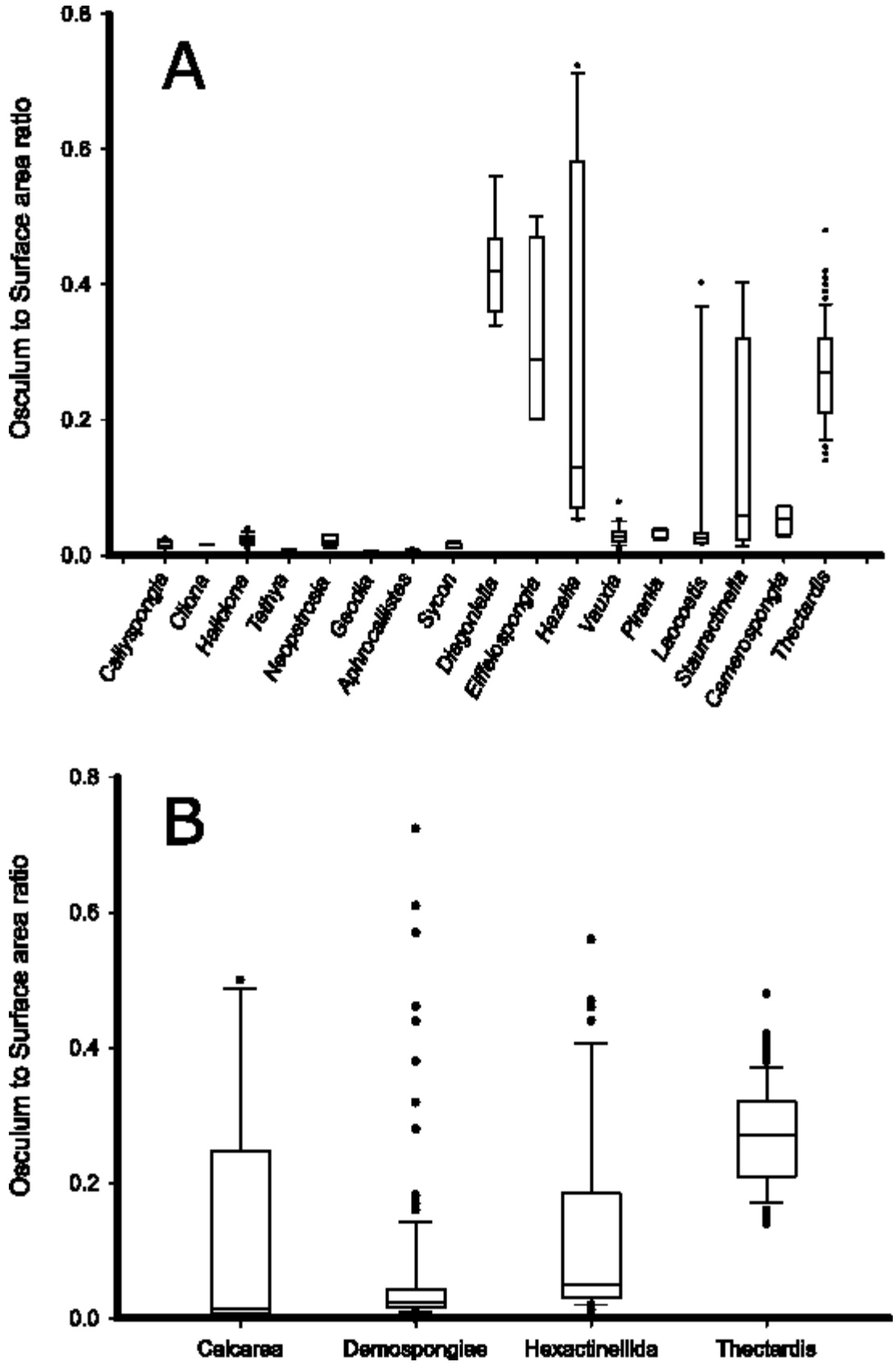
A
Osculum to Surface area ratio
0.0
0.2
0.4
0.6
0.8
Callyspongia
Clona
Haliclona
Tethya
Neopetrosia
Geodia
Aphrocallistes
Sycon
Diagoniella
Euplectellidae
Hazelia
Vazuta
Pirania
Lanceatis
Staurocalyptus
Cameronispongia
Thectarditis
B
Osculum to Surface area ratio
0.0
0.2
0.4
0.6
0.8
Calcarea
Demospongiae
Hexactinellida
Thectarditis

Table 2.3. Slopes of the correlation of osculum area vs surface area comparing modern and fossil forms. Note that slopes are plotted on log scale.

Grouping category	OSA to SA equation	R^2	p	slope	intercept	Slope 95% bootstrapped CI N=1999	Intercept 95% bootstrapped CI N=1999
Fossil Demospongiae	$Y=-1.58X^{1.3}$	0.5	0.0001	1.3	-1.58	1.12, 1.49	-1.74, -1.4
Modern Demospongiae	$Y=-1.56X^{0.88}$	0.9	2E-19	0.88	-1.56	0.82, 0.94	-1.77, -1.54
All Demospongiae	$Y=-1.56X^{1}$	0.7	0.0001	1	-1.567	0.89, 1.09	-1.66, -1.45
Fossil Hexactinellida	$Y=-0.7X^{0.7}$	0.6	2E-08	0.7	-0.7	0.55, 0.84	-0.89, -0.36
Modern Hexactinellida	$Y=-1.67X^{1.1}$	0.9	8E-05	1.1	-1.67	0.75, 1.27	-2.08, -0.79
All Hexactinellida	$Y=-0.7X^{0.7}$	0.7	2E-13	0.7	-0.7	0.59, 0.82	-0.91, -0.39
Fossil Calcarea	$Y=-1.3X^{0.6}$	0.01	0.8	0.6	-1.3	0.29, 2.4	-2.11, -0.74
Modern Calcarea	$Y=-2.1X^{1.8}$	0.99	0.006	1.8	-2.1	1.39, 2.22	-2.12, -1.97
All Calcarea	$Y=-1.6X^{0.8}$	0.01	0.76	0.8	-1.6	0.30869, 3.5242	-2.2873, -1.1095
Thectardis	$Y=-0.6X^{1}$	0.8	5E-52	1	-0.6	0.92, 1.06	-0.69, -0.45

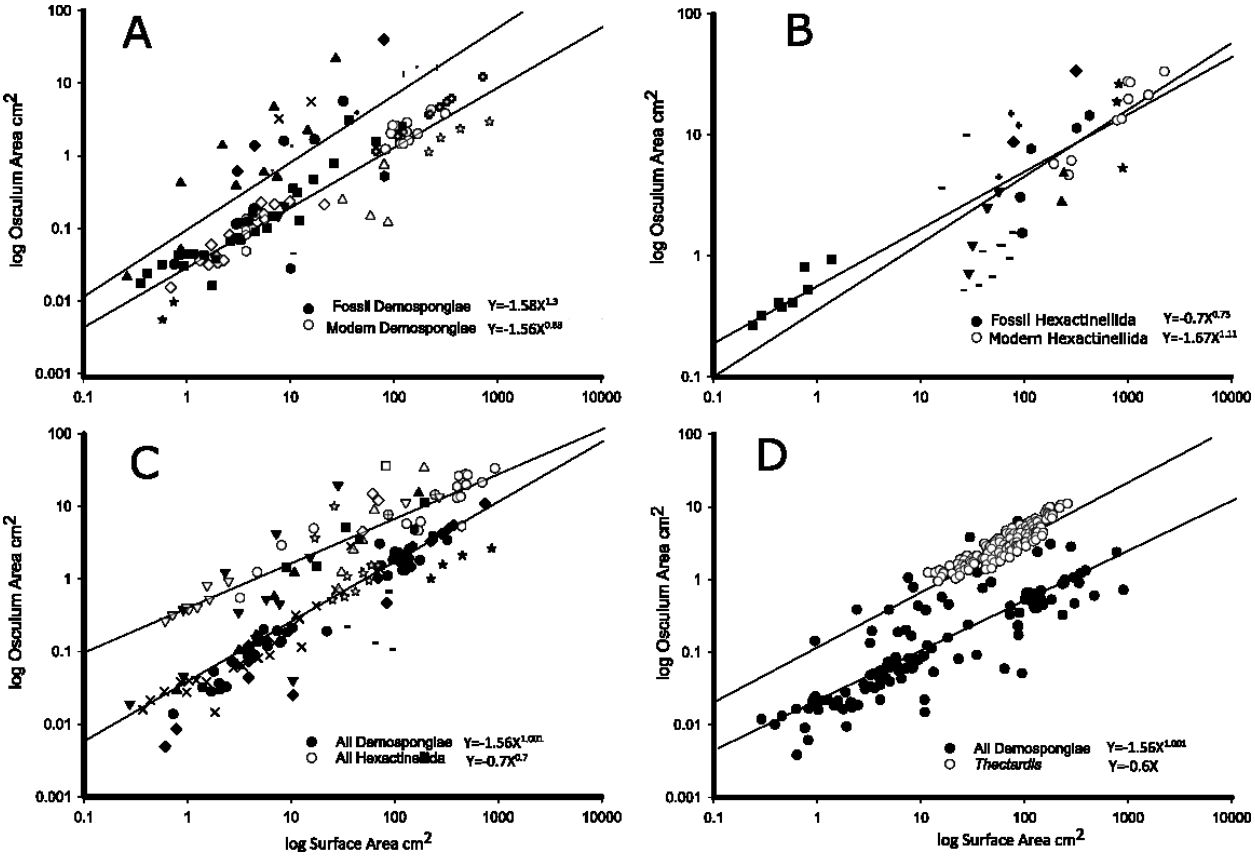

Figure 2.4. Scatter plots of osculum area vs surface area plotted on a log scale. A) Modern demosponges (Y=-1.7+0.9X R^2=0.9 p<0.05) vs fossil demosponges (Y=-1.4+1.3X R^2=0.5; p<0.05). B) Modern hexactinellids (Y=-1.6+1.1X R^2=0.9 p<0.05) vs fossil hexactinellids (Y=-0.7+0.7X R^2=0.7 p<0.05). C) All hexactinellids (Y=-0.7+0.7X R^2=0.7 p<0.05) vs all demosponges (Y=-1.6+1X R^2=0.7 p<0.05). D) All demosponges vs *Thectardis* (*Y=-0.6+1X* R^2=*0.8* p<0.05).

2.4. Discussion

The pump 'character' of extant sponges

A relationship between the total pumping activity of a sponge to the volume of a sponge has long been suggested (Reiswig 1971a, 1975a) indicating that sponges function as a volume-dependent pump. Recent work has confirmed this morphometric relationship showing that the ratio of osculum diameter to spongocoel base (McMurray et al. 2014) and to volume (Goldstein et al. 2019, Kealy et al. 2019, Morganti et al. 2019) are the major determinants of sponge pumping rate. After volume-scaling, smaller sponges tend to pump less water than bigger sponges (Morganti et al. 2019) and multi-oscular sponges pump as a population of single osculum ('module') sponge units (Kealy et al. 2019). Furthermore, scaling is such that the excurrent flow from a sponge can be determined by the area of the osculum (Bidder 1923, Morganti et al. 2021b), which allows these metrics to be effectively used to extrapolate sponge pumping rates *in situ* (Morganti et al. 2021b).

Our analyses take these findings one step further. We show that the 'sponge pump' (excurrent speed and flow rate) is directly proportional to the number of choanocyte chambers, and that the 'sponge pump' is also directly proportional to a ratio we call the OSA/SA, a proportion of the excurrent flow area (the area of the osculum) to incurrent filtration area (the sponge surface area). The available data therefore support the idea that the OSA/SA ratio reflects the number of pumping units in a sponge. We found that for a range of individuals of different sizes, the OSA/SA metric is characteristic for each sponge class, which suggests that each class has distinct pumping capabilities constrained by the structure of the aquiferous system. Finally, we illustrate that this metric is conserved in fossils of the same classes of sponges, and can separate out, by class, well-described fossils of sponges from a range of periods. Applying the same approach to fossils of putative sponges, could provide a powerful tool for classifying a fossil as a sponge or not, as we show using one test on the putative sponge fossil from the Ediacaran, *Thectardis avalonensis*.

The sponge pump and body wall thickness

The scaling of excurrent flow with osculum area is a wonderfully straightforward measure of the sponge pump, and it seems surprising that it should hold true across the vast

range of sponge morphologies and modes of feeding. For example, it might be thought that the excurrent flow would depend on wall thickness because a thick wall should provide more volume for choanocyte chambers. This was considered by Kealy et al. (2019) who pointed out that it has been shown that the pump unit is the individual choanocyte (Asadzadeh et al. 2019). Thick-walled sponges may have more chambers, but smaller chambers and so a similar number of pump units per volume (Ludeman et al. 2017). For example *Geodia barretti*, which is a very thick-walled High Microbial Abundance (HMA) sponge, has a lower chamber density due to the microbe-packed mesohyl and correspondingly filters less volume of water per unit time compared to an equivalent-shaped LMA sponge (Weisz et al. 2008). In general, HMA sponges tend to be thicker with a denser mesohyl, and a lower volume-specific pumping rate. We found that chamber density also did not vary significantly with surface area (Appendix 1 Supplementary Fig. 4). This latter outcome suggests that the sponge form is highly constrained and goes some way to explaining why the filter feeding body plan of sponges is apparently unchanged in so many millions of years.

The geometry of the sponge constrains the pump through the principle of continuity of flow (Vogel 1994). In particular, the constraint comes from the proportion of incurrent to excurrent area. The incurrent area is the combined area of the ostia. This metric is generally not accessible in fossils, but we can assume that it is directly proportional to the external surface area as seen in modern species. One caveat to these relationships is the necessary inadequacy of surface area calculations, as all measurements require assumptions and idealizations of sponge true shape. This bias might have a greater influence in some shapes over others, but for species that are closely conical, tubular or spherical, error can be largely ignored. Even though the best-preserved and complete specimens were included for this study, fossilization may also add error due to tectonic deformation, and specimens may have been preserved at different stages of decay. Nevertheless, despite these assumptions and uncertainties, the relationship of oscula area to surface area seems to hold across a great range of morphologies of extant and fossil genera.

The value of OSA/SA over volume as a metric for other sponge shapes and classes

Traditionally, morphological studies have used volume as a proxy for mass. Nevertheless, volume is a difficult metric to obtain even for modern specimens (Goldstein et al. 2019, McMurray et al. 2014, Strehlow et al. 2017), and if not measured directly, the analysis requires

assumptions about the density of the sponge tissue, which can vary significantly between low and high microbial abundance sponges (Ludeman et al. 2017, Reiswig 1971a, 1975b, Weisz et al. 2008). Because volume is length cubed, the error in volume is three times larger than the error that arises from measured length. On the other hand, a linear dimension such as length alone can overlook the scalar differences from two different shapes of the same length (Corruccini 1987, Junger et al. 1995). Surface area has the advantage of having the same units as osculum cross-sectional area, that results in a dimensionless ratio, the OSA/SA, that can be readily compared among fossil and modern individuals of all sizes and shapes.

However, even a simplified shape ratio like this has complications. The accurate calculation of surface area is not an easy task and it is particularly challenging in sponges with crenulations and those with serious deviations from ideal shapes, and yet with a big enough data set the approximations still converge on a class specific shared slope. While the OSA/SA ratio has a narrow range in a wide diversity of modern sponges, the range is large when fossils are included. Nevertheless, we found that the slope of this metric is distinctive for both demosponges and hexactinellids for which detailed morphometric data were available. The differences in slopes are not too surprising given the marked differences in morphology between the two sponge classes. The syncytial tissue of hexactinellids supports very large acellular flagellated chambers, and makes for a very open aquiferous system, often with very large oscula. In comparison, the cellular tissue of demosponges supports comparatively much smaller choanocyte chambers, narrower canals and a vast range of oscula morphologies.

It is noteworthy that for the few species of Calcarea we studied the slope of the OSA/SA was distinct from both demosponges and hexactinellids, despite being tubular (or conical) like hexactinellids. No homoscleromorph sponges were included in this analysis, but our finding that there is a class-specific slope predicts that the slope of the OSA/SA for Homoscleromorpha will be distinct from the other classes.

The sponge character in the fossil record

Sponges are one of the first animal groups to diverge from the metazoan lineage; however, their time of origin is not resolved, partly because of the lack of undisputed fossils at the time that molecular clocks estimate their origin (Feuda et al. 2017, Ryan et al. 2013, Whelan et al. 2015, Wörheide et al. 2012). Molecular clock estimates place the origin of animals at 800

Ma, and the oldest known sponge at 535 (Antcliffe et al. 2014, Schuster et al. 2018, Sperling and Stockey 2018). Because fossils are necessary to time-calibrate the molecular clock, it is important to have an accurate as possible interpretation of the fossil record. Also needed are methods to combine morphological and molecular data to integrate fossils into divergence time analysis (Peterson and Butterfield 2005). A handful of Precambrian fossils have been proposed as potential pre-metazoan, 'sponge-like' animal, which could close this gap (Brain et al. 2012, Clapham et al. 2004, Maloof et al. 2010, Yin et al. 2015).

Recent paleontological findings suggest the presence of early metazoans deep in the Ediacaran period. Both indirect evidence, such as interpreted bilaterian ichnofossils c.a. 555 Ma (Evans et al. 2020) and exceptional preservation of *Namacalathus hermanastes*, suggest a minimum date for the lophotrochozoan clade at c.a. 550 Ma (Shore et al. 2021). If these findings are corroborated with further observations, the lack of undisputable sponge fossils during this interval (800 – 555 Ma) is puzzling unless the environment was not conducive for preservation of soft tissue, and assuming that early sponges lacked a mineral skeleton (Antcliffe et al. 2014, but see Nadhira et al. 2019). On the other hand, molecular phylogenies suggest a deep Cryogenian divergence for crown group Porifera, implying that spiculate sponges should be present in the late Neoproterozoic (Cryogenian - Ediacaran), but so far none fits the criteria proposed by Antcliffe et al. (2014), who argue that the earliest sponge spicules do not appear until well into the Cambrian at 535 Ma.

The three criteria proposed by Antcliffe et al., (2014) refer to character, diagnosis and time constraints, i.e., the characters used should be useful to identify sponges, should be present in the fossil, and the age of the rocks should be well constrained. There are three body-fossil candidates of unknown affinity to which these criteria could be applied: 1) *Otavia antiqua* from the Otavi and Nama Group, with the oldest occurrence in the Okavuvu Formation in Namibia, is dated at 760 Ma (Brain et al. 2012); 2) *Eocyathispongia qiania* from the Doushantou Formation in central Guizhou, China dated at 600 Ma, is a single specimen folded within (Yin et al. 2015); and 3) *Thectardis avalonensis* from the Mistaken Point and Drook formations dated at 575 Ma, a cone-shaped organism with a putative opening at the top (Clapham et al. 2004).

Otavia is a 0.3 to 5 mm organism with openings of highly irregular morphology that are dispersed throughout the body. It has no clear anchoring point as would be expected for a sessile animal, and so its morphology most readily resembles a testate amoeba or even abiogenic

calciphosphate grains (Antcliffe et al. 2014, Porter and Knoll 2000). *Eocyathispongia* is even smaller than *Otavia* reaching only 1.2 mm across. It has been likened to a sponge because of inner cavities that open to a tube with an osculum-like aperture (Yin et al. 2015) yet the folded shape is unlike sponges, and although the cavities are proposed as chambers (Yin et al. 2015) the surface lacks any obvious openings that might be canals. Moreover, such 'honeycomb' structures have been reported in testate amoeba cast resulting from mineral precipitation (Porter and Knoll 2000). From the morphometrics standpoint, there is only one specimen, which makes any further analysis of dimensions impossible. In contrast, there are tens of specimens of *Thectardis avalonensis*, all of which are cones of different sizes. Sperling et al. (2011) use a length-to-width ratio assuming a conical shape to suggest *Thectardis* has Poriferan affinity, but others suggest *Thectardis* is instead a taphomorph of late decay stage of other Rangeomorphs such as *Charniodiscus* (Antcliffe et al. 2014), like the ivesheadiomorphs (Liu et al. 2011).

If *Thectardis* is a taphomorph, we would expect to find preservational stages from *Charniodiscus* to *Thectardis,* but there is no evidence of this taphonomical succession and more importantly, based in morphology, *Thectardis* is never associated with remnants of a holdfast that are typically the most decay-resistant element of the Rangeomorphs. In addition, *Thectardis* has sharp angles that are not consistent with the soft angles shown by *Charniodiscus* and no taphonomic process has been described that could potentially alter a specimen geometry in this way. A palaeoecological analysis to infer ecological interactions in sessile organisms, which can help distinguish taphomorphs from true taxa, showed that *Thectardis* was the only taxon lacking interspecific interactions or associations (Mitchell and Butterfield 2018). This lack of associations is not based on the low abundance of *Thectardis* relative to the Rangeomorphs, as similarly abundant Rangeomorphs were within the model (e.g., *Hiemalora* and *Bradgatia*). This ecological disparity is consistent with *Thectardis* having a substantially different feeding mode than the osmotrophic feeding typical of the Rangeomorphs.

One suggestion is that some Ediacaran fauna may have fed via symbioses using microbes associated with the surface sediments (McIlroy et al. 2021). While that is a valid option, *Thectardis* is also an ideal candidate to test the effectiveness of the OSA/SA as a metric of sponge pump character. The ratio of width to length of the conical organism means there would be a larger incurrent than excurrent area. The OSA/SA ratio for *Thectardis* was considerably higher (0.25) than that of modern demosponges (0.01), but it lay within the range of the

Cambrian demosponge genera *Hazelia* and *Hamptoniella* (0.1-0.6), and the calcarean *Eiffelospongia* (0.2-0.45). Also, the slope of the OSA/SA ratio of *Thectardis* specimens was not statistically different from the slope that for Demospongiae, which suggests that *Thectardis* could indeed have been a sponge, sharing the gross morphometrics and the pump character of demosponges. The minimum age for *Thectardis,* however, is 575 Ma, so although this could bring the fossil record and the molecular predictions a bit closer, a large fossil gap still remains to be explained. The OSA/SA is another line of evidence to discern the Poriferan affinity for putative fossils and to establish the basis for future palaeoecological reconstructions.

Implications of the sponge pump character for the evolution of sponges

The fact that a dimensionless ratio of very few morphological characters can predict sponge excurrent speed illustrates how tightly constrained the sponge body plan is. It is perhaps surprising that there is such a diversity of sponge types (Hooper and Van Soest 2002, Van Soest et al. 2012). Short of losing choanocyte chambers for carnivory (Vacelet and Boury-Esnault 1995), sponges are tied to a tight set of parameters to maintain the pump character. But having a dimensionless ratio that can predict the sponge pump is especially important when it comes to interpreting body fossils and their ecology. Our analysis of a small set of middle Cambrian and Eocene sponges shows that form is tightly correlated with the OSA/SA ratio over a range of sizes, and modern sponge data shows that osculum area is positively correlated with excurrent flow (McMurray et al. 2014, Morganti et al. 2019). This means that the dimensions of modern sponges are probably very similar to early Cambrian forms, and it implies that the OSA/SA ratio might also be used to estimate the excurrent velocity of known sponge fossils for which we only have osculum size and surface area. In addition, from excurrent velocity it might also be possible to estimate the effect of sponges on the water column in paleoecological contexts, and from that it could be possible to determine whether sponge fossils were HMA or LMA and in turn provide insight into the dissolved and particulate content of the oceans in which those sponges lived (de Goeij et al. 2009, de Goeij et al. 2008, de Goeij et al. 2013, Reiswig 1971b, Reiswig 1981, Weisz et al. 2008).

2.5. Conclusions

The correlations between morphology and pumping rates shown here confirm that the character that best represents a sponge is its total osculum cross sectional area (OSA) because it is

proportional to the total surface area of a sponge (Bidder 1923, Goldstein et al. 2019, Kealy et al. 2019, Morganti et al. 2021b). The total OSA scales allometrically with sponge size and its excurrent speed, and can be considered the main functional trait of a sponge. The ratio of the total OSA to total sponge surface area seems to be conserved across a wide range of sponges justifying its use as a morphometric character for most members of the Porifera. The ratio of osculum cross sectional area to sponge surface area varies very little in most sponges and it is suggested to be a good indicator of elements such as the number of choanocyte chambers and the pumping rate. This analysis suggests that if sponges are, and always were, pumps, then the first sponges should show this relationship of OSA to SA and a decreasing ratio as size scales up. In this light, the putative sponge fossil *Thectardis avalonensis* aligns well with the slope of modern demosponges, and its morphology is consistent with an aquiferous-system filter-feeding mechanism.

Chapter 3. Evidence of sense-induced flow in the deep-sea demosponge *Geodia barretti*

3.1 Introduction

The phylum Porifera is composed almost entirely of highly specialized, sedentary suspension feeders, able to filter up to 900 times their own volume per hour and extract up to 99% of the bacteria and dissolved organic carbon in the water column (Reiswig 1974, Yahel et al. 2003). Early workers established that the choanocytes, flagellated collar cells that are distributed throughout the sponge body, are the power source for the pump (Bowerbank 1864, Grant 1825), and consequently it has generally been considered that moving a lot of water each hour requires considerable energy expenditure (Ludeman et al. 2017, Riisgård and Larsen 1995). In addition, the arrangement of the choanocytes in chambers of a greater combined area than the surface area of the sponge, and the apical position of the osculum, is supposed to favor a higher excurrent speed and decrease the likelihood of recycling water (Bidder 1923). Vogel (1974) suggested that the sponge pump might be assisted by ambient currents due to the porous nature of sponge bodies. In several publications (Vogel 1977, 1978, Vogel and Bretz 1972), he stated that at least some sponges under certain circumstances could benefit from a velocity gradient, filtering more water at no extra metabolic cost. He referred to this phenomenon as "*current-induced flow"*, and over the years, it has become commonly accepted that sponges can use this passive mechanism to filter water and oxygenate their tissues (e.g., Kumala et al. 2017, McMurray et al. 2014, Savarese 1992, Schlappy et al. 2010). Indeed, the idea that sponges use induced-flow has been used indiscriminately to ascribe a wide range of fossils of otherwise unknown phylogenetic affiliation to sponges (Porifera) (Brain et al. 2012, Maloof et al. 2010, Sperling et al. 2011, Sperling et al. 2007, Yin et al. 2015). This is particularly important for Precambrian fossils, because affinities of early fossil assemblages can have a significant impact on our understanding of the history of animal life (Botting and Nettersheim 2018).

The relationship between fluid dynamics and sponge shape is not well understood, however. Savarese and colleagues (Savarese 1992, 1995) studied the hydrodynamic properties of shape-induced flow using models of sponges and archaeocyathids (arguably a sponge-like fossil taxon). They concluded that the sponge shape (tubular, with an apical opening) favored a velocity gradient, which together with continuity of flow (a smaller excurrent area relative to incurrent

area) made it possible for sponges to use induced flow. Even though these pioneering experiments with models were a good starting point for studying how fluids could move through tubular animals, they were inaccurate because important components of the system, namely the small internal canals and the nanometer-sized glycocalyx mesh filter on the sponge choanocyte through which water must pass, were ignored. These fine tissue structures have been shown to greatly contribute to the cost of pumping (Ludeman et al. 2017), and a growing body of evidence shows that the resistance offered by these structures is great enough in some sponge taxa to prevent water from moving passively. For example, Leys et al. (2011) found that the cost of filtration increased with the volume filtered and estimated that for sponges with large oscula like the deep-sea glass sponge *Aphrocallistes vastus,* which filters vast volumes of water hourly, filtration alone was 28% of the total *in situ* respiration (a proxy for metabolic cost). They concluded that this high cost makes it beneficial to use current-induced flow, but it could only happen in thin-walled sponges like the glass sponges, that live in constant and relatively high ambient currents. On the other hand, Ludeman et al. (2017) found that while cost was greater the more water filtered, one demosponge studied responded to increased ambient currents by decreasing the volume of water filtered; they determined that was a behavioral response resulting from closure of oscula and presumably other parts of the canal system. Therefore, the velocity gradient of the apically placed osculum seems unlikely to confer enough energy to overcome the resistance of the sponge filter.

Ambient currents clearly do have an effect on sponge internal and external morphology, because the same species can grow in different shapes that seem to correlate with flow regime (Palumbi 1984). Sponges in high-energy settings tend to have thicker skeletons (denser in spicules) than their low energy counterparts do (Dahihande and Thakur 2019). Nevertheless, the soft tissues of sponges are sensitive and able to respond to environmental stimuli, as any other animal can (Emson 1966, Kahn et al. 2020, Leys et al. 2019). Sponges have a range of behaviors with different cycles of contraction of the aquiferous system (canals) and osculum, and the whole body (Elliott and Leys 2007, Ellwanger et al. 2004, McNair 1923, Parker 1919, Reiswig 1971a, Weissenfels 1990), and can even orient themselves and move (very slowly) towards a location with better flow or food (Bond and Harris 1988, Kahn et al. 2020, Maldonado and Uriz 1999, Morganti et al. 2021a). Sponges therefore can adjust their canal dimensions and their excurrent flow rate to suit both their needs and the requirements of the environment.

Despite this growing understanding of the control that sponges have over their filtration, Vogel's induced current flow hypothesis still receives attention in particular with respect to paleontology of sponges (Maloof et al. 2010, Sperling et al. 2011), because it has been difficult to repeat his experiments with live sponges *in situ*. This is partly because experiments on live sponges are expensive and difficult to do under natural conditions (Leys et al. 2011) and lab or tank experiments have challenges both in terms of instruments that measure flow precisely and in generating laminar flow under different flow rates so that the sponge is considered to behave normally. The only previous work testing changes in ambient current on oxygenation of tissues in a controlled tank setting concluded that the sponges sensed and responded to changes in ambient current (e.g., Schlappy et al. 2010).

Here we set out to reproduce that work by testing the current-induced flow hypothesis using the deep-sea demosponge *Geodia barretti. Geodia barretti* has a high microbial abundance in its tissue (HMA sponge) in the range of 10^{10} microbes per cm^3 of tissue (Hoffmann et al. 2005, Hoffmann et al. 2009). Like other HMA sponges, *Geodia* has a lower oscular flow rate compared to LMA sponges (Weisz et al. 2008). Despite this, the dense populations in which they are found on North Atlantic and Norwegian continental shelves means that they collectively have a major ecological impact on the water column by removal of carbon in the form of pico-plankton (Kutti et al. 2013). In addition, like other HMA sponges *G. barretti* has a higher respiration rate per unit mass compared to LMA sponges (Kutti et al. 2015, Leys et al. 2018), because oxygenation is required for metabolic activity of the microbial symbionts. Generally, *Geodia barretti* has a closely spherical shape and has a thick cortex with a dense network of internal canals (the aquiferous system). This sponge has a large apical osculum and being spherical means its diameter provides a height gradient. All of these factors are thought to favor current-induced flow through the sponge (Vogel 1974).

We tested whether 'current-induced flow' – passively generated excurrent flow – reduces the cost of filtration in *G. barretti* by measuring oxygen removal (respiration) and excurrent flow (filtration) during different ambient current speeds in a large tank experiment. We predicted that if ambient currents cause a pressure differential enhancing the movement of water passively through the sponge, under higher ambient current speeds the oxygen removal should decrease while excurrent speeds should increase. We combined data on oxygen removed with

morphometric analysis of the sponge tissues to estimate the head loss and resistance of the aquiferous system and thereby determined the cost of filtration in this species.

3.2 Methods

Collection and maintenance of *Geodia barretti* was described previously (Leys et al. 2018). Briefly, individuals were collected using a remotely operated underwater vehicle (ROV) and transferred while submerged to a large seawater tank on the ship and from there to a 1000 L flow-through tanks at the Institute of Marine Research's deep-water aquaria facility in Austevoll, Norway. Unfiltered water from 160 m depths was supplied to the tanks at 2000 L h^{-1}. Of over 30 individuals collected, four individuals that were pumping continuously were selected for the flow experiments in tanks. These sponges were small enough to fit in the flow flume yet large enough to be within the reach of the flow and oxygen sensors. We assigned a two-letter code identifier to these individuals, and they had the following volumes and osculum areas. GQ, V=290 cm^3, OSA=1 cm^2; GN, V=430 cm^3, OSA= 1.6 cm^2; GT, V=2200 cm^3, OSA=2.6 cm^2; GU, V=830 cm^3, OSA= 2.1 cm^2 (See table 3.1 for dimensions). Plastic rings were used to hold all the individuals in place. Oscula of these four individuals were at the apical side and large enough to insert the flow and oxygen sensors. We carried out several replicate experiments on each individual and compared the trends using a means plot and a box plot to show the change in excurrent speed and oxygen concentration. To compare the relationship between the two, we performed an ANOVA on the filtration to respiration ratio on low, medium and high ambient flow.

Experiments were carried out in a flume 3 m long and 0.5 m diameter, that was suspended in a tank (4 m *l* x 1m *w* x 0.5 m *d*) supplied with flow-through water (Fig. 3.1 A). Ambient flow velocity was controlled by a propeller located at one end of the tube and water was passed through 20 cm long straws to become laminar. To assess whether the base of sponges was above the boundary layer, the boundary layer δ was calculated as

$$\delta = 5\sqrt{\frac{x\mu}{\rho U}}$$

where μ is dynamic viscosity of water at 20°C, ρ is the density of water at 20°C, U is stream velocity, and x is the distance from the origin of laminar flow to the sponge (Appendix 2).

Current free-stream velocity in the flume was measured upstream at the height of the osculum using a Vectrino Acoustic Doppler Velocimeter (ADV, Nortek, Norway) as well as custom designed thermistor flow probes (LaBarbera and Vogel, 1978), calibrated in the tank using the ADV. Excurrent flow from the sponge was measured using a calibrated thermistor flow probe which could be positioned directly into the osculum (Fig. 3.1 B,C). Ambient oxygen in the tank and oxygen in the excurrent water were measured using two channels of a 4 channel FireSting oxygen sensor (Pyroscience, Germany). Oxygen removed by the sponge (ΔO_2) was calculated by the difference in ambient oxygen (O_{2am}) and the oxygen concentration in the water expelled by the excurrent jet inside the osculum (O_{2ex}).

Sponges were transferred to the tank in a container of water so that they were not exposed to air, instruments were positioned over the osculum, and the animals were left undisturbed for 1-2 hours with the flume running at low speed. The experiment consisted in recording the sponge response to increasing and decreasing ambient flow in the tank. To determine whether changes in flow and oxygen could be caused by the turbulence around the osculum we carried out the same experiment on a glass soy sauce bottle (Kikkoman ®) with an opening roughly the same diameter as the sponges' osculum (2 cm).

The instrument data were recorded in voltage every second and binned in 10 s medians. Thermistor data were then converted to speed in cm s^{-1} using the equation $U = e(\frac{v-intercept}{slope})$ where U is speed, v is voltage and the slope and intercept are calculated from the correlation between the natural-logarithm-transformed speed given by the Vectrino ADV and the voltage recorded by the thermistor during calibration. Oxygen data were recorded in µMol L^{-1} by the FireSting software.

Morphometrics

Sponges were cut into 0.5 cm sized cubes and immersed in a fixative cocktail as described previously (Leys et al. 2018). After 10 minutes those pieces were further cut into pieces roughly 100 μm^3, added to fresh fixative and left at 4 °C for 6 hours. Sponge tissues were rinsed twice for 10 minutes each in distilled water, dehydrated to 70% ethanol and transported to the University of Alberta. Specimens were desilicified in 4% hydrofluoric acid in 70% ethanol for 1-3 days. Pieces were dehydrated further to 100% ethanol and, while in a vial of ethanol, immersed in liquid nitrogen to freeze the ethanol and fracture the tissue. Fragments generated in this way

were transferred in 100% ethanol to a Bal-Tec 030 critical point drier. After drying, samples were mounted on aluminum stubs using nail polish, coated with gold, and viewed in a Zeiss Sigma 300 Field Emission scanning electron microscope.

Head loss and cost of pumping calculations

Dimensions of different components of the aquiferous system were measured in Image J (Schindelin et al. 2012) and head loss calculated following Ludeman et al. (2017). Data were manipulated in MS Excel and graphs were plotted in Sigma Plot 14. Images were trimmed in Adobe Photoshop and figures assembled in Adobe Illustrator or Photoshop (CS 5).

In order to calculate the head loss, we estimated the flow speed through each region from the cross-sectional area of the given region using the formula:

$$U_i = \frac{U_o OSA}{A_i}$$

Where U_o is the excurrent speed at the osculum, OSA is the osculum area, A_i is the estimated total cross-sectional area of the given region, and U_i is the estimated speed at that region. The head loss of each region ΔH_i is calculated as follows:

$$\Delta H_i = \frac{32\mu L_i}{\rho g D_i^2} U_i$$

Where L is the length of the conduit, D is the diameter of the conduit g is the acceleration of gravity, ρ density of water and μ is the dynamic viscosity of water. The total head loss ΔH_t is then calculated as follows:

$$\Delta H_t = \frac{32\mu}{\rho g A_{in}} \left(\sum_i \frac{L_i}{D_i^2 (A_i / A_{in})} \right) Q$$

Where Q is volumetric flow rate. Finally, the cost of filtration (η) is seen as the power (*Pp)* needed to overcome the resistance to water flow through the canals $Pp = \rho g \Delta H_t Q$, and it is calculated using the following equation:

$$\eta = \frac{\rho g \Delta H_t Q}{\Delta O_2}$$

Where ΔO_2 is the oxygen removed by the sponge per volume per second, measured as the difference between ambient and excurrent oxygen concentration. We took the conversion of the oxygen used in watts of energy to be 1 µl O_2 h^{-1}=5.333 µW.

3.3 Results

Flume experiments

Geodia barretti reduced its flow rate in stagnant water and increased its excurrent flow when there was some ambient current. Although the flume held a considerable volume of water (approximately 4 m^3) and was continually replaced with fresh unfiltered seawater from depth (Figure 3.1), we discovered that sponges left in the flume with no additional flow from the propeller pump showed very low excurrent speeds. Conversely, we found that every sponge tested increased the excurrent speed with a slight increase in ambient current speed. However, at the highest ambient current speeds, sponges generally reduced their excurrent speed.

Due to the different sizes of individuals, their different resting excurrent speeds and oxygen removal, and variations in their responses to changes in ambient current speed, data from each experiment were analyzed separately. Despite the individual differences seen, when looking at the whole experiment flow record, each sponge showed the same pattern of excurrent speeds independent of ambient current speeds (Figure 3.2). Sponge GN showed a general decrease in excurrent speed regardless of increased ambient current speed (Figure 3.2 A). Sponge GQ showed an initial increase in excurrent speed with increased ambient current speed, and then excurrent speed decreased regardless of ambient flow, and sponge GT showed an increase in excurrent speed each time ambient current speed was decreased (Figure 3.2 B, C). One sponge, GU, kept at a very high ambient current speed, showed no change in excurrent speed over several hours (Figure 3.2 D), and as this experiment was not stepped like the others it was not used for further analysis.

Each sponge showed an increase in excurrent speed and oxygen removal with increasing ambient flow rates up to 10 cm s^{-1} (Figure 3.3). In addition, in each sponge oxygen removal increased and excurrent speed decreased at ambient current speeds greater than 10 cm s^{-1} (Figure 3.3). It is possible to see the relation of pumping (filtration) to oxygen removal (respiration) directly using the filtration to respiration (FR) ratio, which indicates the volume of water that was filtered per unit of oxygen removed. The FR ratio ranged from 0.2 to 1.5 for the four sponges. For all sponges the FR ratio was not significantly different between low and high ambient current ($p>0.05$) (Figure 3.4).

A control experiment, using a glass bottle with similar sized opening to the sponges, illustrated turbulence in the bottle. The experiment showed a) the same changes in velocity when

the probe was held in the opening (the 'excurrent' probe) as the ambient flow probe, and b) no change in oxygen concentration between ambient and excurrent probes over the duration of the experiment (Figure S3 in Appendix 2). This experiment confirms that any change in the FR ratio is directly caused by the sponge metabolism and is not an artifact of the oxygen sensors being exposed to higher flow. It also shows that turbulence can artificially increase the readings of the excurrent flow rate, even in a laminar flow regime in a flume.

Morphometrics & Head Loss

The dimensions of passages through the aquiferous system of *Geodia barretti* are shown in Table 3.1 and Figure 3.5. The path of water is as follows: it first enters the ostia, and from there travels through collector canals to a large canal that underlies the cortex, which we refer to here as the subdermal space. From there water passes into large incurrent canals leading to the choanocyte chambers where there is a sudden increase in cross-sectional area with respect to the canals, which slows the flow down, then the flow continues to the excurrent canals and out of the osculum.

The estimated speed through the collar slit was 0.046 mm s^{-1} (Table 3.2) and this region of the aquiferous system presented the highest head loss (5.35 mm H_2O). The head loss is a consequence of the very movement of water creating resistance to flow due to friction in each region, and it is directly proportional to the amount of water and inversely proportional to the dimensions of the canal or structure. The sum of head loss through the whole aquiferous system is estimated to be 15.85 mm H_2O (Table 3.2 and Figure 3.6). The cost of filtration (η) is estimated to be 0.4 W Hr^{-1} equivalent to 2.47% of total metabolism, using the model of Leys et al. (2011) based on the Hagen–Poiseuille equation assuming laminar flow.

Table 3-1. Dimensions, oxygen removed, volumetric flow rate and ratios of 4 individuals of *Geodia barretti*

	Individual of *Geodia barretti*			
	GQ	GN	GT	GU
Osculum area, OSA (cm^2)	1.01	1.6	2.6	2.1
Total sponge surface area, SA (cm^2)	212	275.5	818	427.1
Total sponge tissue volume (cm^3)	290	430	2200	830
Median oscula flow rate, Q ($cm^3\ s^{-1}$)	4.8	7.3	20.1	8.8
Median oxygen removed ($\mu Mol\ L^{-1}\ s^{-1}$)	13.4	16.5	19.6	24.7
Volume-specific oscula flow ($cm^3\ s^{-1}\ cm^{-3}$ sponge)	0.023	0.024	0.014	0.012
Volume-specific oxygen removed ($\mu Mol\ L^{-1}\ s^{-1}\ cm^{-3}$ sponge)	0.051	0.04	0.013	0.034
OSA/SA ratio	0.0053	0.0062	0.0031	0.0053

Table 3-2. Dimensions and flow speed through the elements of the aquiferous system of *Geodia barretti*

	Geodia barretti			
Element of the aquiferous canal system	Diameter (μm)	Path length (μm)	Speed (mm s^{-1})	Head loss (mm H_2O)
Ostia	29.8	10.7	3.70	0.20
Subdermal space	71.80	418.2	1.80	0.64
Large incurrent canal	178.93	179	0.23	0.01
Medium incurrent canal	81.73	23953	0.42	6.65
Small incurrent canal	29.58	29.6	0.67	0.10
Prosopyles	8.188	2	0.27	0.04
Pre-collar space	0.040	0.01	0.05	1.26
Collar slit	**0.063**	**0.10**	**0.05**	**5.35**
Post-collar space	0.040	0.01	0.05	1.26
Chamber	2	0.2	0.14	0.02
Apopyle	8	2	0.30	0.04
Small excurrent canal	50.47	418.2	0.33	0.24
Medium excurrent canal	3041.13	39806.3	0.75	0.01
Large excurrent canal	328.97	468	1.83	0.03
Osculum	12610	2062	46.30	0.003
Head loss, H (mm H2O)	15.85			
Pumping Power, Pp (μW)	779			
Cost of pumping, η (%)	2.47%			

Figure 3.1. Flow tank set up. A) The outer tank into which fresh flow-through seawater is piped from the right. B) Inside the flume tube showing the recording of ambient current by a Vectrino ADV (left) while the thermistor flow sensor and oxygen probe record the excurrent speed and oxygen removed by the sponge. C) The thermistor and bare fiber FireSting oxygen sensor (red dot) recording excurrent speed and oxygen.

Figure 3.2. **Excurrent speed in relation to changes in ambient current velocity.** Recordings showing excurrent speed (black solid lines) and oxygen removed (ΔO_2, green dashed lines) by individual *Geodia barretti* at varying ambient current speed (red dashed lines). Each letter code represents a different individual sponge, A) GQ, B) GN, C) GT, D) GU. Time is given on the x axis, and flow speed on the y axis. Steps of the increasing and decreasing ambient current velocity are indicated with black bars, with the average speed for each shown above each bar.

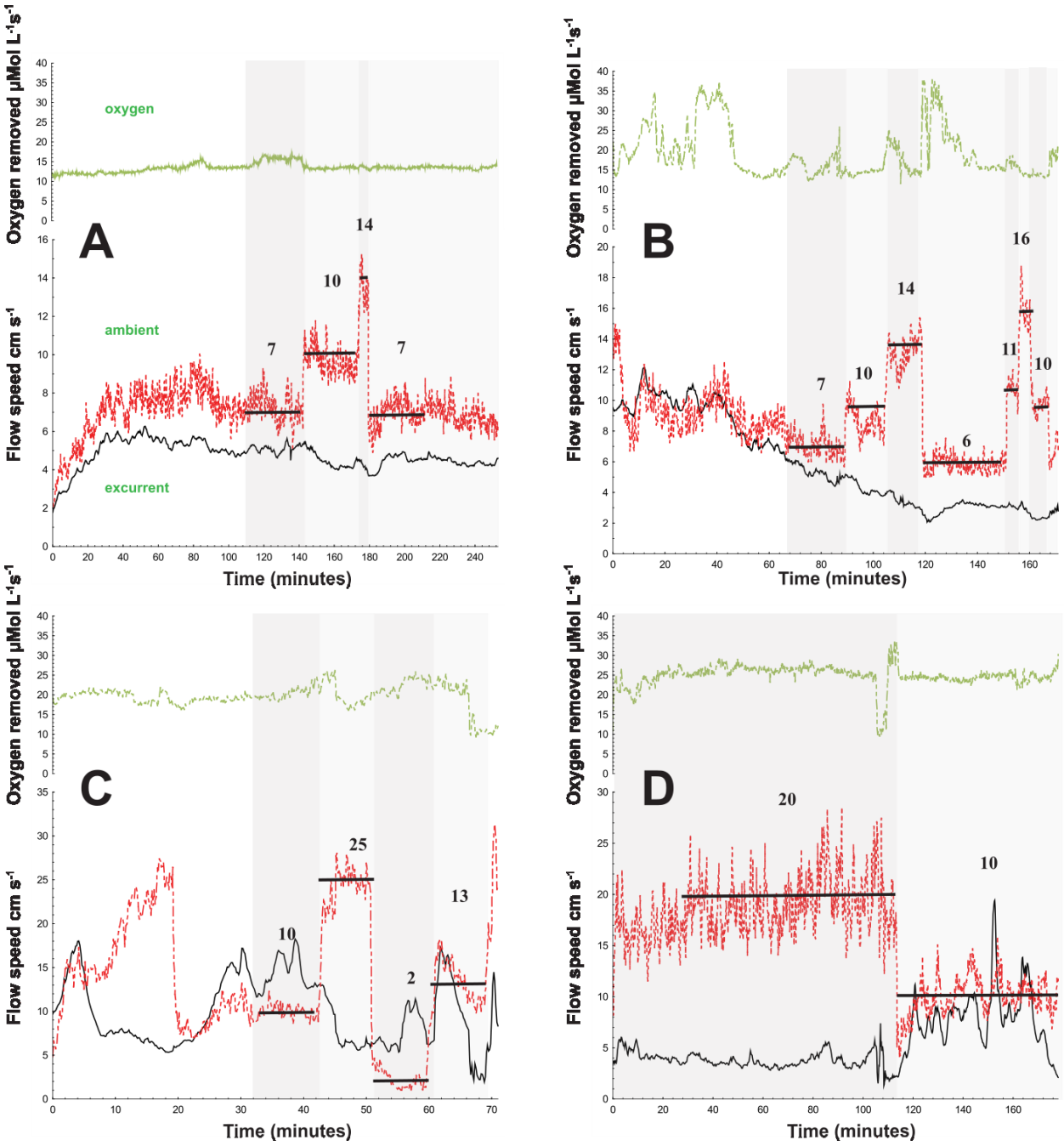
A
oxygen
ambient
excurrent
Oxygen removed µMol L-1s-1
Flow speed cm s-1
Time (minutes)
7
10
14
7
B
7
10
14
6
11
16
10
C
10
25
2
13
D
20
10

Figure 3.3. Effect of ambient flow velocity on excurrent flow speed and oxygen removed by *Geodia barretti.* Record of ambient flow speed (cm s^{-1}, dashed red line), excurrent flow speed (cm s^{-1}, solid black line) and oxygen removed (µmol $L^{-1}s^{-1}$, dashed green line). Data were binned by ambient current speed (cm s^{-1}) for each sponge (GQ, GN, GT, and GU). All three records showed an increase in excurrent speed at low ambient currents (less than 10 cm s^{-1}) and a reduced excurrent speed at higher ambient currents.

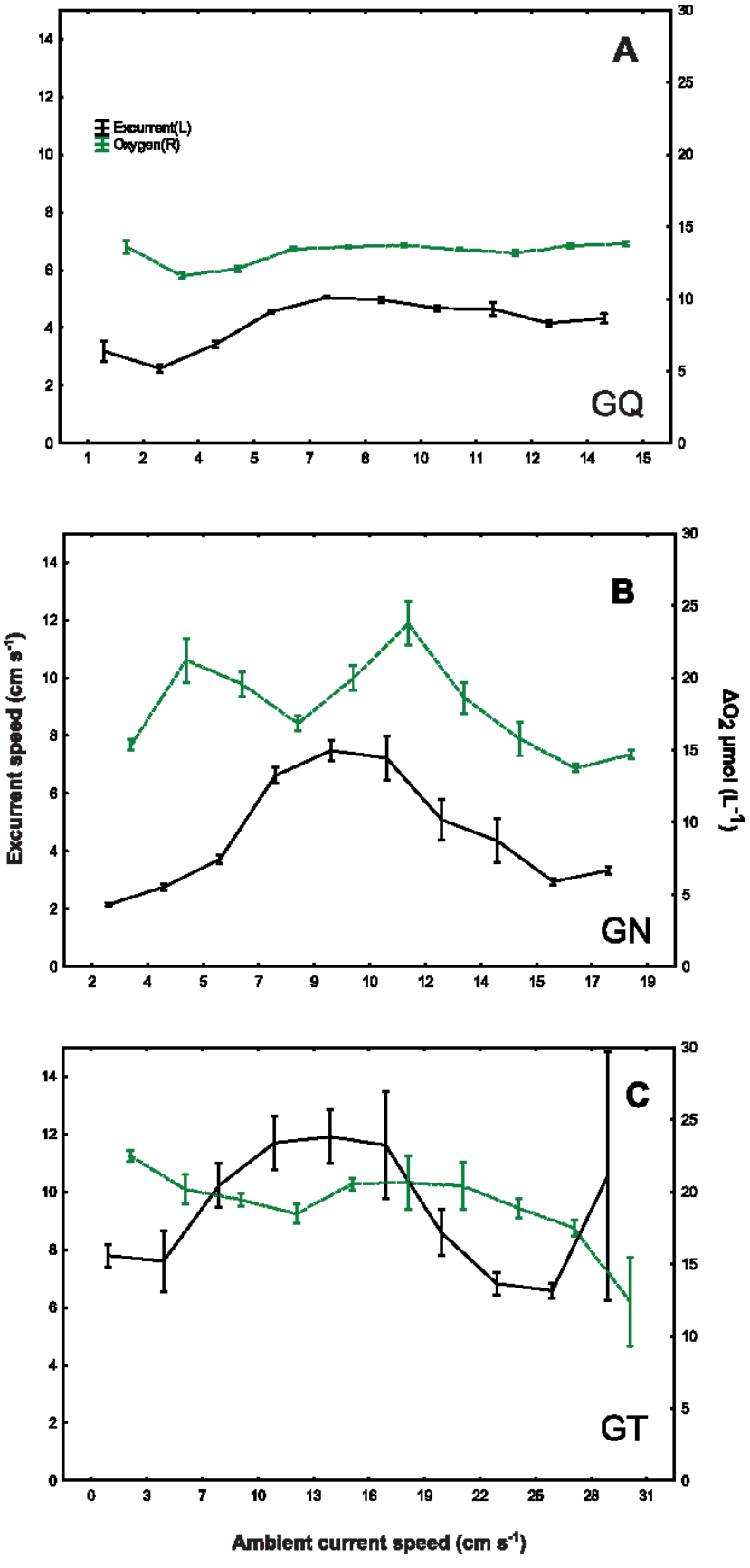
A
Excurrent(L)
Oxygen(R)
GQ
B
GN
C
GT
Excurrent speed (cm s-1)
ΔO2 µmol (L-1)
Ambient current speed (cm s-1)

Figure 3.4. Effect of ambient velocity on excurrent speed (cm s^{-1}) in black and oxygen removed (µmol $L^{-1}s^{-1}$) in green (shaded) by *Geodia barretti*. Data were binned by ambient current speed (cm s^{-1}) for each sponge (A, GQ; B, GN; C, GT). Box plots show median (bar), standard deviation (error bars) and outliers (circles). All three records showed a slight increase in excurrent speed at low ambient currents (<10 cm s^{-1}) and a reduced excurrent speed at higher ambient currents.

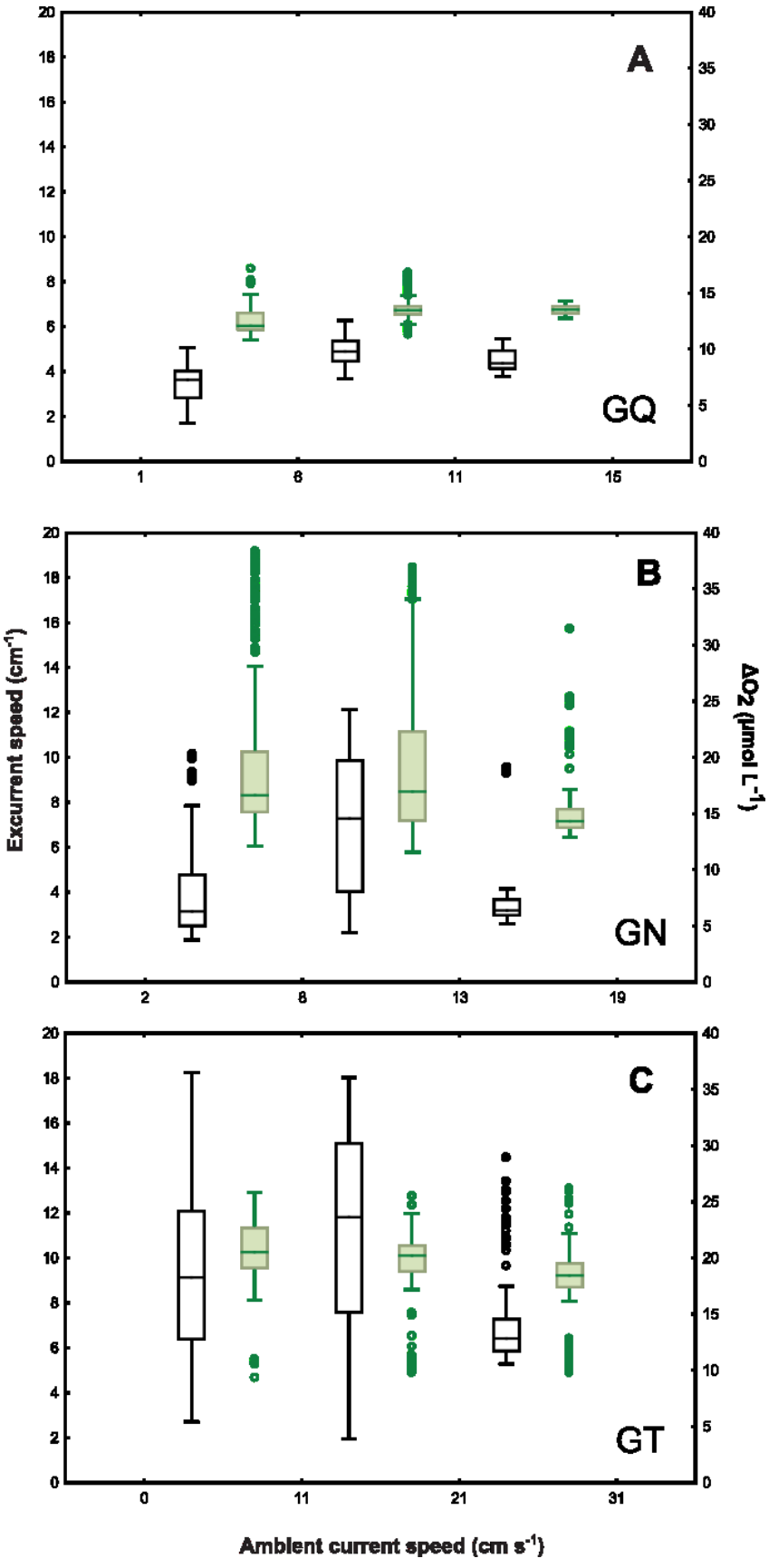
A
GQ
B
GN
C
GT
Excurrent speed (cm-1)
ΔO2 (µmol L-1)
Ambient current speed (cm s-1)

Figure 3.5. Filtration-to-respiration ratio of three individuals of *Geodia barretti.* A-B) GQ and GN experienced lower ambient speeds (<20 cm s^{-1}) and C) GT the highest (<31 cm s^{-1}). Box plots show median (bar), standard deviation (error bars) and outliers (circles). There is an increase in amount of water filtered per oxygen consumed at ambient current speeds lower than 10 cm s^{-1} but not at higher ambient current speeds.

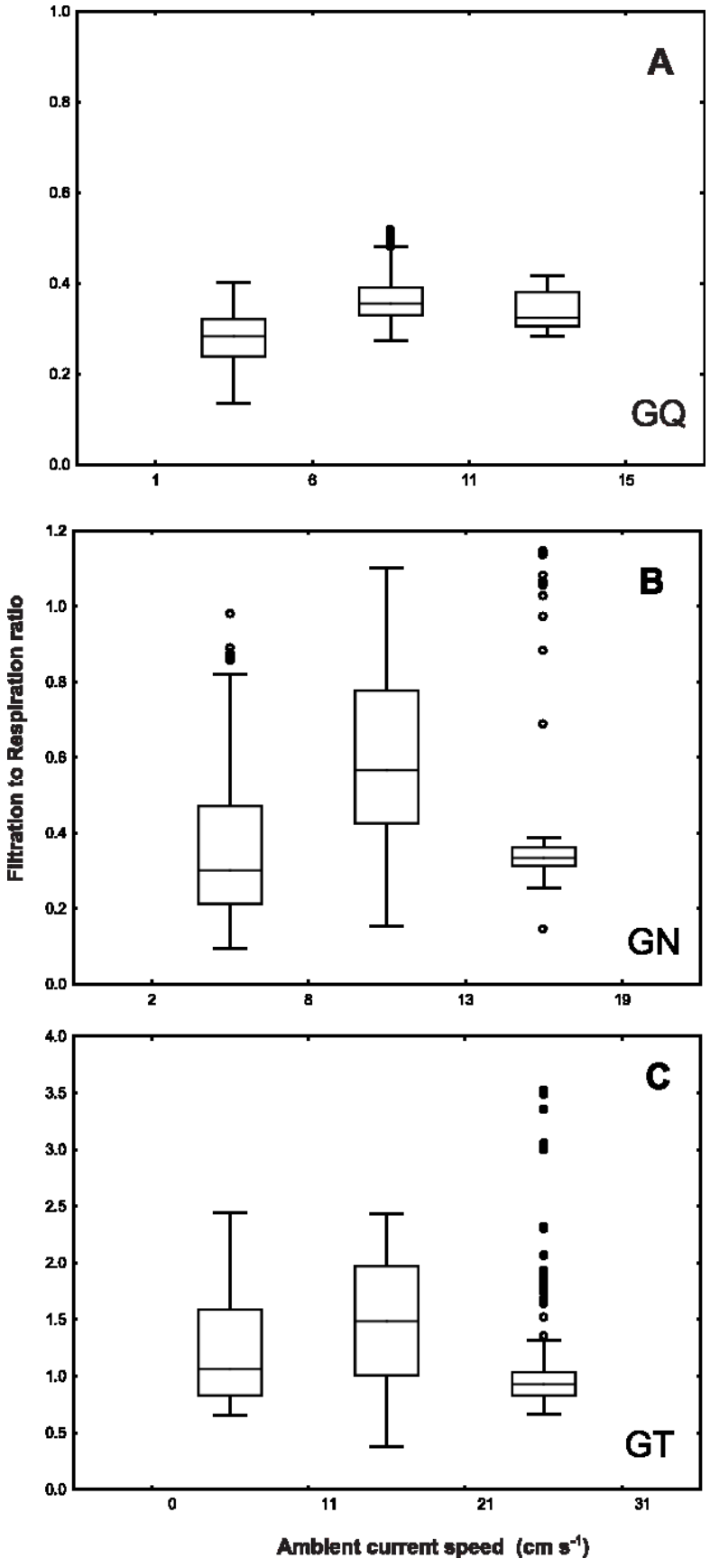
A
GQ
B
GN
C
GT
Filtration to Respiration ratio
Ambient current speed (cm s-1)

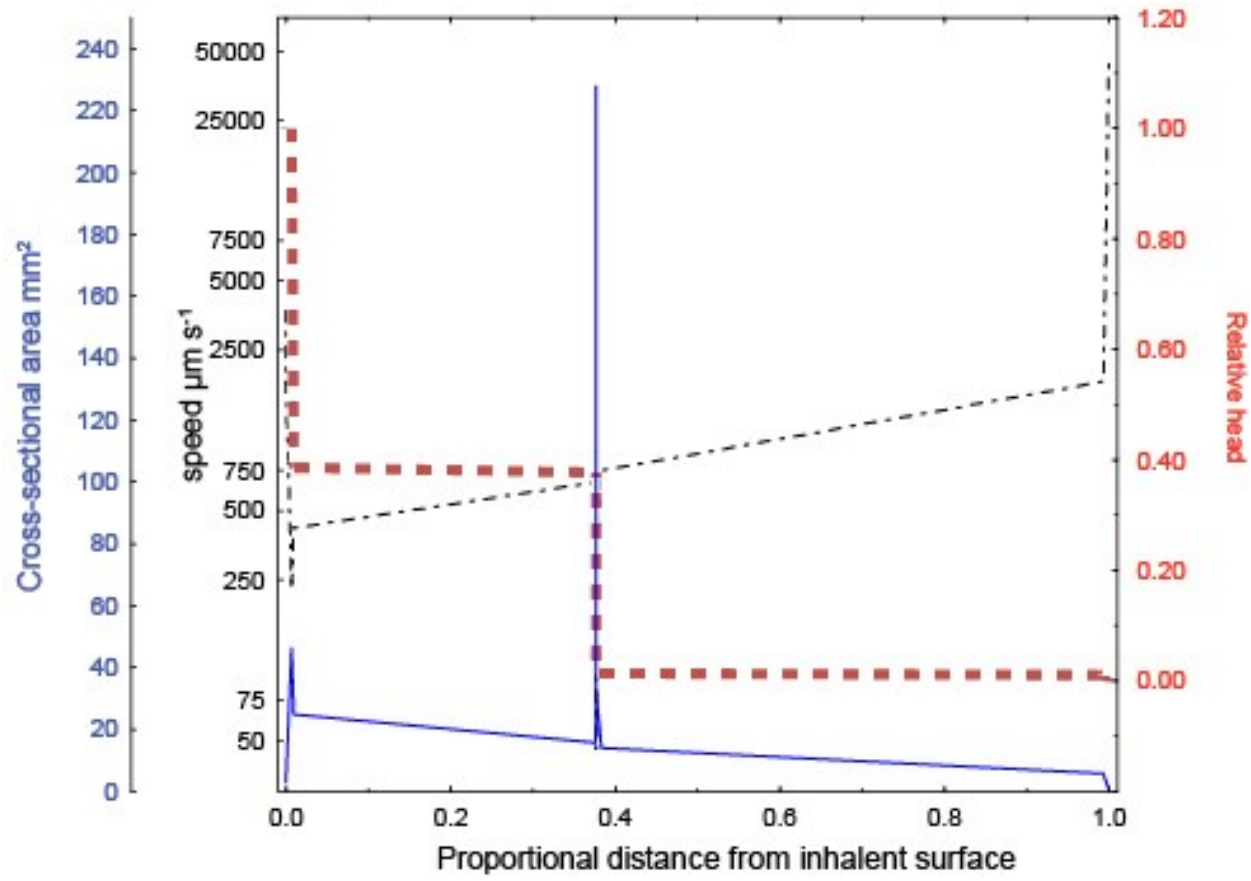

Figure 3.6. Total cross-sectional area, current speed and head loss at each point along the path through the aquiferous system of *Geodia barretti*. This graph shows the change in flow speed through the aquiferous system, with a pronounced change at the choanocyte chambers, where there is a drop in the relative head corresponding to the glycocalyx mesh on the collar, and an increased speed at the osculum. This diagrammatic representation of the water canal system plots the log scale of the cross-sectional area of each region, modelled as a tube, against the proportional distance from inhalant surface.

3.4 Discussion

In this chapter we tested the hypothesis that ambient currents can induce excurrent flow in the deep-sea high-microbial-abundance (HMA) demosponge *Geodia barretti.* This hypothesis aims to explain the mechanism by which sponges could filter water without expending energy from active pumping of the choanocytes (or by reduced pumping) and has been tested in the past with mixed results (Kumala et al. 2017, Leys et al. 2011, Ludeman et al. 2017, McMurray et al. 2014, Savarese 1992, Schlappy et al. 2010). Our results with *G. barretti* suggest that – for three individuals studied here – the sponge does filter more water at no greater oxygen cost when ambient speeds are ~8-10 cm s^{-1} than at lower ambient speeds. However, as ambient current rises above 10 cm s^{-1} the sponge reduces its excurrent flow. Together with the findings of previous workers, our study indicates that current-induced flow in the sense described by Vogel (1974) may occur, but only at lower ambient currents. The mechanism by which this happens is still unclear, but because the sponge does not use more oxygen to increase its excurrent output it is likely that it decreases the resistance through the canal system. This, as with the response of decreased excurrent flow at higher ambient currents, suggests a behavioural response by the sponge.

Morphometrics of the aquiferous system and cost of filtration

To assess the hypothesis of induced flow, it is relevant to understand the morphometrics of the aquiferous system in order to estimate the resistance through the sponge's canal system and filter. Vogel's (1974) and Savarese's (1992, 1995) studies were heavily focused on the gross morphology of the sponge as an explanation of the pump by invoking several fluid dynamic mechanisms, such as viscous entrainment and Bernoulli's principle. Vogel (1974) recorded the excurrent flow out of an actively pumping *Halicondria bowerbanki* and compared it both to a freshly killed or inactivated individual and to an artificial plexiglass and brass models. He did find a correlation of ambient and excurrent flow, but no proxy for metabolic expenditure was provided. A measure of metabolic expenditure is needed to test the induced flow hypothesis, in order to discern if the increase in excurrent flow is due to the sponge pumping more or due to the sponge shape extracting work form the velocity and pressure gradients and viscous entrainment

through the canals. Savarese (1992, 1995) also tested brass models, but of archaeocyathids, and found that the diameter of the internal cavity is the main factor determining the ability of the model to generate excurrent flow. This internal cavity of the archaeocyathids could be considered as an analog for the osculum and atrium of sponges, which is well correlated with excurrent flow in modern sponges (see chapter 2). The phylogenetic affiliation of archaeocyathids is controversial, but Savarese (1992, 1995) and Balsam, and Vogel (1973) showed that it is at least theoretically possible for the archaeocyathids' skeleton to function as a filter feeder, even if they are not related to sponges.

These works were excellent starting points, but the next problem is that there is no information on the non-skeletal tissue structure of archaeocyathids. We do have this information about modern sponges but the aquiferous system is so intricate that it is virtually impossible to replicate either in the lab or in silico. However, besides the external morphology, Leys et al. (2011) suggested that the ability of a sponge to make use of the induced-flow mechanism would strongly depend on the very nature of its aquiferous system, because the dimensions of not only the canals but the substructures of the filter can impose great resistance to the flow.

Early models estimated a low cost of filtration for filter feeders, at 4% of total metabolism (Riisgård and Larsen 1995). The hypothesis was that most filter –suspension-feeders evolved a system for continuous feeding at low metabolic cost (Jørgensen 1975). However, a variation in the rate of feeding corresponding to that of food availability has been observed in both bivalves and sponges (Griffiths and King 1979, Reiswig 1971b). Additionally, direct oxygen uptake measurements from the demosponge *Negombata magnifica* found that 25% of total respiration is allocated to filtration (Hadas et al. 2008). These observations suggest that the cost of pumping might be higher than previous estimations, are unlikely to be universal; and indeed the models are highly sensitive to filter mesh size. Using updated measurements from well-preserved scanning electron micrographs and direct volume flow rate measurements Ludeman et al. (2017) found that estimated cost increases up to five times for several sponges, bivalves, polychaetes and ascidians.

We found that for *Geodia barretti* the estimated velocity through the collar slit was 0.046 mm s^{-1}, around 2.5 times higher than reported for the tropical demosponges *Callyspongia* and *Cliona* at 0.018 and 0.017 respectively (Ludeman et al. 2017), and this region of the aquiferous system also had a higher head loss (5.35 mm H_2O). However, the cost of pumping not only

depends on the velocity at which the water is pumped but the volume of water that is pumped per unit time i.e., volume flow (oscula flow) rate. This explains the ample difference in cost, η=2.47% for *Geodia barretti*, and η=12% for *Cliona delitrix* because *C. delitrix* filters 2668 mL min^{-1}, which is vastly more than *G. barretti*, despite having a similar total head loss (11-16 mm H_2O).

The low metabolic cost of *Geodia* is comparable to other low pumping demosponges e.g., *Haliclona*, *Neopetrosia* and *Tethya*. However, *G. barretti* filters up to 3 times more, at around 300 mL min^{-1}, which is in the same order of magnitude as *Callyspongia* (742 mL min^{-1}) but in *Callyspongia* the cost of pumping is estimated to be around η=5.38%. Therefore, both sponges, *G. barretti* and *C. vaginalis* filter a similar amount of water per unit time but with a difference in metabolic cost. In terms of watts, it cost 0.014W to filter 742 mL min^{-1} for *C. vaginalis*; and it cost almost double, 0.03W to filter 300 mL min^{-1} for *G. barretti*. This difference can be explained by the much higher total head loss through the aquiferous system of *Geodia*, 16 mm H_2O compared to 6 mm H_2O of *Callyspongia*. This result is remarkable, because it suggests that the cost of pumping is affected by the total head loss more than the volume of water filtered and support the hypothesis that the sponge control its flow through the change in canal diameter (thus changing the total head loss) rather than stopping and starting the choanocyte beats.

Morganti et al. (2019) found that bigger sponges pump proportionally less water per unit tissue than smaller sponges, therefore suggesting that size is the major determinant of the volume-specific pumping rate (oscula flow rate normalized for sponge body volume); one implication of this finding is that the density of choanocyte chambers decrease with size. In addition, Morganti et al. (2021b) found that the sponge pump is a function of the oscula size, supporting the argument that body size, oscula size and the proportion between the two intrinsically determine the sponge pump. On the other hand, Asadzadeh et al. (2019) tested the long-standing hypothesis that the choanocyte chamber is the pump unit, showing that the pump unit that overcomes the pressure (head) loss is the choanocyte per se rather than the choanocyte chamber. This is because there are high and low pressure sections in the choanocyte collar effectively separated by the glycocalyx mesh, impeding a synchronous beating of the flagella. Overall, size determines the sponge pump, which in turn determines the pump unit density (total number of choanocytes per unit tissue). Comparing these with the results with *Geodia* and comparison with other demosponges, we argue that size, volume filtered, and canal dimensions

would be the major determinants of cost of pumping, independently of any induced flow mechanism.

Pumping and feeding

The experiment was focused solely on the response, in terms of oscula flow and oxygen uptake, of *Geodia barretti* to increased ambient flow. We did not consider how changes in food concentration affect filtration rates, and the food concentration was considered to remain constant during the experiment. However, if the food concentration is constant, more water filtered also means more carbon intake. Even though the metabolic cost is low for *Geodia* compared to other demosponges, the three individuals showed an increase in the filtration to respiration ratio from low to medium ambient flow. From this increase in volume flow filtered, we estimate that there is a 70% increase in the carbon filtered by the sponge in the medium flow compare to the low flow, which is a substantial gain. As a HMA sponge, *Geodia barretti* removes 99% of the bacteria in the water, but most of its carbon budget is from symbionts (Leys et al. 2018). It has been showed that the volume specific pumping rate of LMA sponges tends to be lower than HMA sponges (Weisz et al. 2008). This lower filtration rate might allow more time for O_2 to reside in tissues to be used by microbes.

Behavioral response of Geodia *to increased ambient current*.

The experiment we carried out consisted of increasing the ambient flow speed from zero to 20 cm s^{-1} in a flow-through flume. A flow-through setting is important when experimenting with living animals as their own waste can accumulate and be detrimental to their performance. Laminar flow is also a prerequisite for this type of experiment as it ensures a velocity gradient between the bottom of the sponge and the apically located osculum. The analysis of the boundary layer in this flow flume showed that the oscula of all 4 sponges were in freestream flow and the base of the sponges were in the boundary layer. The thickness of the boundary layer decreased from 9 cm at the lowest ambient flow to 2 cm when ambient currents reached 20 cm s^{-1} providing a velocity gradient from the base of the sponge to the osculum for all sponges throughout the experiment. It is important to note that any obstacle in the path of laminar flow

can disturb the boundary layer, and therefore it is not clear that sponges in nature can rely on this gradient all the time especially when growing in large population densities.

We had four replicates using different individuals and there was considerable individual variation in excurrent speed and oxygen consumed. Because of this variability, it was not possible to average the data from all individuals and we were forced to analyze each replicate independently. However, we did see some trends among the individuals. For instance, the sponges responded to an ambient current increase up to 10 cm s^{-1} by increasing their excurrent speed. GQ had a steady oxygen record throughout the experiment and the ambient current velocity was not greater than 15 cm s^{-1}. At very low ambient current speeds, this sponge increased excurrent speed and oxygen removal did not increase (Figure 3.3). The filtration to respiration ratio at low ambient flow is slightly lower than at medium and high ambient flow, in the order of 0.1 to 0.4 ml s^{-1} per unit of oxygen in low flow (<10 cm s) (Figure 3.4). In general, *G. barretti,* appears to respond to some ambient flow by increasing its excurrent flow rates, but reduces excurrent flow rates at greater ambient current speeds. Although sponges generally do perform better in low ambient currents compared to still water, there is an optimal ambient current speed for their filtration. Overall, sponges do not always respond to an increase in ambient flow by pumping more but will instead sense the flow around them and increase or reduce pumping. The reduction in pumping at higher ambient current speeds suggests sponges may prevent drawing in disturbed or turbulent water that could potentially damage the filter or bring excess of sediment that could damage the filter.

The mechanism of sensation in sponges is only beginning to be understood and the cilia in the osculum likely play a huge role in this response (Ludeman et al. 2014). Exactly how the sponge controls the excurrent flow rates is not understood. It is anticipated that control takes place throughout the aquiferous system by constricting and relaxing openings and canals rather than changing the speed of the flagella pumps, as described in early experiments by Parker (1910), and future studies should focus on this aspect.

Chapter 4. General Discussion

4.1. Overview

In this thesis I explored two main avenues under the framework of the timing of early animal evolution. I first described a way to quantify the sponge filtration or pumping 'character', which I term simply the 'sponge character', from gross morphology, which allows comparison of extant sponges with many fossil forms; and second, I addressed the question of whether sponges make use of induce flow, an often-made assumption when interpreting fossils as sponges. Overall, my work shows that a good understanding of the biology of modern sponges provides a wealth of information with which to examine the Precambrian record of sponges in particular, and the greater picture of early animal evolution in general, because having a correct interpretation of the fossil record is essential to properly calibrate molecular phylogenies.

The main results from this work are that there is a narrow range of values for the osculum area to surface area ratio (OSA/SA) of modern sponges, and also for the slope plotted for the osculum area to surface area for different sizes of sponges, and both the range and the slope are class-specific for both fossil and extant forms. The OSA/SA ratio is 0.01 - 0.04 for modern demosponges. In fossils this range is wider, although because only the best-preserved specimens were chosen, it cannot be ruled out that there might be some contribution from plastic deformation; even so, the range lies within 0.01 - 0.45 for fossil sponges. *Thectardis avalonensis* stands out as a good fossil sponge candidate to test this hypothesis with, as at least two populations (n=250 known specimens) have been collected, rather than existing solely as an isolated sponge-shaped specimen like many other proposed fossil sponges. The OSA/SA ratio of *T. avalonensis* at 0.25 is different from modern demosponges, albeit closer to two Cambrian demosponge genera *Hamptoniella* and *Hazelia* and the calcarean genera *Eiffelospongia*. The slope of the OSA/SA for *Thectardis avalonensis* is not statistically different from the demosponge slope, but it is different from the slope of the OSA/SA for the hexactinellids. This analysis indicates that the morphometrics (dimensions) of *T. avalonensis* are consistent with a sponge interpretation, possibly with a slightly different pump requirement, which aligns with the paleoenvironmental reconstructions of the oceans (Maliva et al. 1989). However, the original argument for its poriferan affinity is that the width to length ratio, 'Sperling's ratio' (Sperling et

al. 2011) is necessary for a sponge-like structure to move water through its body via induced flow.

The results from the second avenue of the thesis shows that this is not necessarily the case, as sponges do not use induced flow. In early work Bidder (1923) showed that the oscula tend to have a smaller area than the combined area of the choanocyte chambers, and this increased the flow at the osculum expelling excurrent water farthest away from the sponge to avoid recycling. This observation does not imply a passive mechanism, as the choanocytes are still doing the beating part of the job, moving all of the water through the canal system. Data from deep-sea bacteriosponge demosponge *Geodia barretti* confirm previous work on tropical and temperate sponges (Ludeman et al. 2017). *Geodia barretti* exhibits a higher filtration-to-respiration ratio when exposed to some flow, but only up until around 10 cm s^{-1} ambient current, after which it pumps less or even stops.

4.2. Current cannot be easily induced to flow through a sponge

Many authors cite the ability to use induced flow as the *sine qua non* of sponges. They use it as a descriptive character, and a way to elucidate whether a fossil is a sponge if it has the right dimensions for induced flow (e.g., Balsam and Vogel 1973, Savarese 1995, Sperling et al. 2011). That sponges have a combined smaller excurrent than incurrent area, is not necessarily due to their using induced flow, but rather to maximize the pumping power of the choanocytes (see Chapter 1 of this thesis). Vogel (1977, 1978) proposed a few mechanisms to explain how sponges might benefit from induced flow, including the Bernoulli effect provided by a pressure and velocity gradient around the sponge overall shape and viscous entrainment pulling water through the canals. However, these mechanisms do not consider the internal structure of sponges and the great resistance to the passage of water that comes from the sponge tissue and the glycocalyx mesh on the collar (Leys et al. 2011).

Current-induced flow *sensu* Vogel (1974) claims the ability of the sponges to make use of ambient current to filter water at no – or very low – energetic cost. This means that a sponge would expend more energy to filter water at low ambient current and would expend less energy to filter more water at high currents. This is not what happens, however, either in flow flume experiments or in the field (Ludeman et al. 2017). *Geodia barretti* is a deep-sea demosponge and the results of flume experiments show that it does filter more water at 10 cm s^{-1} ambient flow

than with no ambient current, but it reduces its pumping when exposed to ambient currents higher than that. The cost of pumping in *Geodia* is also very low (0.4 W Hr^{-1} or 2.47% of total metabolism) which suggests low selection pressure for exploitation of any induced flow mechanism in this sponge.

4.3. The slope of osculum area to surface area can distinguish sponge classes

Shape is inherited and can be measured, so it should be analyzable, even for a developmentally plastic organism. Sponges are plastic but still have constraints on their body plan, i.e., the total osculum area has to be smaller than the surface area, and that results in a very small and narrow OSA/SA ratio and permits us to discriminate types of sponges from other shapes that are not limited to a narrow ratio. The analysis of the scaling properties of modern sponges indicates that the osculum area is a major predictor of the pumping of a sponge, which in turn links the OSA/SA ratio to the pumping rate of the sponge. Considering modern and fossil sponges, the range of the OSA/SA ratio was 0.01 - 0.45. This means we can identify shapes that lie outside this range as not typical for a sponge; additionally, and perhaps surprisingly, the slope of osculum area to surface area for individuals of different sizes can discriminate between classes even when considering both fossil and modern forms. That indicates there is a class difference in how the aquiferous system is built, which can be distilled down to one ratio and one slope for individuals in the class. The fact that Cambrian sponges had a bigger OSA/SA ratio might suggest that these sponges had a slightly different pumping requirement, in a sea richer in bacteria and less filled with filter-feeding competitors; a hypothesis that could be tested with extant animals. This approach proves valuable as it permits us to compare neontological data and paleontological data with the same tools.

4.4. *Thectardis avalonensis* and the sponge fossil gap

In the sections above, I discussed my results on the form and function of a sponge and now I will discuss its implications for the Precambrian sponge fossil gap. In this thesis I show evidence that sponges do not rely on current-induced flow to filter water, but nevertheless their morphology can indicate a class-specific pump character. This character can only be applied to a population of organisms, because a single specimen with a particular shape could randomly have an

osculum to surface area ratio similar to the sponges. But it is unlikely that this proportion (OSA/SA) is reflected in the whole population. I applied this test (the OSA/SA ratio) to a population of specimens of *Thectardis avalonensis* from the Ediacaran fauna of Mistaken Point, Newfoundland (565 – 575 Ma) as this was the best candidate population to be a sponge (Sperling et al. 2011). The ratio was considerably higher (0.25) for *T. avalonensis* compared to 0.01 of modern demosponges, but it was surprisingly similar to the Cambrian demosponge genera *Hazelia*, *Fieldospongia*, *Hamptoniella,* and the calcarean *Eiffelospongia.* Also, the slope of the osculum area to surface area of *T. avalonensis* was not statistically different from the slope for Demospongiae (both fossil and modern). I propose that *T. avalonensis* was indeed a sponge, and it shared the gross morphometrics and the pump character of the demosponges.

The stratigraphic range of *Thectardis avalonensis,* however, is restricted to the Mistaken Point era and does not exceed 575 Ma. The question remains as to the 200 million years of absence of sponge fossils at 800 Ma when molecular clocks and phylogenetic analysis imply that they were present (Schuster et al. 2018, Sperling and Stockey 2018). Again, this gap cannot be attributed to lack of preservation as the same preservation styles where we find sponge fossil assemblages of exquisite detail in the Cambrian, are also found in the Ediacaran, including pyritization and carbonaceous compressions. This is reflected in several Ediacaran assemblages e.g., Vendobiota or Lantian Biota (Yuan et al. 2013), Miaohe Biota (Xiao et al. 2002), Zuun-Arts Biota (Dornbos et al. 2016) and Gaojiashan Biota (Cai et al. 2012). Additionally, dissolved silica content reached saturation levels in the Ediacaran world's oceans which could have enhanced spicule preservation, but did not (Tarhan et al. 2016).

Another important transition at the Precambrian-Phanerozoic boundary was deep-sea oxygenation. The Neoproterozoic deep-sea basin was mostly euxinic (both anoxic and sulfidic), but rich in dissolved organic carbon (DOC), which likely was the main nutrient source for the rangeomorphs biota and the vendobionts in general (Anbar and Knoll 2002, Canfield 1998, Laflamme and Narbonne 2008, Sperling et al. 2007). Only after this transition, do we observe the onset of biomineralization, but specially silica biomineralization. The silica-saturated seas changed to low concentrations of silica during the Phanerozoic. It is hypothesized that the reduction of the silica to modern day levels was mainly because of biosilification by diatoms, but sponges also played a major role after the Cambrian (Maliva et al. 1989). Molecular phylogenies however suggest a deep Cryogenian divergence for crown group Porifera, implying that spiculate

sponges should be present in the late Neoproterozoic (Cryogenian - Ediacaran). Alternatively, the scenario of Ctenophora as the sister group of the rest of Metazoa, implying that the divergence of sponges post-dates the origin of animals, would reduce the minimum gap (Borowiec et al. 2015, Dunn et al. 2015). In summary, even if *Thectardis avalonensis* is indeed a sponge, the problem of the missing Precambrian sponge fossil record is not resolved, and the ratio I have highlighted here (OSA/SA) is worth exploring in a wider set of taxa, modern and fossil, to make inferences of the sponge pump, palaeoecological reconstructions, and even as another line of evidence of poriferan affinity for putative fossils.

4.5. Concluding statement

In this thesis I presented yet another line of evidence against the induce flow hypothesis in sponges, with the consequence that induce flow should not be taken as a criterion for ascribing to the sponges any structure based on this assumption. Sponges are far from being passive conduits. They behave, sense and respond to the currents around them. Although sponges are asymmetrical, they do have a body ratio that relates to the pumping character, the osculum area to surface area ratio. This ratio can be applied to modern and fossil forms, and the slope can discriminate between sponge classes and give valuable insight into the putative Precambrian sponge fossil record.

Bibliography

Allison, P.A., and D.E.G. Briggs. 1993. Exceptional fossil record: Distribution of soft-tissue preservation through the Phanerozoic. Geology 21(6):527-530.

Anbar, A.D., and A.H. Knoll. 2002. Proterozoic Ocean Chemistry and Evolution: A Bioinorganic Bridge? Science 297(5584):1137.

Antcliffe, J.B. 2013. Questioning the evidence of organic compounds called sponge biomarkers. Palaeontology 56(5):917-925.

Antcliffe, J.B., R.H.T. Callow, and M.D. Brasier. 2014. Giving the early fossil record of sponges a squeeze. Biological Reviews 89(4):972-1004.

Asadzadeh, S.S., T. Kiørboe, P.S. Larsen, S.P. Leys, G. Yahel, and J.H. Walther. 2020. Hydrodynamics of sponge pumps and evolution of the sponge body plan. eLife 9:e61012.

Asadzadeh, S.S., P.S. Larsen, H.U. Riisgård, and J.H. Walther. 2019. Hydrodynamics of the leucon sponge pump. Journal of The Royal Society Interface 16(150):20180630.

Balsam, W.L., and S. Vogel. 1973. Water Movement in Archaeocyathids: Evidence and Implications of Passive Flow in Models. Journal of Paleontology 47(5):979-984.

Barghoorn, E.S., and S.A. Tyler. 1965. Microorganisms from the Gunflint Chert. Science 147(3658):563.

Bavestrello, G., G. Corriero, and M. Sarà 2008. Differences between two sympatric species of Tethya (Porifera, Demospongiae) concerning the growth and final form of their megasters. Zoological Journal of the Linnean Society 104(1):81-87.

Bell, G., and S. Collins. 2008. Adaptation, extinction and global change. Evolutionary Applications 1(1):3-16.

Bell, J.J. 2008. The functional roles of marine sponges. Estuarine, Coastal and Shelf Science 79(3):341-353.

Bergquist, P.R. 1978. Sponges. Hutchinson and Co., London.

Bidder, G.P. 1923. The relation of the form of a sponge to its currents. Quarterly journal of microscopical science 67:293-323.

Bond, C., and A.K. Harris. 1988. Locomotion of sponges and its physical mechanism. Journal of Experimental Zoology 246:271-284.

Borowiec, M.L., E.K. Lee, J.C. Chiu, and D.C. Plachetzki. 2015. Extracting phylogenetic signal and accounting for bias in whole-genome data sets supports the Ctenophora as sister to remaining Metazoa. BMC Genomics 16(1):987.

Botting, J.P., and B.J. Nettersheim. 2018. Searching for sponge origins. Nature Ecology and Evolution 2(11):1685-1686.

Botting, J.P., Y. Zhang, and L.A. Muir. 2017. Discovery of missing link between demosponges and hexactinellids confirms palaeontological model of sponge evolution. Scientific Reports 7(1):5286.

Bowerbank, J.S. 1864. A Monograph of the British Spongiadae. Vol 1. Ray Society, London.

Brain , C.K.B., A.R. Prave , K.-H. Hoffmann , A.E. Fallick , A. Botha , D.A. Herd , C. Sturrock , I. Young , D.J. Condon , and S.G. Allison 2012. The first animals : ca. 760-million-year-old sponge-like fossils from Namibia. South African Journal of Science 108 (1/2):658.

Brusca, R., and G. Brusca. 2003. Invertebrates. Sinauer Associates, Massachusetts.

Butterfield, N. 2007. Macroevolution and Macroecology through deep time. Palaeontology 50(1):41-55.

Cai, Y., J. Schiffbauer, H. Hua, and S. Xiao. 2012. Preservational modes in the Ediacaran Gaojiashan Lagerstätte: Pyritization, aluminosilicification, and carbonaceous compression. Palaeogeography, Palaeoclimatology, Palaeoecology 326:109-117.

Canfield, D.E. 1998. A new model for Proterozoic ocean chemistry. Nature 396(6710):450-453.

Carter, M.C., D.P. Gordon, and J.P.A. Gardner. 2010. Polymorphism and vestigiality: comparative anatomy and morphology of bryozoan avicularia. Zoomorphology 129(3):195-211.

Clapham, M., G. Narbonne, J.G. Gehling, and M. Anderson. 2004. *Thectardis avalonensis*: A new Ediacaran fossil from the Mistaken Point biota, Newfoundland. Journal of Paleontology 78(6):1031-1036.

Corruccini, R.S. 1987. Shape in morphometrics: Comparative analyses. American Journal of Physical Anthropology 73(3):289-303.

Cunningham, J., A. Liu, S. Bengtson, and P. Donoghue. 2017. The origin of animals: Can molecular clocks and the fossil record be reconciled? BioEssays 39(1):e201600120.

Dahihande, A.S., and N.L. Thakur. 2019. Temperature- and size-associated differences in the skeletal structures and osculum cross-sectional area influence the pumping rate of contractile sponge Cinachyrella cf. cavernosa. Marine ecology 40(5):e12565.

Darwin, C. 1859. On the Origin of Species. Murray, London.

de Goeij, J.M., A. De Kluijver, F.C. Van Duyl, J. Vacelet, R.H. Wijffels, A.F.P.M. De Goeij, J.P.M. Cleutjens, and B. Schutte. 2009. Cell kinetics of the marine sponge *Halisarca caerulea* reveal rapid cell turnover and shedding. Journal of Experimental Biology 212(23):3892-3900.

de Goeij, J.M., L. Moodley, M. Houtekamer, N.M. Carballeira, and F.C. van Duyl. 2008. Tracing 13C-enriched dissolved and particulate organic carbon in the bacteria-containing coral reef sponge *Halisarca caerulea*: Evidence for DOM-feeding. Limnology and Oceanography 53(4):1376-1386.

de Goeij, J.M., D. van Oevelen, M.J.A. Vermeij, R. Osinga, J.J. Middelburg, A.F.P.M. de Goeij, and W. Admiraal. 2013. Surviving in a Marine Desert: The Sponge Loop Retains Resources Within Coral Reefs. Science 342(6154):108-110.

Dohrmann, M., and G. Wörheide. 2017. Dating early animal evolution using phylogenomic data. Scientific Reports 7(1):3599-3599.

Dong, X.-P., P.C.J. Donoghue, H. Cheng, and J.-B. Liu. 2004. Fossil embryos from the Middle and Late Cambrian period of Hunan, south China. Nature 427:237-240.

Dornbos, S.Q., T. Oji, A. Kanayama, and S. Gonchigdorj. 2016. A new Burgess Shale-type deposit from the Ediacaran of western Mongolia. Scientific Reports 6(1):23438.

Dunn, C.W., S.P. Leys, and S.H.D. Haddock. 2015. The hidden biology of sponges and ctenophores. Trends in Ecology & Evolution 30(5):282-291.

Edgecombe, G.D., G. Giribet, C.W. Dunn, A. Hejnol, R.M. Kristensen, R.C. Neves, G.W. Rouse, K. Worsaae, and M.V. Sørensen. 2011. Higher-level metazoan relationships: recent progress and remaining questions. Organisms Diversity & Evolution 11(2):151-172.

Eernisse, D.J., and K.J. Peterson. 2004. The history of animals. P. 591. *In* J. Cracraft, and M. Donoghue, eds. Assembling the Tree of Life. Oxford University Press.

Elliott, G.R.D., and S.P. Leys. 2007. Coordinated contractions effectively expel water from the aquiferous system of a fresh water sponge. Journal of Experimental Biology 210(21):3736-3748.

Ellwanger, K., F. Brümmer, and M. Nickel. 2004. Glutamate, GABA and serotonin induce contractions in the sponge *Tethya wilhelma* (Porifera: Demospongiae). P. 157. Jahrestagung der Deutschen Zoologischen Gesellschaft. Zoologisches Institut der Universität Rostock, Rostock.

Emson, R.H. 1966. The reactions of the sponge *Cliona celata* to applied stimuli. Comparative Biochemistry and Physiology 18:805-827.

Ereskovsky, A.V., D.V. Lavrov, and P. Willenz. 2014. Five new species of Homoscleromorpha (Porifera) from the Caribbean Sea and re-description of Plakina jamaicensis. Journal of the Marine Biological Association of the United Kingdom 94(2):285-307.

Erpenbeck, D., and G. Wörheide. 2007. On the molecular phylogeny of sponges (Porifera). Zootaxa 1668:107-126.

Evans, S.D., I.V. Hughes, J.G. Gehling, and M.L. Droser. 2020. Discovery of the oldest bilaterian from the Ediacaran of South Australia. Proceedings of the National Academy of Sciences 117(14):7845-7850.

Feuda, R., M. Dohrmann, W. Pett, H. Philippe, O. Rota-Stabelli, N. Lartillot, G. Wörheide, and D. Pisani. 2017. Improved modeling of compositional heterogeneity supports sponges as sister to all other animals. Current Biology 27(24):3864-3870.e4.

Frisone, V., A. Pisera, and N. Preto. 2016. A highly diverse siliceous sponge fauna (Porifera: Hexactinellida, Demospongiae) from the Eocene of north-eastern Italy: systematics and palaeoecology. Journal of Systematic Palaeontology 14(11):949-1002.

Gökalp, M., T. Kooistra, M.S. Rocha, T.H. Silva, R. Osinga, A.J. Murk, and T. Wijgerde. 2020. The Effect of Depth on the Morphology, Bacterial Clearance, and Respiration of the Mediterranean Sponge *Chondrosia reniformis* (Nardo, 1847). Marine Drugs 18(7):358.

Goldstein, J., H.U. Riisgård, and P.S. Larsen. 2019. Exhalant jet speed of single-osculum explants of the demosponge *Halichondria panicea* and basic properties of the sponge-pump. Journal of Experimental Marine Biology and Ecology 511:82-90.

Goloboff, P.A., and S.A. Catalano. 2011. Phylogenetic morphometrics (II): algorithms for landmark optimization. Cladistics 27(1):42-51.

Gould, S.J. 1966. Allometry and size in ontogeny and phylogeny. Biol Rev Camb Philos Soc 41(4):587-640.

Gould, S.J. 1971. D'Arcy Thompson and the Science of Form. New Literary History 2(2):229-258.

Gould, S.J. 1976. D'Arcy Thompson and the Science of Form. Pp. 66-97. *In* M. Grene, and E. Mendelsohn, eds. Topics in the Philosophy of Biology. Springer Netherlands, Dordrecht.

Grant, R. 1825. Observations and experiments on the structure and functions of the sponge. Edinburgh Philosophical Journal 8:94-107.

Griffiths, C.L., and J.A. King. 1979. Energy expended on growth and gonad output in the ribbed mussel *Aulacomya ater*. Marine Biology 53(3):217-222.

Gröger, H., and V. Schmid. 2001. Larval development in Cnidaria: A connection to Bilateria? Genesis 29:110-114.

Hadas, E., M. Ilan, and M. Shpigel. 2008. Oxygen consumption by a coral reef sponge. Journal of Experimental Biology 211(13):2185-2190.

Hammer, Ø., D. Harper, and P. Ryan. 2001. PAST: Paleontological statistics software package for education and data analysis. Palaeontologia Electronica 4(1):9.

Heiko, S., R. Dirk, W.L. Raymond, L. Peter, and S. Erwin. 2002. Macrofaunal community structure and sulfide flux at gas hydrate deposits from the Cascadia convergent margin, NE Pacific. Marine Ecology Progress Series 231:121-138.

Hentschel, U., L. Fieseler, M. Wehrl, C. Gernert, M. Steinert, J. Hacker, and M. Horn. 2003. Microbial Diversity of Marine Sponges. Pp. 59-88. *In* W. E. G. Müller, ed. Sponges (Porifera). Springer Berlin Heidelberg, Berlin, Heidelberg.

Hentschel, U., K.M. Usher, and M.W. Taylor. 2006. Marine sponges as microbial fermenters. FEMS Microbiology Ecology 55(2):167-177.

Hoffmann, F., O. Larsen, V. Thiel, H.T. Rapp, T. Pape, W. Michaelis, and J. Reitner. 2005. An Anaerobic World in Sponges. Geomicrobiology Journal 22:1-10.

Hoffmann, F., R. Radax, D. Woebken, M. Holtappels, G. Lavik, H.T. Rapp, M.-L. Schläppy, C. Schleper, and M.M.M. Kuypers. 2009. Complex nitrogen cycling in the sponge *Geodia barretti*. Environmental Microbiology 11(9):2228-2243.

Hooper, J.A., and R.W.M. Van Soest. 2002. Systema Porifera. A Guide to the Classification of Sponges. Kluwer Academic/Plenum Publ., New York.

Jensen, S., J.G. Gehling, and M.L. Droser. 1998. Ediacara-type fossils in Cambrian sediments. Nature 393(6685):567-569.

Jørgensen, C. 1975. Comparative physiology of suspension feeding. Annual review of physiology 37:57-79.

Junger, W., A. Falsetti, and C. Wall. 1995. Shape, Relative Size, and Size-Adjustments in Morphometrics. Yearbook of Physical Anthropology 38:137-161.

Kaandorp, J.A., J.G. Blom, J. Verhoef, M. Filatov, M. Postma, and W.E.G. Müller. 2008. Modelling genetic regulation of growth and form in a branching sponge. Proceedings of the Royal Society B: Biological Sciences 275(1651):2569-2575.

Kaandorp, J.A., and R.A.G. Leiva. 2004. Morphological analysis of two- and three- dimensional images of branching sponges and corals. Pp. 83-96. *In* A. M. T. Elewa, ed. Morphometrics: Applications in Biology and Paleontology. Springer Berlin Heidelberg, Berlin, Heidelberg.

Kahn, A.S., C.W. Pennelly, P.R. McGill, and S.P. Leys. 2020. Behaviors of sessile benthic animals in the abyssal northeast Pacific Ocean. Deep Sea Research Part II: Topical Studies in Oceanography 173:104729.

Kealy, R.A., T. Busk, J. Goldstein, P.S. Larsen, and H.U. Riisgård. 2019. Hydrodynamic characteristics of aquiferous modules in the demosponge *Halichondria panicea*. Marine Biology Research 15(10):531-540.

Kelley, D., J. Baross, and J. Delaney. 2002. Volcanoes, Fluids, and Life at Mid-Ocean Ridge Spreading Centers. Annual Review of Earth and Planetary Sciences 30(1):385-491.

Kendall, D.G. 1989. A Survey of the Statistical Theory of Shape. Statistical Science 4(2):87-99, 13.

Kumala, L., H.U. Riisgård, and D.E. Canfield. 2017. Osculum dynamics and filtration activity in small single-osculum explants of the demosponge *Halichondria panicea*. Marine Ecology Progress Series 572:117-128.

Kutti, T., R.J. Bannister, and J.H. Fosså. 2013. Community structure and ecological function of deep-water sponge grounds in the Traenadypet MPA—Northern Norwegian continental shelf. Continental Shelf Research 69:21-30.

Kutti, T., R.J. Bannister, J.H. Fosså, C.M. Krogness, I. Tjensvoll, and G. Søvik. 2015. Metabolic responses of the deep-water sponge Geodia barretti to suspended bottom sediment, simulated mine tailings and drill cuttings. Journal of Experimental Marine Biology and Ecology 473:64-72.

LaBarbera, M., and S. Vogel. 1976. An Inexpensive Thermistor Flowmeter for Aquatic Biology. Limnology and Oceanography 21(5):750-756.

Laflamme, M., and G.M. Narbonne. 2008. Competition in a Precambrian world: palaeoecology of Ediacaran fronds. Geology Today 24(5):182-187.

Leys, S.P., and A. Hill. 2012. The Physiology and Molecular Biology of Sponge Tissues. Advances in Marine Biology 62:1-56.

Leys, S.P., A.S. Kahn, J.K.H. Fang, T. Kutti, and R.J. Bannister. 2018. Phagocytosis of microbial symbionts balances the carbon and nitrogen budget for the deep-water boreal sponge *Geodia barretti*. Limnology and Oceanography 63(1):187-202.

Leys, S.P., J.L. Mah, P.R. McGill, L. Hamonic, F.C. De Leo, and A.S. Kahn. 2019. Sponge Behavior and the Chemical Basis of Responses: A Post-Genomic View. Integrative and Comparative Biology 59(4):751–764.

Leys, S.P., G. Yahel, M.A. Reidenbach, V. Tunnicliffe, U. Shavit, and H.M. Reiswig. 2011. The sponge pump: the role of current induced flow in the design of the sponge body plan. PLoS One 6 (12):e27787.

Liu, A., D. McIlroy, J.B. Antcliffe, and M.D. Brasier. 2011. Effaced preservation in the Ediacara biota and its implications for the early macrofossil record. Palaeontology 54(3):607-630.

Love, G.D., E. Grosjean, C. Stalvies, D.A. Fike, J.P. Grotzinger, A.S. Bradley, A.E. Kelly, M. Bhatia, W. Meredith, C.E. Snape, S.A. Bowring, D.J. Condon, and R.E. Summons. 2009. Fossil steroids record the appearance of Demospongiae during the Cryogenian period. Nature 457(7230):718-721.

Ludeman, D.A., N. Farrar, A. Riesgo, J. Paps, and S.P. Leys. 2014. Evolutionary origins of sensation in metazoans: functional evidence for a new sensory organ in sponges. BMC Evol Biol 14, 3.

Ludeman, D.A., M.A. Reidenbach, and S.P. Leys. 2017. The energetic cost of filtration by demosponges and their behavioural response to ambient currents. The Journal of Experimental Biology 220:995-1007.

Maldonado, M., and M.J. Uriz. 1999. An experimental approach to the ecological significance of microhabitat-scale movement in an encrusting sponge. Marine Ecology Progress Series 185:239-255.

Maliva, R.G., A.H. Knoll, and R. Siever. 1989. Secular change in chert distribution: a reflection of evolving biological participation in the silica cycle. Palaios 4:519-32.

Maloof, A.C., C.V. Rose, R. Beach, B.M. Samuels, C.C. Calmet, D.H. Erwin, G.R. Poirier, N. Yao, and F.J. Simons. 2010. Possible animal-body fossils in pre-Marinoan limestones from South Australia. Nature Geosci 3(9):653-659.

Manuel, M., C. Borchiellini, E. Alivon, Y. Le Parco, J. Vacelet, and N. Boury-Esnault. 2003. Phylogeny and evolution of calcareous sponges: monophyly of Calcinea and Calcaronea, high level of morphological homoplasy, and the primitive nature of axial symmetry. Systematic Biology 3:311-333.

Maynard Smith, J., and E. Szathmary. 1995. The Major Transitions in Evolution. Freeman, Oxford.

McIlroy, D., S.C. Dufour, R. Taylor, and R. Nicholls. 2021. The role of symbiosis in the first colonization of the seafloor by macrobiota: Insights from the oldest Ediacaran biota (Newfoundland, Canada). BioSystems 205:104413.

McMurray, S.E., J.R. Pawlik, and C.M. Finelli. 2014. Trait-mediated ecosystem impacts: how morphology and size affect pumping rates of the Caribbean giant barrel sponge. Aquatic Biology 23(1):1-13.

McNair, G.T. 1923. Motor reactions of the fresh-water sponge *Ephydatia fluviatilis*. Biological Bulletin 44:153-166.

Mitchell, E.G., and N.J. Butterfield. 2018. Spatial analyses of Ediacaran communities at Mistaken Point. Paleobiology 44(1):40-57.

Mitteroecker, P., and S.M. Huttegger. 2009. The Concept of Morphospaces in Evolutionary and Developmental Biology: Mathematics and Metaphors. Biological Theory 4(1):54-67.

Morganti, T.M., A. Purser, H.T. Rapp, C.R. German, M.V. Jakuba, L. Hehemann, J. Blendl, B.M. Slaby, and A. Boetius. 2021a. In situ observation of sponge trails suggests common sponge locomotion in the deep central Arctic. Current Biology 31(8):R368-R370.

Morganti, T.M., M. Ribes, R. Moskovich, J.B. Weisz, G. Yahel, and R. Coma. 2021b. *In situ* Pumping Rate of 20 Marine Demosponges Is a Function of Osculum Area. Frontiers in Marine Science 8(19).

Morganti, T.M., M. Ribes, G. Yahel, and R. Coma. 2019. Size Is the Major Determinant of Pumping Rates in Marine Sponges. Frontiers in Physiology 10(1474).

Nadhira, A., M.D. Sutton, J.P. Botting, L.A. Muir, P. Gueriau, A. King, D.E.G. Briggs, D.J. Siveter, and D.J. Siveter. 2019. Three-dimensionally preserved soft tissues and calcareous hexactins in a Silurian sponge: implications for early sponge evolution. Royal Society Open Science 6(7):190911.

Nettersheim, B.J., J.J. Brocks, A. Schwelm, J.M. Hope, F. Not, M. Lomas, C. Schmidt, R. Schiebel, E.C.M. Nowack, P. De Deckker, J. Pawlowski, S.S. Bowser, I. Bobrovskiy, K. Zonneveld, M. Kucera, M. Stuhr, and C. Hallmann. 2019. Putative sponge biomarkers in unicellular Rhizaria question an early rise of animals. Nature Ecology & Evolution 3(4):577-581.

Palumbi, S.R. 1984. Tactics of acclimation: morphological changes of sponges in an unpredictable environment. Science 225(4669):1478-1480.

Parker, G.H. 1910. The reactions of sponges with a consideration of the origin of the nervous system. Journal of Experimental Zoology 8:765-805.

Parker, G.H. 1919. The elementary nervous system. Monographs on experimental biology:25-49.

Peng, S., L.E. Babcock, and R.A. Cooper. 2012. The Cambrian Period. Pp. 437-488. The Geologic Time Scale.

Peterson, K., M. McPeek, and D. Evans. 2005. Tempo and mode of early animal evolution: inferences from rocks, Hox, and molecular clocks. Paleobiology 31:36-55.

Peterson, K.J., and N.J. Butterfield. 2005. Origin of the Eumetazoa: testing ecological predictions of molecular clocks agains the Proterozoic fossil record. Proceedings of the National Academy of Sciences USA 102(27):9547-9552.

Peterson, K.J., J.A. Cotton, J.G. Gehling, and D. Pisani. 2008. The Ediacaran emergence of bilaterians: congruence between the genetic and the geological fossil records. Philosophical transactions of the Royal Society of London. Series B, Biological sciences 363(1496):1435-43.

Philippe, H., H. Brinkmann, D.V. Lavrov, D.T.J. Littlewood, M. Manuel, G. Wörheide, and D. Baurain. 2011. Resolving Difficult Phylogenetic Questions: Why More Sequences Are Not Enough. PLoS biology 9(3):e1000602.

Philippe, H., R. Derelle, P. Lopez, K. Pick, C. Borchiellini, N. Boury-Esnault, J. Vacelet, E. Renard, E. Houliston, E. Queinnec, C. Da Silva, P. Winicker, H. Le Guayader, S. Leys, D. Jackson, F. Schreiber, D. Erpenbeck, B. Morgenstern, and G. Woerheide. 2009. Phylogeomics revives traditional views on deep animal relationships. Current Biology 19:706-712.

Pita, L., M.P. Hoeppner, M. Ribes, and U. Hentschel. 2018. Differential expression of immune receptors in two marine sponges upon exposure to microbial-associated molecular patterns. Scientific Reports 8(1):16081.

Poppell, E., J. Weisz, L. Spicer, A. Massaro, A. Hill, and M. Hill. 2014. Sponge heterotrophic capacity and bacterial community structure in high- and low-microbial abundance sponges. Marine ecology 35(4):414-424.

Porter, S.M., and A.H. Knoll. 2000. Testate amoebae in the Neoproterozoic Era: evidence from vase-shaped microfossils in the Chuar Group, Grand Canyon. Paleobiology 26(3):360-385.

Raff, E.C., J.T. Villinski, F.R. Turner, P.C.J. Donoghue, and R.A. Raff. 2006. Experimental taphonomy shows the feasibility of fossil embryos. Proceedings of the National Academy of Science (USA) 103(15):5846-5851.

Reiswig, H.M. 1971a. *In situ* pumping activities of tropical Demospongiae. Marine Biology 9:38-50.

Reiswig, H.M. 1971b. Particle feeding in natural populations of three marine demosponges. The Biological Bulletin 141(3):568-591.

Reiswig, H.M. 1974. Water transport, respiration and energetics of three tropical marine sponges. Journal of Experimental Marine Biology and Ecology 14(3):231-249.

Reiswig, H.M. 1975a. The aquiferous systems of three marine Demospongiae. Journal of Morphology 145:493-502.

Reiswig, H.M. 1975b. Bacteria as food for temperate-water marine sponges. Canadian Journal of Zoology 53:582-589.

Reiswig, H.M. 1981. Partial carbon and energy budgets of the bacteriosponge *Verongia fistularis* (Porifera: Demospongiae) in Barbados. Marine ecology 2(4):273-293.

Richtsmeier, J.T., V. Burke Deleon, and S.R. Lele. 2002. The promise of geometric morphometrics. American Journal of Physical Anthropology 119(S35):63-91.

Riisgård, H., and P. Larsen. 1995. Filter-feeding in marine macro-invertebrates: pump characteristics, modelling and energy cost. Biological Reviews 70(1):67-106.

Rohlf, F.J. 2015. The tps series of software. Hystrix, the Italian Journal of Mammalogy 26(1):9-12.

Rohlf, F.J., and M. Corti. 2000. Use of Two-Block Partial Least-Squares to Study Covariation in Shape. Systematic Biology 49(4):740-753.

Ryan, J.F., K. Pang, C.E. Schnitzler, A.-D. Nguyen, R.T. Moreland, D.K. Simmons, B.J. Koch, W.R. Francis, P. Havlak, S.A. Smith, N.H. Putnam, S.H.D. Haddock, C.W. Dunn, T.G. Wolfsberg, J.C. Mullikin, M.Q. Martindale, and A.D. Baxevanis. 2013. The genome of the ctenophore *Mnemiopsis leidyi* and its implications for cell type evolution. Science 342(6164):1242592.

Savarese, M. 1992. Functional Analysis of Archaeocyathan Skeletal Morphology and Its Paleobiological Implications. Paleobiology 18(4):464-480.

Savarese, M. 1995. Functional significance of regular archaeocyathan central cavity diameter: a biomechanical and paleoecological test. Paleobiology 21(3):356-378.

Schindelin, J., I. Arganda-Carreras, E. Frise, V. Kaynig, M. Longair, T. Pietzsch, S. Preibisch, C. Rueden, S. Saalfeld, and B. Schmid. 2012. Fiji: an open-source platform for biological-image analysis. Nature Methods 9(7):676-682.

Schlappy, M.-L., M. Weber, D. Mendola, F. Hoffmann, and D. De Beer. 2010. Heterogeneous oxygenation resulting from active and passive flow in two Meterirranean sponges, *Dysidea avara* and *Chondrosia reniformis*. Limnology and Oceanography 55(3):1289-1300.

Schmitt, S., P. Tsai, J. Bell, J. Fromont, M. Ilan, N. Lindquist, T. Perez, A. Rodrigo, P.J. Schupp, J. Vacelet, N. Webster, U. Hentschel, and M.W. Taylor. 2012. Assessing the complex sponge microbiota: core, variable and species-specific bacterial communities in marine sponges. Isme j 6(3):564-76.

Schuster, A., S. Vargas, I.S. Knapp, S.A. Pomponi, R.J. Toonen, D. Erpenbeck, and G. Wörheide. 2018. Divergence times in demosponges (Porifera): first insights from new mitogenomes and the inclusion of fossils in a birth-death clock model. BMC Evolutionary Biology 18(1):114.

Shore, A.J., R.A. Wood, I.B. Butler, A.Y. Zhuravlev, S. McMahon, A. Curtis, and F.T. Bowyer. 2021. Ediacaran metazoan reveals lophotrochozoan affinity and deepens root of Cambrian Explosion. Science Advances 7(1):eabf2933.

Simister, R.L., P. Deines, E.S. Botté, N.S. Webster, and M.W. Taylor. 2012. Sponge-specific clusters revisited: a comprehensive phylogeny of sponge-associated microorganisms. Environ Microbiol 14(2):517-24.

Sperling, E.A., K.J. Peterson, and M. Laflamme. 2011. Rangeomorphs, Thectardis (Porifera?) and dissolved organic carbon in the Ediacaran oceans. Geobiology 9(1):24-33.

Sperling, E.a., D. Pisani, and K.J. Peterson. 2007. Poriferan paraphyly and its implications for Precambrian palaeobiology. Pp. 355-368. *In* P. Vickers-Rich, and P. Komarower, eds.

The Rise and Fall of the Ediacaran Biota. The Geological Socitey Publishing House, Bath, UK.

Sperling, E.A., and R.G. Stockey. 2018. The Temporal and Environmental Context of Early Animal Evolution: Considering All the Ingredients of an "Explosion". Integrative and Comparative Biology 58(4):605-622.

Stearn, C.W. 1983. Stromatoporoids: Affinity with Modern Organisms. Notes for a Short Course: Studies in Geology 7:164-166.

Strehlow, B.W., M.-C. Pineda, A. Duckworth, G.A. Kendrick, M. Renton, M.A. Abdul Wahab, N.S. Webster, and P.L. Clode. 2017. Sediment tolerance mechanisms identified in sponges using advanced imaging techniques. PeerJ 5:e3904.

Tarhan, L., A.V.S. Hood, M. Droser, J.G. Gehling, and D. Briggs. 2016. EXCEPTIONAL PRESERVATION OF SOFT-BODIED EDIACARA BIOTA PROMOTED BY SILICA-RICH OCEANS.

Thomas, R.D.K., and W.E. Reif. 1993. The Skeleton Space: A Finite Set of Organic Designs. Evolution 47(2):341-360.

Thompson, D.A.W. 1992. On Growth and Form. Cambridge University Press, Cambridge.

Tyler, C.L., and L.R. Leighton. 2011. Detecting competition in the fossil record: Support for character displacement among Ordovician brachiopods. Palaeogeography, Palaeoclimatology, Palaeoecology 307(1):205-217.

Vacelet, J., and N. Boury-Esnault. 1995. Carnivorous sponges. Nature 373:333-335.

Vacelet, J., and C. Donadey. 1977. Electron microscope study of the association between some sponges and bacteria. Journal of Experimental Marine Biology and Ecology 30(3):301-314.

Van Soest, R.W.M., N. Boury-Esnault, J. Vacelet, M. Dohrmann, D. Erpenbeck, N.J. De Voogd, N. Santodomingo, B. Vanhoorne, M. Kelly, and J.N.A. Hooper. 2012. Global Diversity of Sponges (Porifera). Public Library of Science One 7(4):e35105.

Vogel, S. 1974. Current-induced flow through the sponge, *Halichondria*. Biological Bulletin 147:443-456.

Vogel, S. 1977. Current-induced flow through living sponges in nature. Proceedings of the National Academy of Science USA 74(5):2069-2071.

Vogel, S. 1978. Evidence for one-way valves in the water-flow system of sponges. Journal of Experimental Biology 76:137-148.

Vogel, S. 1994. Life in Moving Fluids: The physical biology of flow. Princeton University Press, Princeton, NJ.

Vogel, S., and W.L. Bretz. 1972. Interfacial Organisms: Passive Ventilation in the Velocity Gradients near Surfaces. Science 175(4018):210.

Warton, D.I., I.J. Wright, D.S. Falster, and M. Westoby. 2006. Bivariate line-fitting methods for allometry. Biological Reviews 81(2):259-291.

Webster, N.S., M.W. Taylor, F. Behnam, S. Lücker, T. Rattei, S. Whalan, M. Horn, and M. Wagner. 2010. Deep sequencing reveals exceptional diversity and modes of transmission for bacterial sponge symbionts. Environmental Microbiology 12(8):2070-2082.

Weissenfels, N. 1990. Condensation rhythm of fresh-water sponges (Spongillidae, Porifera). European Journal of Cell Biology 53:373-383.

Weisz, J., N. Lindquist, and C. Martens. 2008. Do associated microbial abundances impact marine demosponge pumping rates and tissue densities? Oecologia 155:367-376.

Whelan, N.V., K.M. Kocot, L.L. Moroz, and K.M. Halanych. 2015. Error, signal, and the placement of Ctenophora sister to all other animals. Proceedings of the National Academy of Sciences 112(18):5773-5778.

Whelan, N.V., K.M. Kocot, T.P. Moroz, K. Mukherjee, P. Williams, G. Paulay, L.L. Moroz, and K.M. Halanych. 2017. Ctenophore relationships and their placement as the sister group to all other animals. Nature Ecology & Evolution 1(11):1737-1746.

Wörheide, G., M. Dohrmann, D. Erpenbeck, C. Larroux, M. Maldonado, O. Voigt, C. Borchiellini, and D.V. Lavrov. 2012. Deep phylogeny and evolution of sponges (phylum Porifera). Pp. 1-78. *In* M. A. Becerro, M. J. Uriz, M. Maldonado, and X. Turon, eds. Advances in Sponge Science: Phylogeny, Systematics, Ecology. Academic Press, London, UK.

Xiao, S., J. Hu, X. Yuan, R.L. Parsley, and R. Cao. 2005. Articulated sponges from the Lower Cambrian Hetang Formation in southern Anhui, South China: their age and implications for the early evolution of sponges. Palaeogeography, Palaeoclimatology, Palaeoecology 220:89-117.

Xiao, S., X. Yuan, M. Steiner, and A.H. Knoll. 2002. Macroscopic carbonaceous compressions in a terminal Proterozoic shale: A systematic reassessment of the Miaohe biota, south China. Journal of Paleontology 76(2):347-376.

Yahel, G., J.H. Sharp, D. Marie, C. Hase, and A. Genin. 2003. In situ feeding and element removal in the symbiont-bearing sponge *Theonella swinhoei* : bulk DOC is the major source for carbon. Limnology and Oceanography 48(1):141-149.

Yin, L., M. Zhu, A.H. Knoll, X. Yuan, J. Zhang, and J. Hu. 2007. Doushantuo embryos preserved inside diapause egg cysts. Nature 446(7136):661-3.

Yin, Z., M. Zhu, E.H. Davidson, D.J. Bottjer, F. Zhao, and P. Tafforeau. 2015. Sponge grade body fossil with cellular resolution dating 60 Myr before the Cambrian. Proceedings of the National Academy of Sciences 112(12):E1453-E1460.

Yuan, X., Z. Chen, S. Xiao, B. Wan, C. Guan, W. Wang, C. Zhou, and H. Hua. 2013. The Lantian biota: A new window onto the origin and early evolution of multicellular organisms. Chinese Science Bulletin 58(7):701-707.

Zhang, Y., X. Yuan, and L. Yin. 1998. Interpreting Late Precambrian Microfossils. Science 282(5395):1783.

Zumberge, J.A., G.D. Love, P. Cárdenas, E.A. Sperling, S. Gunasekera, M. Rohrssen, E. Grosjean, J.P. Grotzinger, and R.E. Summons. 2018. Demosponge steroid biomarker 26-methylstigmastane provides evidence for Neoproterozoic animals. Nature Ecology & Evolution 2(11):1709-1714.

Appendix 1

Likelihood of preservation: Biostratinomy of the sponge tissue

Background & Summary

How likely it is to find fine details of tissues and cell types, and larvae (sponges with cellular structure) in the fossil record? As a prerequisite for fossilization, tissues need to be preserved long enough for the mineralization process to occur. Cell autolysis can be stopped by action of a reducing agent e.g., H_2S. However, due to the high toxicity of H_2S, β-ME (beta-mercaptoethanol) is often used as a substitute because their reducing potential is similar (Raff et al. 2006). Raff et al., (2006) used 100 mM β-ME in experimental taphonomic studies with echinoderm larvae because some authors reported concentrations of H_2S around 30-100 mM in some modern marine environments (Heiko et al. 2002, Kelley et al. 2002). In addition, pyrite rich sediments in Ediacaran and Cambrian deposits are evidence that H_2S was involved in the fossilization process in these localities (Dong et al. 2004). Here I asked whether enough sponge tissue could remain after 2 weeks in a reducing environment, and whether that would be long enough for early mineralization to start. I predicted that tissues exposed to different concentrations of the reducing agent β-ME will show less decay after two weeks, compared to tissues in sea water. The level of preservation obtained by β-ME is expected to be the highest achievable, and so if tissues are not recognizable after two weeks, it is unlikely that sponge tissue (and cells, such as choanocytes) could be found in the fossil record.

Sponge fine structures are very unlikely to be preserved unless in anoxic and reducing conditions for long enough time to allow replacement of tissue by minerals. A general outline can still be preserved by retention of the skeleton (Supplementary Figure 1). I tested the likelihood of sponge tissue preservation in first seawater and in β-ME, and then in a mineral solution plus β-ME. The first experiment, decay, looked at three different sponges over two and four weeks. *Neopetrosia problematica* had the most resilient structure; although not much of the sponge tissue was recovered after four weeks, the skeleton remained articulated. After even two weeks, *Tethya californiana* had no recognizable tissue but lots of spicules remained. For *Haliclona mollis*, some spongin lasted, but soft tissue was lost. The calcareous sponge *Sycon coactum* decayed even more quickly than the other species, with no structure remaining at all

after two weeks. The results from the first experiment suggest that sponges, and sponge tissues decay very rapidly, even within 15 days, and so we now have a time frame within which to explore biostratinomy, or the processes of decay (supplementary figure 2). Chronologically, biostratinomy can be seen as the analysis of what happens to the organisms after death (necrology) and before final burial (diagenesis). The second experiment addressed how the tissue decays in reducing and mineral solutions. β-ME was used as a reducing agent, and treatments included silicate, sulfate and phosphate. In short, the only tissue element remaining in one specimen was collagen and perhaps a few cells but with no tissue structure. However, using scanning electron microscopy, crystals were found attached to the spicule surfaces (Supplementary Figure 3). I found that silicates form bigger crystals and sulfate and phosphates, smaller crystals. I also found calcium crystals attached to the spicules but not to the remains of tissues.

Materials and methods

Field work was carried out at the Bamfield Marine Sciences Centre during the summer of 2019. The preservation potential of the sponge tissue was examined using the representative demosponge species *Neopetrosia problematica* (de Laubenfels, 1930) (ord. Haplosclerida), *Haliclona mollis* (Lambe, 1893) (ord. Haplosclerida), and *Tethya californiana* (de Laubenfels, 1932) (ord. Tethyida) and the calcarean sponge *Sycon coactum* (ord. Leucosolenida). β-ME (beta-mercaptoethanol) was used to create reducing conditions rather than the typically used H_2S. β-ME is less toxic and has similar reducing potential (Raff et al., 2006). I used 100 mM β-ME based on reported concentrations of H_2S around 30-100 mM in modern marine sediments (Heiko et al. 2002, Kelley et al. 2002, Raff et al. 2006). In addition, pyrite rich sediments in Ediacaran and Cambrian deposits are evidence that H_2S was involved in the fossilization process in these localities (Dong et al. 2004)(Dong et al., 2004).

Two questions are tackled here. The first tests the time frame of sponge tissue decay. I tested 15 and 30 days, following Allison & Briggs (1993) for invertebrate experimental taphonomy. For this experiment I tested whether the tissue could persist for 15 days under 'standard' conditions, i.e. living pieces of sponge placed in sea water with and without β-ME in a closed vial at room temperature. This first experiment tests whether reducing conditions alone

can significantly slow down decay to potentially allow for tissue-detailed preservation in a fossil. For convenience, and following the methods of Raff et al. (2006), β-ME was used *in lieu* of H_2S that would normally be present in natural settings. The treatments were 5 mm^2 pieces of sponge in 20 mL vials at three concentrations of β-ME (50, 100 and 150 mM) and one vial with only filtered sea water. The second experiment tests the potential for mineralization under conditions of sea water saturated with silicate, sulfate and phosphate. The treatments for the second experiment were sodium metasilicate (Na_2SiO_3), sodium sulfite (Na_2SO_3) and sodium phosphate (Na_3PO_4) (Sigma-Aldrich, Ont. Canada), left undisturbed for two weeks in sealed vials with β-ME. Controls consisted of sponge tissue left in 50 mM β-ME with no added salt i.e. the only different between experimental and control groups is the mineral salt added.

After two weeks samples were fixed for SEM. First, immersed in a fixative cocktail as described previously (Leys et al. 2018). After 10 minutes those pieces were immersed in fresh fixative and left at 4 °C for 6 hours. Sponge tissues were rinsed twice for 10 minutes each in distilled water, and dehydrated to 70% ethanol and transported to the University of Alberta. Fragments generated in this way were transferred in 100% ethanol to a Bal-Tec 030 critical point drier. After drying, samples were mounted on aluminum stubs using nail polish, coated with gold, and viewed in a Zeiss Sigma 300 Field Emission scanning electron microscope.

Results

The results from the first experiment suggest that sponge tissue decayed quickly within 15 days (Figure S1). No sponge tissue was recovered even at two weeks, but collagen remained in good shape in *Neopetrosia problematica* after 2 weeks and only the skeleton was present after four weeks; therefore this species had the most resilient organic matrix. For *Tethya californiana* no organic material remained, but lots of spicules were present after 4 weeks. *Haliclona mollis* had some collagen that lasted for the whole 4 weeks experiment. Nothing was found of *Sycon coactum* after 4 weeks in even at the highest concentration of β-ME.

In the second experiment – seawater saturated with silicate, sulfate and phosphate - and β-ME as a reducing agent – no tissue remained but crystal-like concretions were found using Energy

Dispersive X-ray analysis (EDX) in *Neopetrosia problematica*. Silicates formed bigger and more numerous crystals than sulfate and phosphate. Interestingly, I also found calcium crystals attached to the spicules of *Neopetrosia problematica* even in the absence of any treatment.

Conclusions

The experimental taphonomy suggests that sponge tissues decay quickly, at least within two weeks, and that all soft tissue is lost after four weeks despite being in a reducing medium such as β-ME. Early mineralization should take place before four weeks in order to preserve some sponge tissue. These experiments showed that in that period crystals can be formed and attached to spicules, which show signs of mild dissolution. Silicate saturated media gave rise to bigger crystals compared to sulfate and phosphate saturated media. Both results – decay and mineralization – align with the expected fossilization of sponge tissues in a silica saturated ocean.

It is true that short-term taphonomy experiments are problematic because attempting to recreate the time and environment for fossilization is extremely difficult. However, this sort of work, which is so much needed for a proper reading of the fossil record, is not common, especially not for invertebrates. There is no equivalent work on sponges and it therefore has value as a first step for opening up an avenue for research. This sort of work is vital to our understanding of fossilization, and directly affects our interpretation of the fossil data, which in turn affects our understanding of the unfolding of the evolutionary process in which the first multicellular animals arose. In the conditions tested here, it is very unlikely that cellular details of sponge tissues would be preserved, but even under these conditions collagen was preserved, which suggests that it might be possible under exceptional circumstances, to preserve sponge tissues just as we have the precedent of phosphatized fossil embryos (Dong et al., 2004), for instance. Future work can include experimental taphonomy with larvae and with choanocyte chambers, as well as using more combinations of mineral solutions, in particular iron, phosphate, sulphate, carbonates, silicates and reducing conditions in different combinations. Experimental taphonomy with sponges should also focus its effort on spicule taphonomy.

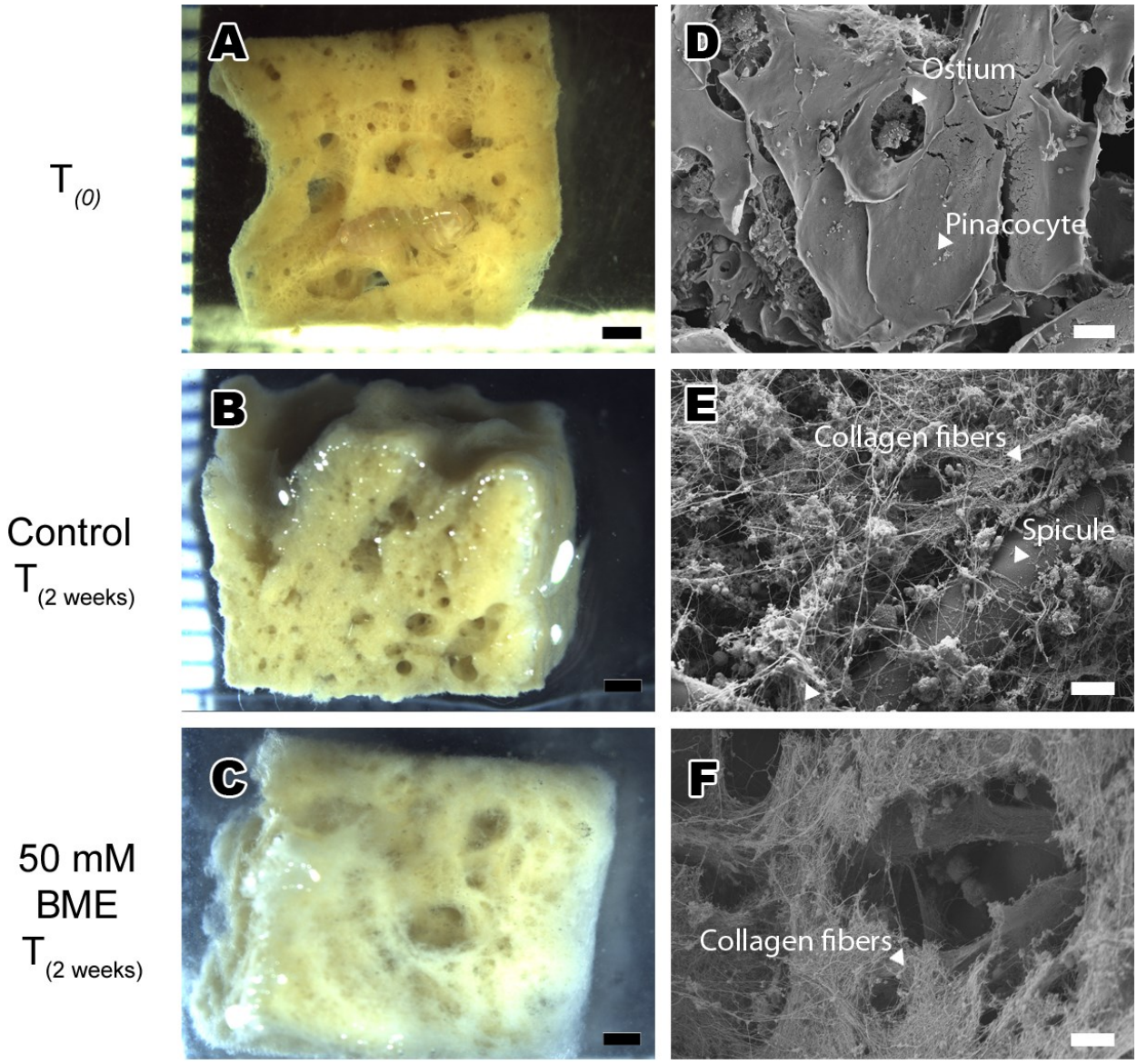

Supplementary Figure 1. Experimental decay by *Neopetrosia problematic*a. Comparison of fixed tissue at T_0 to decaying tissue after two weeks (T_{2weeks}) under control conditions (i.e. filtered seawater and no treatment) and 50 mM β-ME. (A-C) Light micrographs of tissue. Internal structure is lost as internal canals lose definite boundaries, but the skeleton maintains its gross shape: scale bar 1 cm. (D-F) Scanning electron micrographs comparing regular tissue to decayed tissue. (D) Fixed regular tissue shows poorly preserved pinacocytes and ostia; scale bar 10 µm. (E). Decayed tissue after two weeks in plain seawater. Collagen fibers and spicules are present: scale bar 5 µm. F) After two weeks in 50 mM β-ME treatment, collagen fibers networks outlining the decayed tissue are better preserved; scale bar 5 µm.

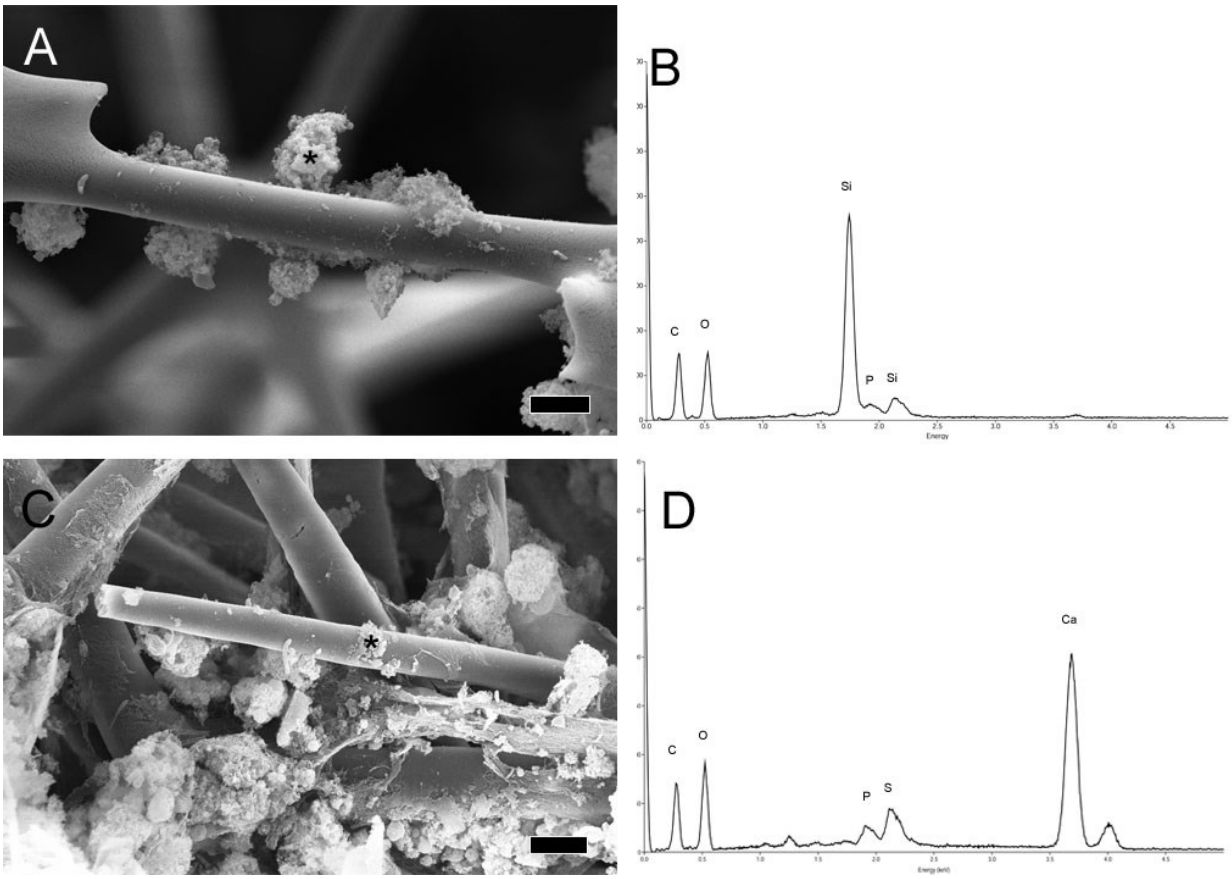

Supplementary Figure 2. Crystal formation and attachment to *Neopetrosia problematica* spicules after 15 days of decay. A) 100 mM β-ME and a silicate solution treatment with attached crystals, and Energy Dispersive X-ray Spectroscopy (EDX) spectrum was obtained (*) B) EDX shows a silicate predominance, and carbon and oxygen. C) Control of decayed tissue in 100 mM β-ME. Crystals were recovered and D) EDX shows a predominance of calcium. Scale bars 5 μm.

Supplementary Table 1. Percent error and mean percent error of measurements of Osculum Area (OSA, cm^2) in a sample of 20 measurements using area function in ImageJ, and calculated from diameter dimensions.

n	species	OSA calculated from diameter	OSA measured (Image J)	Percent error %
1	*Laocetis emiliana*	1.55	1.54	0.9
2	*Laocetis emiliana*	1.23	1.15	6.3
3	*Laocetis emiliana*	0.95	0.93	2.1
4	*Laocetis emiliana*	0.67	0.65	2.7
5	*Laocetis emiliana*	1.09	1.02	6.7
6	*Laocetis emiliana*	0.52	0.53	1.7
7	*Laocetis emiliana*	1.21	1.15	5.0
10	*Haliclona permollis*	0.203	0.19	4.4
11	*Haliclona permollis*	0.135	0.098	27.4
12	*Haliclona permollis*	0.211	0.212	0.5
13	*Haliclona permollis*	0.053	0.05	11.3
14	*Haliclona permollis*	0.032	0.03	12.5
15	*Haliclona permollis*	0.028	0.03	2.5
16	*Haliclona permollis*	0.03	0.04	30.0
17	*Haliclona permollis*	0.014	0.01	19.9
18	*Haliclona permollis*	0.099	0.09	13.9
19	*Haliclona permollis*	0.033	0.03	14.0
20	*Haliclona permollis*	0.152	0.178	17.1
			Mean Percent Error	0.7%

Supplementary Table 2. Measurements of 17 *Haliclona* cf. *permollis* patches in Bamfield, B.C., Canada showing the change in OSA/SA ratio with size and the distribution of oscula sizes.

Sponge	**length** (cm)	**Surface Area (SA**, cm^2)	**Average Osculum area (xOSA**, cm^2)	**Total Osculum area (tOSA**, cm^2)	**xOSA:SA**	**tOSA:SA**
1	2.26	5.1	0.008	0.20	0.002	0.04
2	2.12	4.5	0.006	0.14	0.001	0.03
3	3.11	9.7	0.004	0.21	0.000	0.02
4	1.30	1.7	0.004	0.05	0.003	0.03
5	1.15	1.3	0.005	0.03	0.004	0.02
6	1.27	1.6	0.002	0.03	0.001	0.02
7	1.40	2.0	0.003	0.03	0.001	0.02
8	0.83	0.7	0.002	0.01	0.003	0.02
9	1.88	3.5	0.003	0.10	0.001	0.03
10	1.49	2.2	0.002	0.03	0.001	0.01
11	2.13	4.5	0.003	0.15	0.001	0.03
12	2.33	5.4	0.005	0.14	0.001	0.03
13	1.38	1.9	0.001	0.04	0.001	0.02
14	2.05	4.2	0.008	0.09	0.002	0.02
15	2.36	5.6	0.002	0.12	0.0004	0.02
16	1.59	2.5	0.003	0.07	0.001	0.03
17	2.63	6.9	0.011	0.19	0.002	0.03
Average	1.8	3.7	0.004	0.10	0.001	0.025
SE	0.15	0.57	6.48E-04	0.02	2.25E-04	1.64E-03
SD	0.6	2.4	0.003	0.07	0.001	0.007
Max	3.1	9.7	0.011	0.21	0.004	0.040
Min	0.8	0.7	0.001	0.01	0.0004	0.015
Median	1.9	3.5	0.003	0.09	0.001	0.024

Supplementary Table 3. Correlation of length to average osculum area (xOSA) and osculum to surface area (OSASA) in *Haliclona* cf *permollis*.

Grouping category	equation	R^2	p	slope	intercept	Slope 95% bootstrapped CI N=1999	Intercept 95% bootstrapped CI N=1999
length to xOSA	Y=-0.004+0.004X	0.25	0.04	0.004	-0.0039	0.002, 0.007	-0.007, 0.0001
length to OSASA	Y=0.003+0.012X	0.11	0.19	0.012	0.003	0.004, 0.03	-0.04, 0.016

Supplementary Figure 3. Scatterplot showing volumetric flow rate Q and sponge volume for extant species of demosponges: *Cliona delitrix* (inverted open triangle), *Geodia barretti* (open circle), *Callyspongia vaginalis* (filled triangle), *Haliclona mollis* (filled square), *Neopetrosia problematica* (filled diamond), *Tethya californiana* (open diamond) (R^2=0.54 p<0.001).

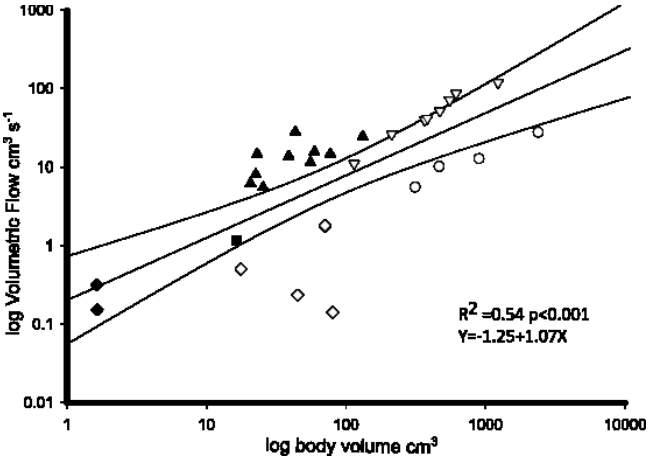

Supplementary Figure 4. Correlation of surface area to choanocyte chamber density demosponges *Cliona delitrix* (inverted open triangle), *Geodia barretti* (open circle), *Callyspongia vaginalis* (filled triangle), *Haliclona mollis* (filled square), *Neopetrosia problematica* (filled diamond), *Tethya californiana* (open diamond). We found that chamber density did not vary significantly with surface area (R^2=0.21 p=0.34).

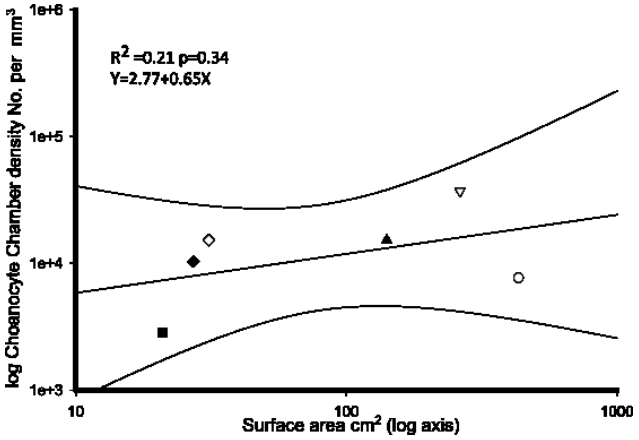

Supplementary Figure 5. Change in the oscula dimensions with respect to length in *Haliclona permollis*. A) Average osculum area does not increase with size, (R^2=0.25 p=0.04) B) The osculum to surface area ratio does not increase with size in this species (R^2=0.11 p=0.19) C) Median osculum to surface area ratio is 0.025±0.007SD D) The average osculum area is 0.003±0.003SD cm^2.

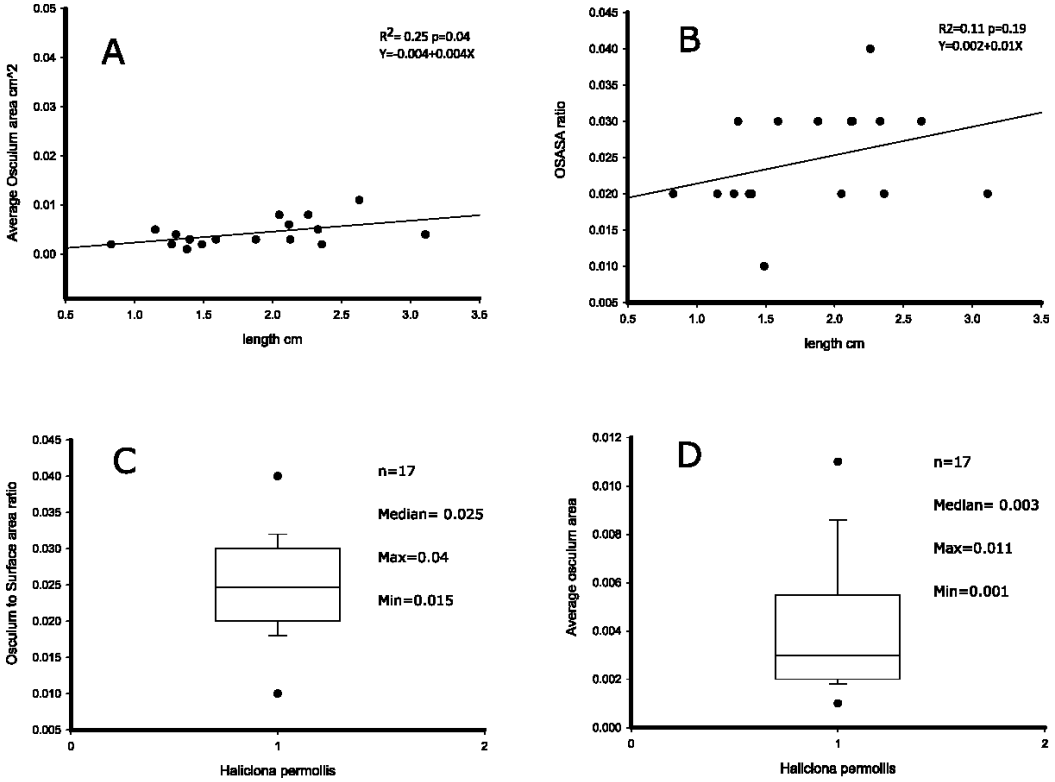

Supplementary Figure 6. Scatterplot and correlation of surface area (SA) to osculum area (OSA) in log scale of *Haliclona permollis* (R^2=0.91 p<0.001).

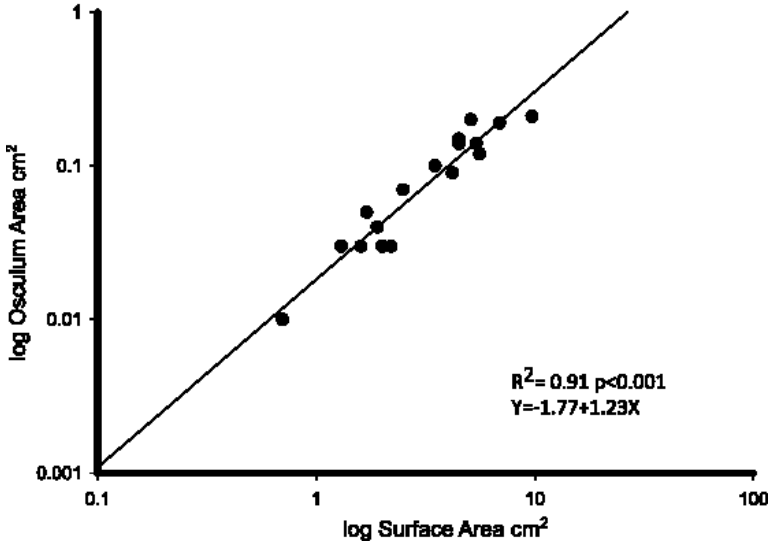

Appendix 2

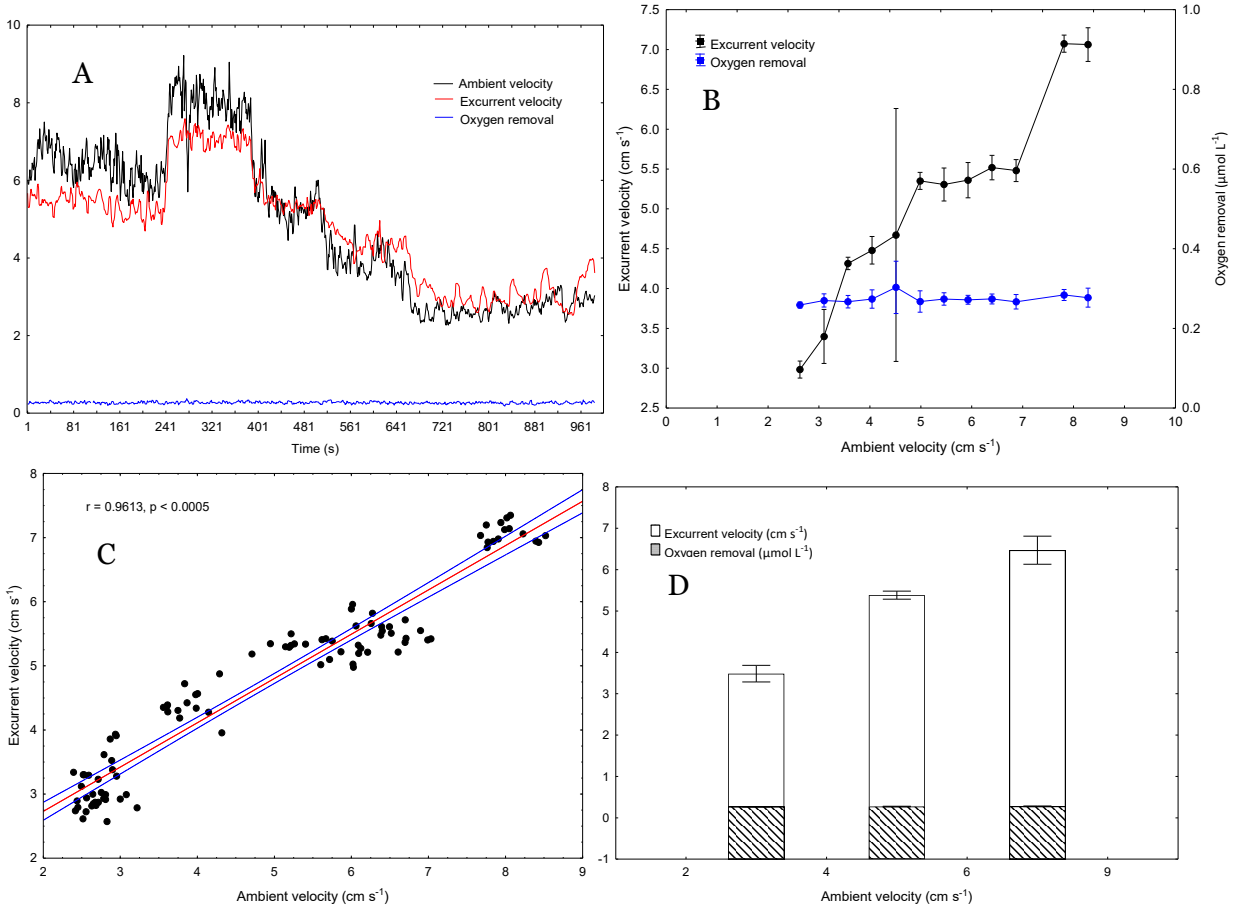

Supplementary Figure 3. Control flow experiment with an inert 'sponge' model. It shows that the oxygen sensor accurately captures the oxygen removal by a sponge, and that turbulence in the osculum can artificially increase the apparent excurrent speed.

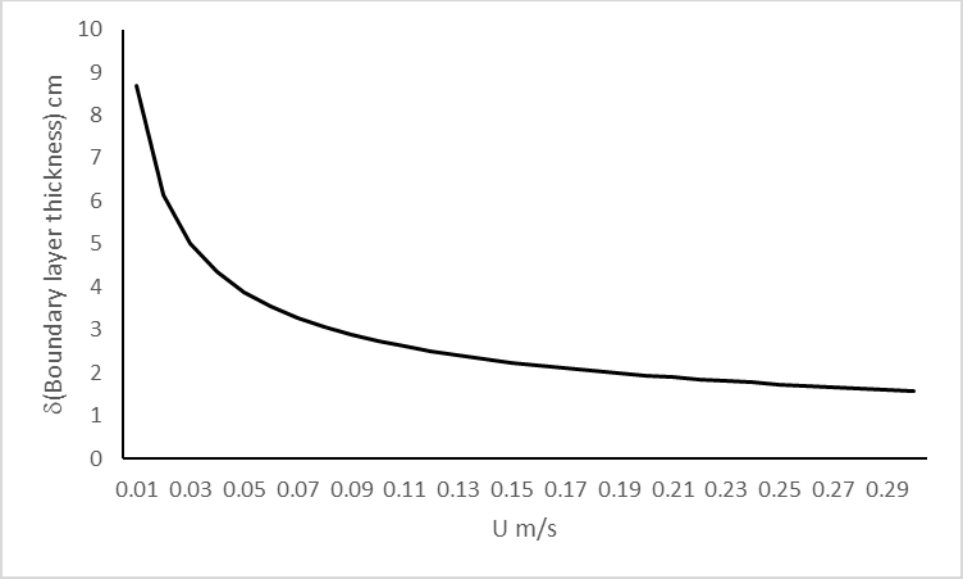

Supplementary Figure 4. Calculation of the boundary layer in laminar flow in a 3 m length and 0.5 m diameter. It is estimated to be 9 cm at velocities of 2 cm s^{-1}